

**Dissertation zur Erlangung des Doktorgrades
der Fakultät für Chemie und Pharmazie
der Ludwig-Maximilians-Universität München**

**Adeno-associated virus type 2 as vector for human gene therapy:
Characterization of virus-host interactions**

Nadja Angelika Huttner

aus

München

2003

Erklärung

Diese Dissertation wurde im Sinne von § 13 Abs. 3 bzw. 4 der Promotionsordnung vom 29. Januar 1998 von PD Dr. Stefan Weiß betreut.

Ehrenwörtliche Versicherung

Diese Dissertation wurde selbständig, ohne unerlaubte Hilfe erarbeitet.

München, am 09.05.2003

Nadja Huttner

Dissertation eingereicht am: 12.05.2003

1. Gutachter: PD Dr. Stefan Weiß
2. Gutachter: Prof. Dr. Michael Hallek

Mündliche Prüfung am: 23.06.2003

DANKSAGUNG

Herrn PD Dr. Stefan Weiß danke ich für die Betreuung meiner Promotionsarbeit und die Erstellung des Erstgutachtens.

Mein besonderer Dank gilt Prof. Dr. Michael Hallek für die Vergabe des Themas meiner Doktorarbeit und die kontinuierliche Unterstützung während meiner gesamten Promotionszeit. Besonders danke ich ihm, dass er mir die Teilnahme an nationalen und internationalen Kongressen ermöglicht hat. Des Weiteren danke ich für die Erstellung des Zweitgutachtens.

Mein Dank gilt auch Prof. Dr. Rudolf Grosschedl, der das Genzentrum mit innovativer Kraft leitet. Vor allem die Genzentrums Retreats in Wildbad Kreuth waren sowohl wissenschaftlich als auch sozial sehr interessant und förderlich. Prof. Dr. Ernst-Ludwig Winnacker bin ich für die Schaffung der hervorragenden Arbeitsbedingungen am Genzentrum zu großem Dank verpflichtet, ohne die diese Dissertation nur schwer durchzuführen gewesen wäre.

Ferner bedanke ich mich bei allen aktuellen und ehemaligen Mitgliedern der Arbeitsgruppe Hallek, sowohl am Genzentrum als auch an der GSF, für das gute Arbeitsklima, viele interessante Diskussionen, und ihre stete Hilfsbereitschaft. Hildegard Büning danke ich für Ihre Unterstützung und Zusammenarbeit vor allem in meiner Anfangszeit, in der ich in vielerlei Hinsicht gelernt habe. Allen anderen Mitarbeitern des 4. Stockwerks danke ich für die gute Zusammenarbeit und das freundschaftliche Klima.

Für die großartige Hilfestellung bei den AFM Analysen und Kopplungsexperimenten danke ich Dr. Reinhard Guckenberger, Dr. Martin Stark und Dr. Christian Plank.

Einen großen Dank auch an Siegi Kastenmüller für ihre Hilfe bei verwaltungstechnischen Angelegenheiten.

Nur schwer vorstellbar wäre meine Promotionszeit für mich gewesen ohne Anne Girod (leckere Crêpes und unzählige Korrekturen), Kristin „Grottenolm“ Leike (schnürzelbrünft... grunz), Eddie Speckbauer inklusive Knut Hennecke (beide knuddelsüchtig), Petra Nicklaus („Ich bin heut irgendwie etwas verpeilt“), Karin Forster („Hallo Süße“) und alle anderen Freunde außerhalb des Labor. Einen besonders herzlichen Dank für physischen und mentalen Beistand vor allem während der Durststrecken, für Freundschaft, jede Menge Spaß und vieles mehr.

Mein ganz besonderer Dank gilt meinen Eltern für ihre großartige Unterstützung in jeglicher Hinsicht und für alles, was sie mir mit auf den Weg gegeben haben.

Die vorliegende Arbeit wurde in der Zeit von September 1997 bis Oktober 2002 am Institut für Biochemie der Ludwig-Maximilians-Universität München unter der Anleitung von Prof. Dr. Michael Hallek angefertigt.

Im Verlauf dieser Arbeit wurden folgende Veröffentlichungen angefertigt:

Huttner NA, Girod A, Schnittger S, Schoch C, Hallek M, and Büning H. (2003) Analysis of site-specific transgene integration following cotransduction with recombinant adeno-associated virus and a Rep encoding plasmid. *J Gene Med* 5: 120-129.

Huttner NA, Stark M, Endress T, Girod A, Guckenberger R, Bräuchle C, Hallek M, Büning H. PLL/DNA complexes coupled to adeno-associated virus vectors allow for simultaneous gene transfer of a Rep encoding plasmid. *Virology*. (submitted for publication)

Huttner NA, Girod A, Perabo L, Edbauer D, Kleinschmidt JA, Büning H, and Hallek M. (2003) Genetic modifications of the adeno-associated virus type 2 capsid reduce the affinity and the neutralizing effects of human serum antibodies. *Gene Ther.* (in press)

Büning H, Ried MU, Perabo L, Gerner FM, **Huttner NA**, Enssle J, and Hallek M. (2003) Retargeting of Adeno-Associated Virus Vectors. *Gene Ther* 10: 1142-1151

Verliere den ganzen Verstand, ein halber verwirrt nur

C. F. Hill

Für meine Eltern

SUMMARY		II
CHAPTER I	Introduction	1
CHAPTER II	Analysis of site-specific transgene integration following co-transduction with recombinant adeno-associated virus and a Rep encoding plasmid	27
CHAPTER III	PLL/DNA complexes coupled to adeno-associated virus vectors allow for simultaneous gene transfer of a Rep encoding plasmid	47
CHAPTER IV	Genetic modifications of the adeno-associated virus type 2 capsid reduce the affinity and the neutralizing effects of human serum antibodies	65
CHAPTER V	Receptor targeting of adeno-associated virus vectors	87
CHAPTER VI	References	107
ABBREVIATIONS		133
CURRICULUM VITAE		135

SUMMARY

Vectors based on adeno-associated virus type 2 (AAV) offer considerable promise for somatic gene therapy of various diseases (e.g. cystic fibrosis, hemophilia B, cancer). Limitations, however, still exist and require further improvement. The study presented here addresses two major problems that hamper a widespread use of AAV in human gene therapy: First, the loss of site-specific integration of recombinant AAV vectors (rAAV) due to the deletion of the *rep* gene, and secondly, the potential neutralization of AAV gene therapy vectors by preexisting antibodies.

A unique advantage of wild-type AAV (wtAAV) is the ability to integrate into the host genome at a specific site within the human chromosome 19 (AAVS1), especially with regard to stable transgene expression and avoiding the risk of insertional mutagenesis by random integration. Site-specific integration depends on the presence of the viral *rep* gene. Currently available rAAV vectors are devoid of all viral genes and therefore do not target AAVS1. In order to define whether targeted integration of a rAAV vector can be restored by providing the *rep* gene in *trans*, HeLa cells were transfected with a plasmid expressing Rep under control of its natural promoter followed by transduction with a rAAV vector, and analyzed for site-specific integration of the transgene cassette. Similar to wtAAV in these experiments, 70% of the analyzed cell clones exhibited site-specific integration of the ITR flanked transgene cassette into chromosome 19 without adverse effects on the cells, while control transduction with rAAV alone resulted in random integration. This demonstrated that site-specific integration of a transgene encoding rAAV vector can be efficiently restored by providing the *rep* gene in *trans*.

Based on these findings a rAAV vector was developed where a plasmid coding for Rep was coupled as polylysine/DNA complex (PLL/DNA) directly to the capsid of the virion which would allow for targeted integration of rAAV. Plasmid DNA of various sizes could be complexed by polylysine to small compact particles and efficiently coupled to the AAV capsid via a biotin-streptavidin bridge. Biotinylation of AAV as well as conjugation of streptavidin did not interfere with the viral infection process. Furthermore, co-transduction of a PLL/DNA complex coupled to the AAV capsid was demonstrated by single virus tracing and FACS analysis, thus providing the basis for the generation of specifically integrating rAAV vectors.

Another limitation for the *in vivo* application of AAV vectors is the high prevalence of human serum antibodies against the AAV capsid. In particular neutralizing antibodies

represent a severe problem as they can reduce or even eliminate transgene expression of the delivered vector. To characterize immunogenic domains of the AAV capsid and to develop strategies to circumvent neutralization by antibodies, six AAV capsid mutants carrying peptide insertions in surface exposed loop regions were investigated in binding and neutralization assays. Mutations at position 534 and 573 reduced the affinity of human antisera in the majority of the analyzed serum samples, indicating that these capsid domains might be preferentially recognized by the human antibodies. Additionally, AAV vectors carrying two different targeting peptides inserted in position 587 escaped neutralization by human antibodies without losing their ability to infect cells via the targeted receptors. These data suggest that some major disadvantages of neutralizing antibodies might be overcome by an AAV retargeting vector modified at position 587.

Taken together, these results should be useful for the design of an improved generation of rAAV vectors: Providing *rep*-DNA as PLL/DNA should allow rAAV vectors to integrate specifically at chromosome 19. Furthermore, capsid modifications could help to overcome binding and neutralization by human antisera in clinical gene therapy applications.

CHAPTER I

Introduction

1	Human Gene Therapy: A Short Overview	4
2	Adeno-Associated Virus.....	5
2.1	Genomic Organization of AAV	8
2.2	Production of AAV Vectors	10
2.3	Infection Biology of AAV	11
2.4	The Structure of the AAV Capsid.....	14
2.5	The AAV Rep Proteins and their Role in Site-Specific Integration	17
2.6	Immune Response against AAV	19
3	AAV as Gene Therapy Vector: Pros and Cons	21

1 Human Gene Therapy: A Short Overview

Human gene therapy is a very young discipline when compared to other medical sciences. It can be broadly defined as the transfer of genetic material to cure a disease or at least to improve the clinical status of a patient. Key findings in molecular biology which have provided the basis for gene therapy, identification of the DNA structure and genetic code and lately the sequencing of the human genome, have been accomplished only within the last five decades. A milestone in experimental medicine was the first phase I gene-based clinical trial in 1990 which dealt with the treatment of adenosine deaminase deficiency (Blaese et al. 1995). The initial success of this clinical trial gave rise to the submission of many other human gene therapy protocols. Over the last decade, more than 600 phase I and phase II gene-based clinical trials have been conducted worldwide for the treatment of cancer and inherited or acquired genetic disorders. Recently, these trials have also been extended to the treatment of other diseases like AIDS and cardiovascular diseases. Presently available gene delivery vehicles for somatic gene transfer can be broadly divided into two categories: viral and nonviral vectors (Table 1). Based on the nature of their genome, viral vectors can be divided into RNA (retroviruses) and DNA (adeno-associated virus, adenovirus, herpes simplex virus, pox virus) viral vectors. Viruses are intracellular parasites that have developed efficient strategies to invade host cells, and in most cases, transport their genetic information into the nucleus. The major advantages of viral vectors are their high transduction efficiency and the potential stable expression of the therapeutic gene (retroviruses, adeno-associated virus). A limitation, however, is the risk of toxicity of the vector and induction of immunological reactions against the vector or its transgene (e.g. adenoviral vectors). The nonviral vectors, also known as synthetic gene delivery systems, represent the second category of delivery vehicles and rely on direct delivery of either naked DNA or RNA with cationic lipids. Nonviral vectors do not share the safety risks of the viral transfer systems, but suffer from low efficiency of gene transfer and only transient expression of the delivered genes. Although distinct classes of vectors have different combinations of favorable features, the ideal vector system has not yet been found. Constant investigations, however, will further improve the existing vector systems and many disadvantages can be overcome.

Table 1. Gene therapy clinical trials worldwide (www.wiley.co.uk/genmed/clinical/)

Vector	Trials¹	Example of diseases	pros / cons
Viral			
Adeno-associated virus (AAV)	15 (2.4%)	Cystic fibrosis, hemophilia B, prostate cancer, neurological disorders, muscular dystrophy	
Adenovirus	171 (26.9%)	Many cancers, peripheral artery disease, cystic fibrosis, Canavan disease	
Herpes simplex virus (HSV)	5 (0.8%)	Brain tumor, colon carcinoma	+ high efficiency, stable gene expression (AAV, retroviruses)
Pox virus	39 (6.1%)	Many cancers	- low selectivity, risk of immunogenicity or toxicity, limited coding capacity (except HSV)
Retrovirus	217 (34.1%)	Many cancers, AIDS, SCID, rheumatoid arthritis, graft-versus-host disease, multiple sclerosis, osteodysplasia, hemophilia	
Nonviral			
Gene gun ²	5 (0.8%)	Melanoma, sarcoma	
Lipofection ³	77 (12.1%)	Many cancers, cystic fibrosis, coronary artery disease, restenosis	
Naked DNA (plasmid)	70 (11.0%)	Many cancers, peripheral artery disease, coronary artery disease, peripheral neuropathy, open bone fractures	+ high safety, unlimited coding capacity - low efficiency, low selectivity, transient gene expression
RNA transfer	6 (0.9%)	Many cancers	
Other	25 (3.9%)		

¹ Number of open clinical trials world wide

² DNA coated on small gold particles and shot with a special gun into target tissue

³ Includes liposomes and various packages of lipid, polymer, and other molecules

2 Adeno-Associated Virus

Adeno-associated virus (AAV) is a particularly promising delivery system for gene therapy. In 1994 the first clinical trial was conducted with this vector system dealing with cystic fibrosis (Flotte & Carter 1995). AAV is a member of the parvovirus family. Viruses of this

family have a single-stranded DNA genome of approximately 5 kb and a non-enveloped icosahedral capsid. With a diameter of only 18 to 30 nm the parvoviruses are among the smallest known viruses. The family *Parvoviridae* includes two subfamilies: the *Parvovirinae*, which infect vertebrates, and the *Densovirinae*, which infect insects. Each of the subfamilies includes three genera. Adeno-associated viruses belong to the Dependovirus genus. In contrast to members of the Parvovirus genus (e.g. canine parvovirus, porcine parvovirus, Aleutian mink disease virus) and the Erythrovirus genus (human parvovirus B19), which are autonomous parvoviruses, adeno-associated viruses naturally depend on co-infection of an unrelated helper virus, e.g. adenovirus (Ad), herpesvirus (HSV), human cytomegalovirus, or papillomavirus, for productive infection (for review see Muzyczka & Berns 2001). Originally, the first serotype of AAV, AAV type 2, was found as a contaminant in laboratory stocks of adenovirus, hence the name “adeno-associated virus” (Atchison et al. 1965; Hoggan et al. 1966). Up to now eight serotypes (AAV type 1 – AAV type 8), which share different levels of sequence homology, have been identified. Although the other serotypes have attracted increasing attention during recent years, AAV type 2 is the most prominent serotype for gene therapy, being the first isolated, cloned, and best characterized. Since all following descriptions will refer to AAV type 2, it will be termed AAV throughout this chapter.

The life cycle of AAV has two distinct intracellular phases (Fig. 1). In the absence of co-infection by a helper virus the latent cycle is initiated. AAV enters the cell, and after a limited expression of viral regulatory proteins (Rep proteins), the virion integrates into the host genome in the q arm of chromosome 19 at a specific locus (AAVS1). After super-infection with a helper virus, the integrated genome is activated by entering the lytic cycle, leading to viral gene expression, rescue and replication of the AAV genome with subsequent production of viral progeny (Berns & Giraud 1996). Besides helper virus also genotoxic agents (e.g. UV-irradiation, γ -irradiation, hydroxyurea, topoisomerase inhibitors, and various chemical carcinogens) can support a productive infection (Heilbronn et al. 1985; Russell et al. 1995; Yakobson et al. 1989; Yalkinoglu et al. 1991; Yalkinoglu et al. 1988). These observations led to the conclusion that the role of helper functions is rather the induction of the appropriate cellular milieu (expression of stress response genes) required for AAV DNA replication than direct involvement of helper virus gene products (Yakobson et al. 1987).

The natural route for AAV infections is assumed to occur via the respiratory or gastrointestinal route as is the case for Ad, because *in vivo* AAV has been typically found as a contaminant of Ad isolates (Blacklow et al. 1971). However, it is not yet clear what tissue or

organ is a preferred site of latency in humans. Nevertheless, recombinant AAV vectors have demonstrated infection and long-term gene expression in a wide variety of tissues, including brain, liver, muscle, lung, and retina in animals (Fisher et al. 1997; Flannery et al. 1997; Flotte et al. 1993; Kaplitt et al. 1994; Snyder et al. 1997; Xiao et al. 1996). Although AAV is widespread, no disease has been associated with the virus (Berns & Linden 1995). On the contrary, AAV seems to be protective against bovine papillomavirus and Ad mediated cellular transformation (de la Maza & Carter 1981; Hermonat 1989; Khleif et al. 1991; Mayor et al. 1973), and to have cytotoxic effects in malignant cells (Raj et al. 2001).

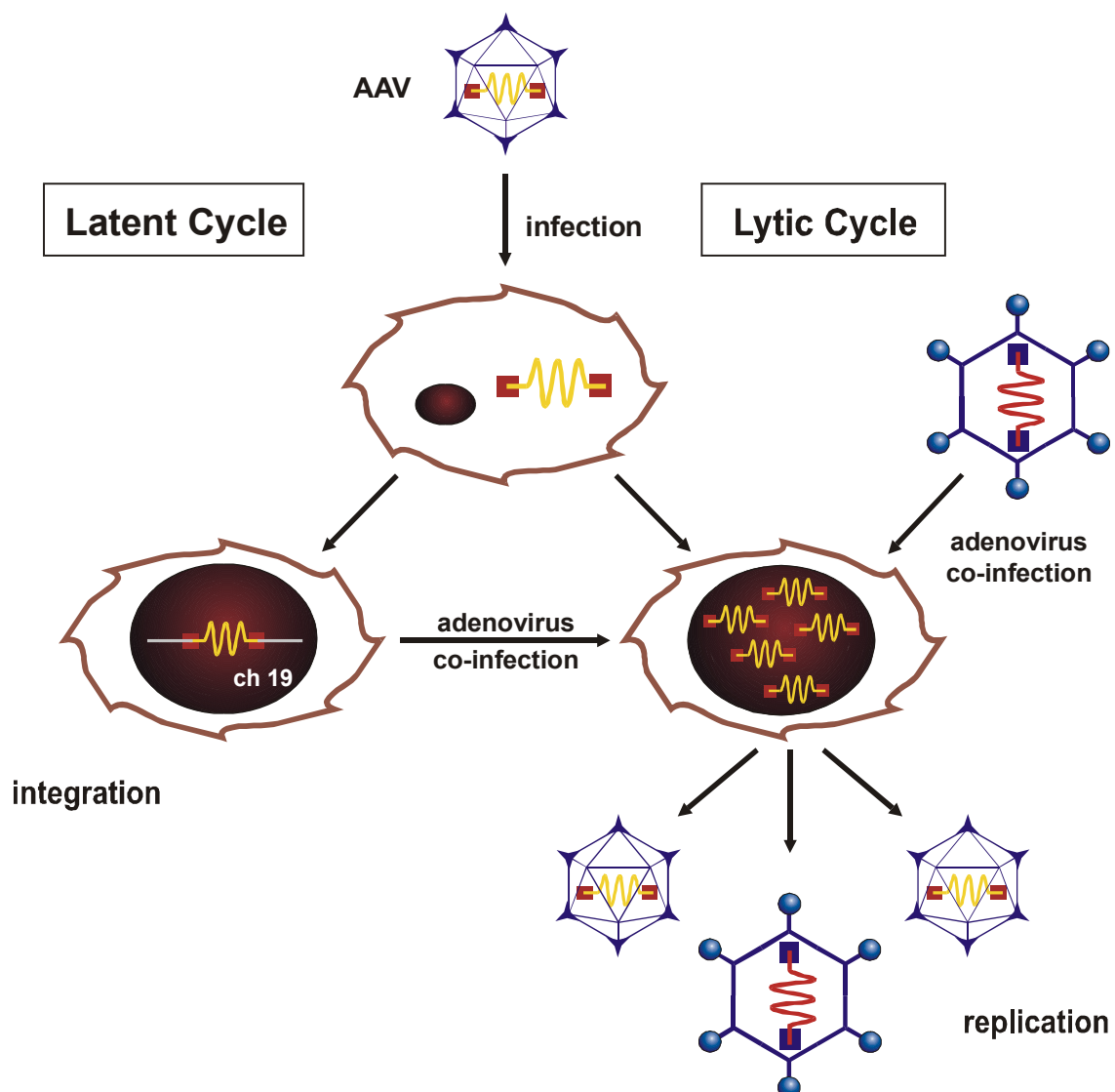


Figure 1. The biphasic life cycle of AAV. In the presence of a helper virus, adenovirus or herpesvirus, AAV enters the lytic cycle and undergoes a productive infection. Lacking a helper virus the AAV DNA can stably integrate preferentially into chromosome 19 of the host genome (AAVS1). After super-infection with a helper virus AAV can be rescued from the latent state and reenter the lytic cycle.

2.1 Genomic Organization of AAV

The wild-type AAV (wtAAV) has a single-stranded DNA genome of 4680 nucleotides. Two large open reading frames (ORF) occupy the right and the left half of the genome, respectively. These ORF are flanked by palindromic sequences, the inverted terminal repeats (Fig. 2).

- The 145 nucleotide long inverted terminal repeats (ITR) form a T-shaped structure on either side of the symmetry axis. The ITRs contain a Rep binding site (RBS) and a specific cleavage site for the bound Rep protein (terminal resolution site, TRS) (Im & Muzyczka 1990; McCarty et al. 1994; Snyder et al. 1993; Snyder et al. 1990). They constitute an important *cis*-acting signal which serves as origin of replication (*ori*) and primer for initiation of DNA synthesis. Furthermore they are critical for regulation of gene expression, and essential for site-specific integration of AAV and rescue of the viral genome from the integrated state (Labow & Berns 1988; McLaughlin et al. 1988; Samulski et al. 1987).
- The 5'-ORF *rep* encodes the non-structural, regulatory Rep proteins. Two promoters, p5 and p19, direct expression of the *rep* gene. A common intron results in the production of four Rep proteins: p5 initiated Rep78, Rep68 and p19 initiated Rep52, Rep40. Rep78 and Rep68 are multifunctional proteins with diverse biochemical activities, including DNA binding, DNA ligase, ATPase, DNA helicase, and strand-specific, site-specific endonuclease activities (Im & Muzyczka 1990; Im & Muzyczka 1992; Smith & Kotin 2000; Zhou et al. 1999). They are involved in AAV DNA replication, transcriptional control and targeted integration. The two smaller proteins, Rep52 and Rep40, appear to be involved directly in the accumulation and encapsidation of single-stranded genomes into preformed capsids and have also been shown to possess ATPase and helicase activities but seem to lack DNA binding activity (Chejanovsky & Carter 1989; Dubielzig et al. 1999; King et al. 2001; Smith & Kotin 1998). The Rep proteins can act as both repressors and transactivators of AAV transcription by regulating the activities of the three viral promoters. In the absence of helper virus, all Rep proteins have been observed to repress p5 and p19 transcription (Kyostio et al. 1994).
- The 3'-ORF *cap* encodes three structural proteins with overlapping amino acid sequence, VP1, VP2, and VP3, which form the viral capsid. They are all transcribed from the p40 promoter and expressed in a ratio of approximately 1:1:8 (Kronenberg et al. 2001). The

different translation efficiency is a consequence of differential splicing of the intron for synthesis of VP1, and the use of an unusual initiator codon (ACG) for VP2 synthesis. VP3 is translated from the initiator codon AUG and is the major capsid protein (Becerra et al. 1988; Becerra et al. 1985). All three capsid proteins use a common stop codon. The molecular weight of VP1, VP2, and VP3 is 90 kDa, 72 kDa, and 60 kDa, respectively. VP2 and VP3 are sufficient for capsid formation, yet VP1 is required for viral infection (Hermonat et al. 1984; Smuda & Carter 1991; Tratschin et al. 1984). The N-terminus of VP2 contains a nuclear localization signal which is required for translocation of VP3 to the nucleus (Hoque et al. 1999; Ruffing et al. 1992).

The half life of the Rep and Cap proteins is 15 h, and of the AAV mRNA approx. 4 to 6 h (Carter & Rose 1974; Redemann et al. 1989). The AAV particle has a molecular weight between 5.4 and 6.0×10^6 g/mol. Approximately 70% of the mass is protein, and the remaining is DNA. AAV particles are very resistant to inactivation. They are stable between pH 3 and 9 and at 56°C for 60 min. Inactivation of the virus is possible by formalin, β -propiolactone, hydroxylamine, and oxidizing agents (Berns et al. 2000).

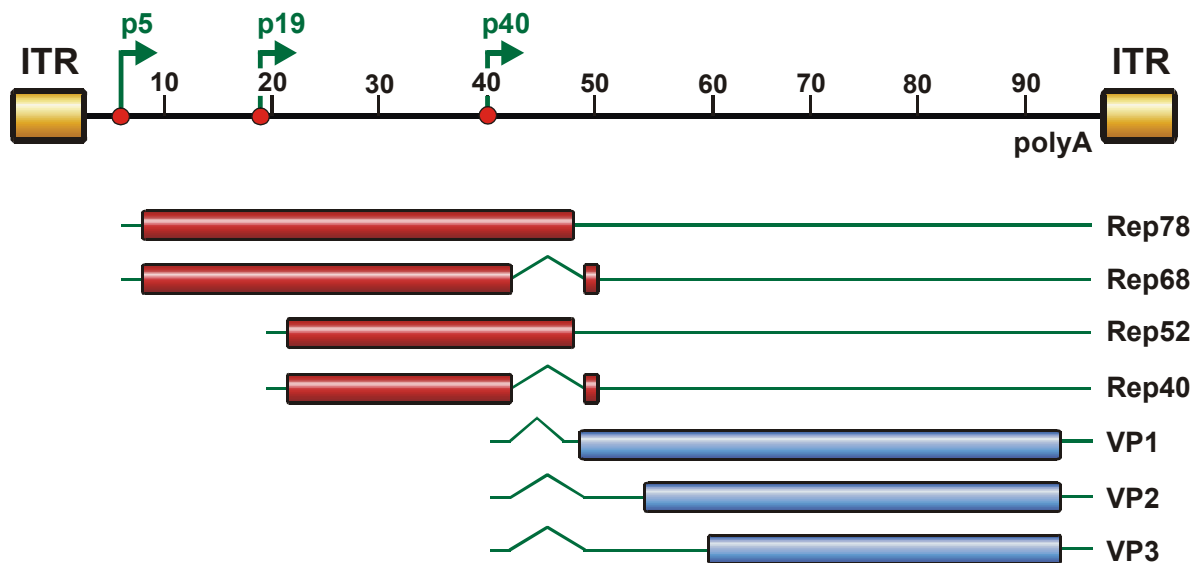
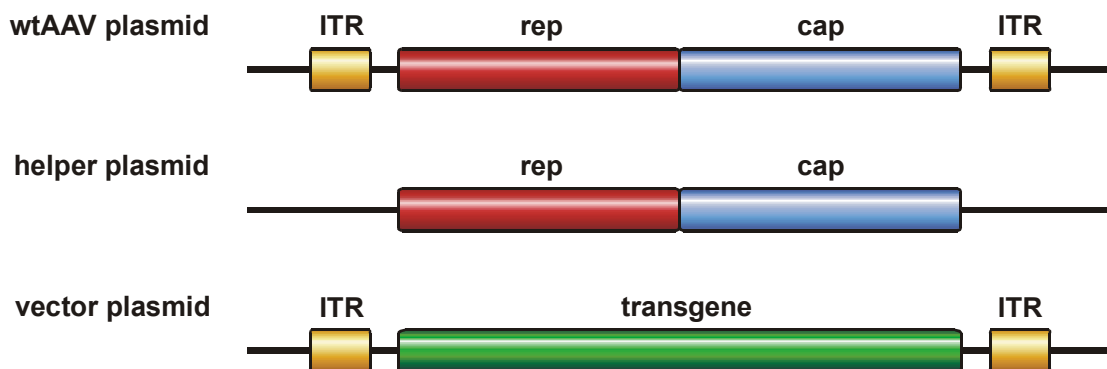


Figure 2. Map of the AAV genome. The AAV genome encompasses 4680 nucleotides, divided into 100 map units. Indicated are the two inverted terminal repeats (ITRs), the three viral promoters at map position 5, 19, and 40 (p5, p19, and p40) and the polyadenylation signal at map position 96 (poly A). The open reading frames are represented by rectangles, untranslated regions by solid lines and the introns by carats. Large Rep proteins (Rep78 and Rep68) under the control of the p5 promoter and small Rep proteins (Rep52 and Rep40) driven by the p19 promoter exist in spliced and unspliced isoforms. The *cap* genes encoding the three different capsid proteins VP1, VP2, and VP3 are under control of the p40 promoter.

2.2 Production of AAV Vectors

For the generation of recombinant AAV vectors (rAAV) *rep* and *cap* are deleted by removing 96% of the genome, leaving only the ITR sequences of the parent virus, which are the solely required *cis* elements for the production of viral particles (replication and packaging). Due to the limited coding capacity of AAV, the removal of all viral genes is, amongst other reasons, required to create space for a heterologous gene, a marker gene (GFP, lacZ) or a therapeutic gene, which is cloned in place of the *rep* and *cap* genes between the ITRs.

For the production of rAAV vectors two different plasmids are needed (Fig. 3A). The “vector plasmid” contains the transgene flanked by the viral ITRs. The two AAV-specific genes required in *trans*, *rep* and *cap*, are cloned onto a “helper plasmid” which does not carry the ITR sequences. These two plasmids are co-transfected together with a third plasmid providing the adenoviral functions necessary for AAV replication (Fig. 3B). Instead of the adenoviral plasmid, co-infection with wild-type Ad is also possible, but this procedure yields AAV preparations that are contaminated with Ad particles. After transcription and translation of the Rep and Cap proteins the ITR flanked transgene cassette from the vector plasmid is replicated, and the single-stranded DNA molecules are encapsidated into preformed AAV capsids (Dubielzig et al. 1999; Samulski et al. 1989). Thereafter viral particles can be harvested and purified, either by gradient centrifugation (CsCl, Iodixanol) and/or column chromatography (Zolotukhin et al. 1999).

A

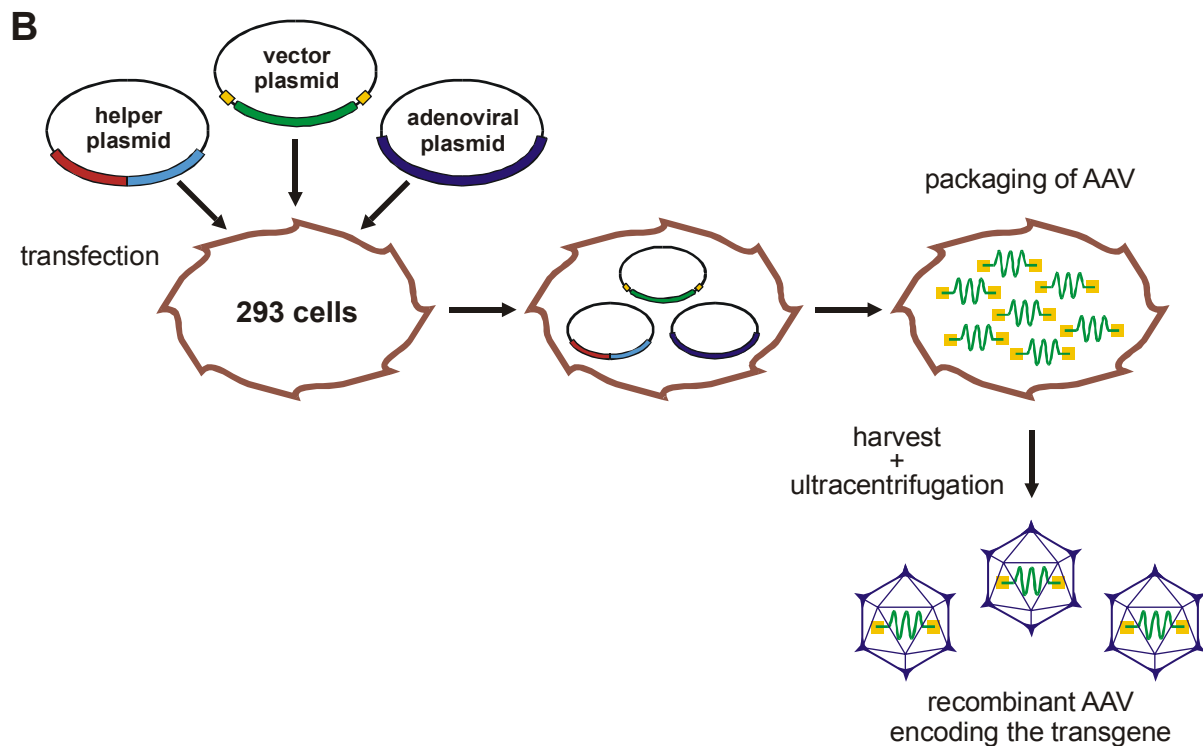


Figure 3. Packaging of AAV. (A) Plasmid constructs used for packaging of rAAV. In contrast to the wild-type AAV-plasmid, which contains the viral *rep* and *cap* gene and the ITRs, the vector plasmid is devoid of all viral genes. Only the ITRs are left which flank the transgene and serve as packaging signal. The helper plasmid provides the regulatory proteins (Rep) and the capsid proteins (Cap) required for replication of the ITR flanked transgene cassette and packaging into preformed capsids. (B) Packaging of AAV. Vector plasmid, helper plasmid, and adenoviral plasmid are transfected into 293 cells. After replication and assembly of viral particles cells are lysed and AAV virions are harvested and purified by iodixanol gradient centrifugation.

2.3 Infection Biology of AAV

The infection pathway of AAV is a multistep process which involves attachment of AAV to the cell surface, binding to the cellular receptors, internalization of the virion, intracellular trafficking, and transport to the nucleus where the viral genome can be replicated and, in the presence of helper functions, synthesis of new viral particles can take place.

A model of the infection process is depicted in figure 4. The first step in this process is the interaction of AAV with its putative primary receptor heparan sulfate proteoglycan (HSPG) that mediates attachment of the virion to the host cell membrane (Summerford & Samulski 1998). Heparan sulfate proteoglycans are widely distributed on the surface of many cell types. This might explain the broad host tropism of AAV. Also two co-receptors have

been suggested so far, $\alpha_v\beta_5$ integrin and fibroblast growth factor receptor 1 (FGFR) (Qing et al. 1999; Summerford et al. 1999). While $\alpha_v\beta_5$ integrin seems to be involved in endocytosis, FGFR is believed to additionally enhance the attachment process. Receptor mediated endocytosis via clathrin-coated pits seems to be the predominant, but not exclusive, pathway for AAV entry, at least in HeLa cells. A possible model postulates that $\alpha_v\beta_5$ integrin clustering facilitates the localization of virus particles to coated pits, similar to adenovirus. In the subsequent internalization process dynamin, a 100 kDa cytosolic GTPase, is involved (Bartlett et al. 2000; Duan et al. 1999; Wang et al. 1998). Specifically, oligomerization of dynamin into a ring structure is required for the formation of clathrin coated vesicles and subsequent pinching of coated pits from the cell membrane (Hinshaw & Schmid 1995; Sever et al. 2000). Additionally, integrin clustering has been shown to activate Rac1, a GTP binding protein, which facilitates internalization. Subsequently, activation of Rac1 leads to activation of PI3K signaling pathways (PI3K, phosphatidylinositol-3 kinase) which are required for efficient trafficking of endosomal vesicles containing virus along microfilaments and microtubules to the nucleus (Sanlioglu et al. 2000).

In contrast to its natural helper virus, adenovirus, AAV particles seem to be delivered to the late endosome before they are released into the cytoplasm (Douar et al. 2001). The maturation of endosomes involves a progressive decrease of their internal pH. This acidic milieu may trigger conformational changes of the viral capsid, exposing domains which disrupt the endosomal membrane. Interestingly, the unique region of the AAV VP1 protein contains a phospholipase A₂ (PLA₂) motif (HDXXY) which is conserved among parvoviruses (Girod et al. 2002; Zadori et al. 2001). It can be speculated that externalization of this domain would expose the PLA₂ group together with other functions located in the VP1 unique region (DNA binding, nuclear localization) which may be required for endosome exit and transfer of the viral genome to the nucleus. Notably, a significant proportion of viral particles can be degraded by the proteasome before they reach the nuclear compartment (Douar et al. 2001).

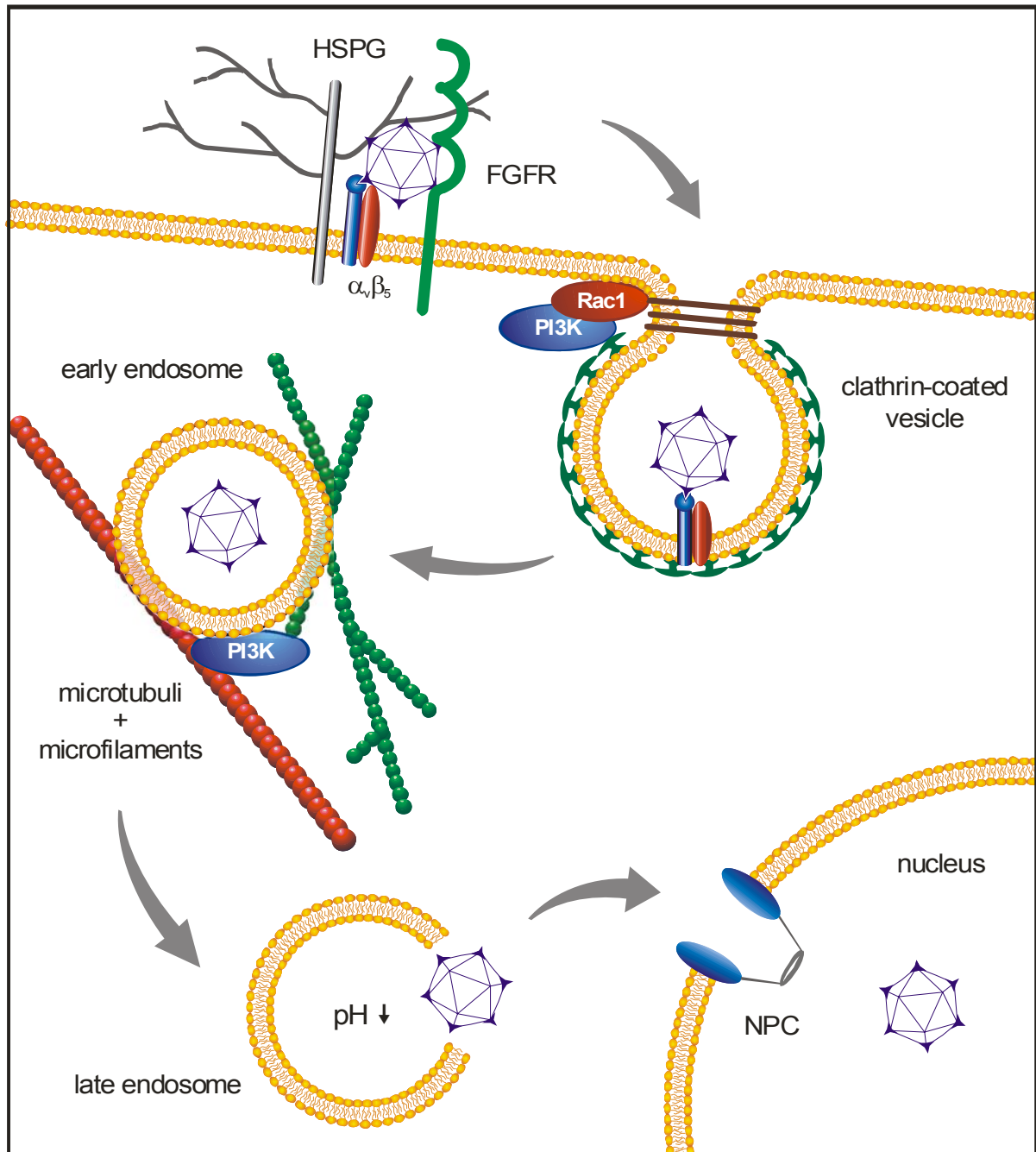


Figure 4. The AAV infection pathway. After binding to its primary attachment receptor HSPG and co-receptors FGFR and $\alpha_v\beta_5$ integrin AAV is internalized by receptor-mediated endocytosis in a dynamin dependent manner into clathrin coated pits. This internalization is facilitated by the action of Rac1. Activation of Rac1 subsequently stimulates PI3K pathways which regulate endosome trafficking along the cytoskeleton. After transition to the late endosomal compartment AAV is released into the cytoplasm and enters the nucleus by an unknown mechanism.

Relatively little is known about how the virus enters the nucleus and where viral uncoating occurs. Several studies have observed a perinuclear accumulation and subsequent

slow nuclear entry of fluorescent labeled viral particles (Bartlett et al. 2000; Sanlioglu et al. 2000). In contrast, Seisenberger and coworkers (2001) observed by single molecule imaging a very quick transfer of viral particles, within minutes, to the nuclear area. Whether viral particles localized in the nucleus are partially uncoated or otherwise modified remains unclear in all studies. However, all cellular factors required for uncoating and second-strand synthesis are contained within the nucleus and transport across the nuclear envelope itself seems not to depend on active transport through nuclear pore complexes (NPC) (Hansen et al. 2001).

In the course of a productive infection, replication of the AAV genome proceeds via a self-priming strand displacement mechanism in which the two large Rep proteins, Rep78 and Rep68, play an essential role (for review see Muzyczka & Berns 2001). At early stages of virus production, capsid assembly and viral DNA replication are found at distinct sites within the cell nucleus. Assembly of empty capsids seems to take place in the nucleolus, whereas DNA replication and the subsequent encapsidation of the viral genome takes place in the nucleoplasm (Wistuba et al. 1997; Wistuba et al. 1995). During this assembly process, first complexes are formed between empty capsids and large Rep-bound AAV genomes mediated by the interaction of large and small Rep proteins with one another and empty capsids (Dubielzig et al. 1999). Then helicase activity of capsid-immobilized Rep52 and Rep40 drives the translocation of single-stranded AAV genomes into the preformed capsids (King et al. 2001). Both positive and negative strands of the viral genome are separately encapsidated in AAV virions (Mayor et al. 1969).

2.4 The Structure of the AAV Capsid

Recently the atomic structure of AAV has been determined to 3 Å resolution by x-ray crystallography (Xie et al. 2002) (Fig. 5). It was the first structure of a dependovirus to be determined. While the atomic structures of related autonomous parvoviruses, including canine parvovirus (CPV), feline panleukopenia virus (FPV), minute virus of mice (MVM), Aleutian mink disease virus (ADV), and the human parvovirus B19, have been resolved during the past decade, the three-dimensional structure of the AAV capsid remained unknown (Agbandje et al. 1994; Agbandje-McKenna et al. 1998; Chang et al. 1992; Chapman & Rossmann 1993; Chipman et al. 1996; McKenna et al. 1999; Strassheim et al. 1994; Tsao et al. 1991). Instead, alignments of these related parvoviruses with AAV had led to hypothetical models of the AAV capsid. Random and systematic mutagenesis approaches helped to identify functional

sites on the capsid, including putative binding sites for the primary receptor HSPG, immunogenic epitopes and flexible loop regions at the capsid surface that accept the insertion of targeting ligands (Girod et al. 1999; Rabinowitz et al. 1999; Wobus et al. 2000; Wu et al. 2000). Now that the three-dimensional structure has been resolved, function can be mapped to the structure.

Striking similarities but also notable differences exist between AAV and related autonomous parvoviruses. Each viral capsid is composed of 60 subunits arranged with T=1 icosahedral symmetry (Xie et al. 2002). The three structural proteins VP1, VP2, and VP3, which share overlapping sequences and differ only at their N-termini, build the AAV capsid with a relative stoichiometry of about 1:1:8 (Kronenberg et al. 2001). The central motif of each subunit is an anti-parallel β -barrel which is highly conserved among parvoviruses (Fig. 5A). This β -barrel motif forms elongated smooth lumps at the inner surface of the capsid at the 2-fold symmetry axis (Kronenberg et al. 2001). Between the strands of the β -barrel core large loop insertions are found that share only low similarity among the parvovirus family. These loops comprise two-thirds of the capsid structure and constitute the capsid surface features that interact with antibodies and cellular receptors. These surface features include a hollow cylinder at the 5-fold axis of symmetry which is surrounded by a circular depression (canyon), and a depression spanning the 2-fold axis (dimple) (Fig. 5B). The most prominent features of the capsid are the 3-fold-proximal peaks, which cluster around the 3-fold symmetry axis. The peaks are not derived from one capsid subunit protein but from the interaction of two adjacent subunits. The sequences that compose these structures belong to the GH loop (between the β -sheets G and H) which, with approximately 220 amino acids, is the longest loop insertion. Other interactions between loops of neighboring subunits are found at the 5-fold cylinder, where amino acids from the HI loop interact with residues from the BC and EF loop. Overall, the outside surface of AAV is positively charged with clusters of positive charges in the canyon, surrounding the 5-fold cylinder, and at the 3-fold symmetry axis. Regions of negative charges are mainly found at the top of the 5-fold cylinder and at the sides of the 2-fold dimple facing the 3-fold axes (Fig. 5B and C). The N-terminal unique regions of VP1 and VP2 could not be resolved by x-ray crystallography, because of low electron density. Kronenberg and coworkers (2001), who performed cryo-electron microscopy assumed that globular structures at the inner surface of the capsid at the 2-fold axes of symmetry, which are attached to the smooth lumps, represent the positions for the N-terminal extensions of VP1 and VP2.

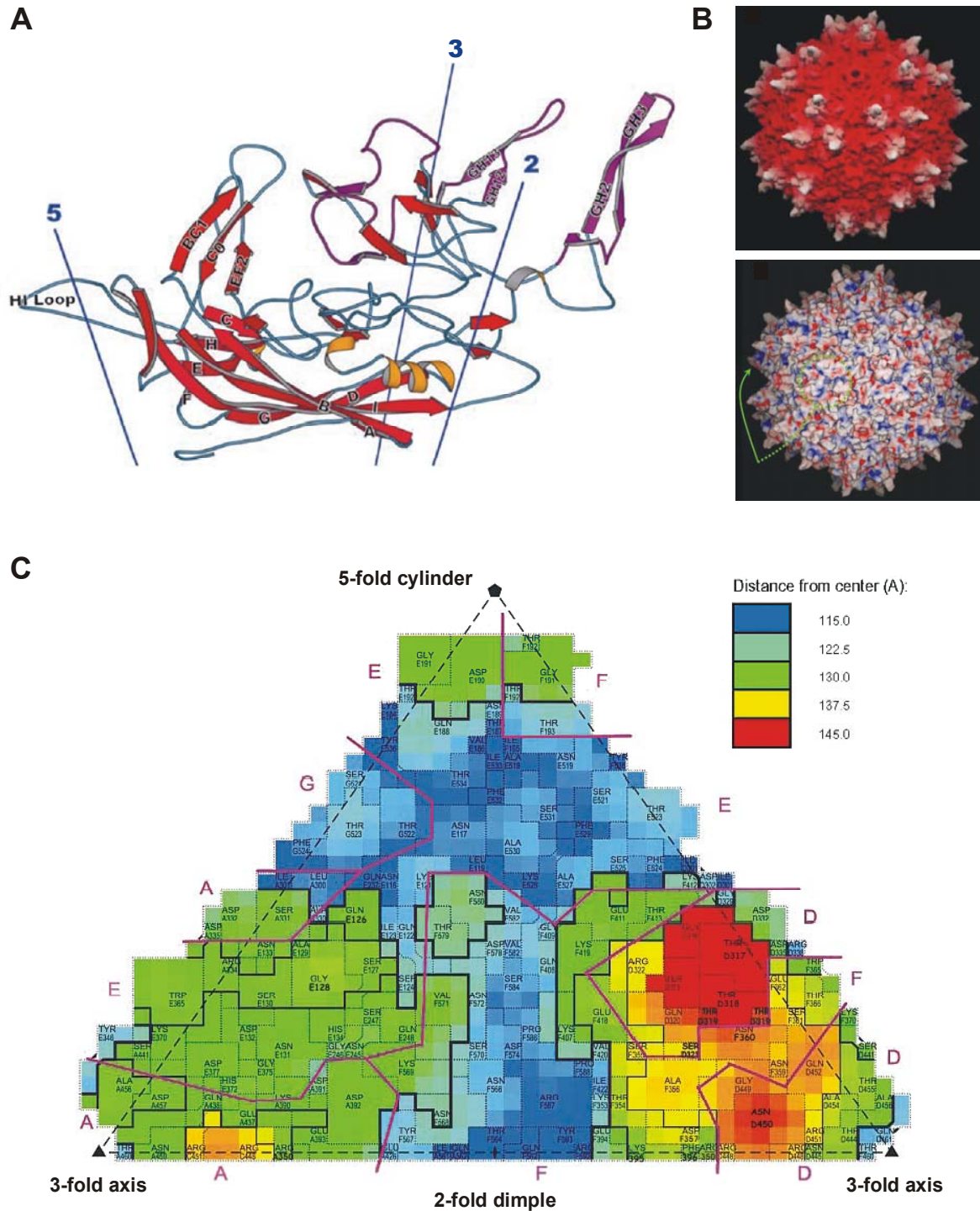


Figure 5. The structure of the AAV capsid (images taken from Xie et al. 2002). (A) Ribbon drawing of a VP3 protein. The position of the 2-fold, 3-fold, and 5-fold axis is indicated. The β -barrel core comprising two anti-parallel β -sheets (strands A to I) is on the inner surface of the capsid. The inter-strand loops are labeled according to the flanking strands. (B) Surface topology (top row) and electrostatic surface potential (bottom row) of the AAV capsid. Red colors indicate clusters of negative charges and blue colors indicate positive charges. The view is down the 2-fold symmetry axis. (C) One of the 60 triangular asymmetric subunits showing the surface amino acids of the capsid. The amino acids are numbered according to VP2.

After resolution of the crystal structure of AAV important functions obtained from genetic data could be mapped to the structure. At the 3-fold-proximal peaks, in the valleys separating the three peaks of one 3-fold axis, clusters of positive charges are located, which are implicated in receptor binding. Although no definitive HSPG binding motif has been found on the capsid surface so far, mutational analyses have identified these locations being involved in binding to the primary receptor HSPG (Wu et al. 2000). Especially the basic amino acids (aa) R487 (R350), R585 (R448), R588 (R451) and H509 (H372), which are at the side of the peak, seem to play a crucial role (numbers in parentheses refer to VP2 numbering) (Fig. 5C) (Grifman et al. 2001; Wu et al. 2000; Xie et al. 2002). Interestingly, the separation between these clusters at the side of the peaks is 20 Å, consistent with binding neighboring disaccharides of the heparan sulfate moiety. These findings are supported by the fact that the neutralizing monoclonal antibody C37-B which inhibits binding of AAV to the host cell has its epitope adjacent to these residues in the three-dimensional structure, namely between aa 492 and 503 (corresponds to aa 355-366 in VP2 numbering) at the shoulder of a peak (Wobus et al. 2000). The epitope of another neutralizing antibody, A20, could also be mapped to the 3-fold spike region. It is situated in the valley between the peaks of one 3-fold axis (Wobus et al. 2000). In contrast to C37-B, A20 does not block receptor binding but neutralizes AAV infection at a post-binding step, possibly by interfering with internalization, endosomal release or viral uncoating (Smith 2001). These data implicate the 3-fold proximal peaks not only in receptor binding, but also show their possible role in recognition by the host immune system. Moreover, it is supposable that other important viral functions are additionally located at this prominent feature.

2.5 The AAV Rep Proteins and their Role in Site-Specific Integration

Adeno-associated viruses utilize a biphasic life cycle to persist in nature. In the presence of helper virus, adenovirus or herpesvirus, wtAAV undergoes a productive infection. Lacking a helper virus, the virion latently infects by integrating into the host genome. This integration occurs in 70% at a specific locus in the q arm of human chromosome 19 within 19q13.4 termed AAVS1 (Giraud et al. 1994; Kotin et al. 1992; Kotin et al. 1990; Samulski et al. 1991). Recently this AAV integration site has been identified to lie within a muscle-specific DNA region of the human genome (Dutheil et al. 2000).

The only viral *cis* elements required for site-specific integration are the ITRs, or at least partial ITR-like sequences. The ITRs contain a Rep binding site (RBS) and a specific cleavage site for the large Rep proteins (TRS) which seem to play an essential role for this integration process (Xiao et al. 1997b). Additionally, targeted integration depends on the large Rep proteins, Rep78 and/or Rep68, which can be provided in *trans* (Balague et al. 1997; Huttner et al. 2003; Surosky et al. 1997). Mutational analysis of Rep78 and Rep68 indicated that sequence specific DNA binding, site-specific endonuclease activity, and helicase activity are essential for site-specific recombination (Linden et al. 1996a; Urabe et al. 1999). On the host chromosomal side a 33 bp region within the AAVS1 has been identified as the minimal requirement for the targeted integration process. Interestingly, the AAVS1 also comprises a RBS and an abbreviated version of the TRS which are essential to target integration to AAVS1 (Giraud et al. 1994; Giraud et al. 1995; Linden et al. 1996a; Linden et al. 1996b). Recently, a spacer sequence containing either a GCTC motif or two CTC triplets embedded in a pyrimidine-rich sequence has been determined to be the third requisite necessary for specific integration (Meneses et al. 2000). The specific combination of these three parameters seems to be unique to AAVS1 within the human chromosome which would explain the specificity of the integration process.

The exact mechanism of the integration process, however, is still unclear. Several models have been proposed:

- One current model for targeted integration proposes that Rep68/78 binds as a hexamer to the RBS motifs on the chromosomal DNA and the viral DNA and thereby positions the incoming infecting genome at AAVS1 (Weitzman et al. 1994). This represents a Rep protein mediated alignment of the recombination partners AAV and AAVS1, initiating the non-homologous recombination event observed. Then a nick is introduced by Rep68/78 at the TRS in AAVS1, and DNA synthesis is initiated following a single-strand displacement mechanism involving the cellular polymerase complex. As DNA synthesis at the AAVS1 proceeds, a series of DNA template switches (copy choice) links the viral DNA to the chromosomal DNA (Brister & Muzyczka 2000; Chiorini et al. 1996; Linden et al. 1996a; Linden et al. 1996b). This model has been referred to as copy-choice model.
- A second, more recent model supposes a cleavage-ligation mechanism for targeted integration which does not imply template strand switching. Smith and colleagues demonstrated that the large Rep proteins not only possess sequence specific binding

and nicking activity but also have the ability to catalyze the ligation of single-stranded AAV *ori* DNA. They proposed that Rep68/78 may mediate recombination between an AAV replication intermediate, which might have been generated after limited Rep expression during latent infection, and the chromosomal AAVS1 locus by a strand cleavage and exchange mechanism (Smith & Kotin 2000).

Very often site-specific integration seems to be accompanied by rearrangements of the viral genome and the AAVS1 locus (Giraud et al. 1995; Kotin & Berns 1989; Kotin et al. 1992; McLaughlin et al. 1988; Surosky et al. 1997). These rearrangements include deletions of AAV sequences and the disruption of the preintegration site. Recombination junctions are clustered near the RBS of the AAVS1 target locus and within the ITR or the p5 promoter in AAV. In most latently infected cell lines the viral DNA is integrated as head-to-tail concatamer (Cheung et al. 1980; Laughlin et al. 1986; McLaughlin et al. 1988), but also inverted tandem arrays (head-to-head, tail-to-tail) have been observed (Kotin & Berns 1989). For rescue of AAV from the latent state after helper virus co-infection at least one intact ITR is required. Interestingly, one ITR copy between integrated tandems is normally found to be intact after integration. Therefore rescue was only observed when AAV had integrated as concatamer and not after monomer integration because of substantial rearrangements and deletions in the ITR sequences.

As recombinant AAV (rAAV) vectors are devoid of all viral genes, they have lost the ability of targeted integration. rAAV vectors can still integrate through the ITR sequences, but at a lower frequency and only randomly into the host genome. One challenge for human gene therapy is to restore the ability of targeted integration of rAAV and to design specifically integrating vector systems. This is especially of importance with respect to a safe transfer system that avoids the risk of insertional mutagenesis because of random integration as it is the case for retroviral vectors.

2.6 Immune Response against AAV

An obstacle for the application of AAV as a gene therapy tool is the preexisting immunity against the virus. Generally humoral and cellular immune responses against viral gene therapy vectors can limit sustained transgene expression and their potential readministration. As rAAVs are deleted of all viral genes, these vectors are believed to be relatively non-immunogenic which may contribute to the prolonged expression observed after AAV

transduction in animal studies. However, several studies have determined a high prevalence of serum antibodies (Ab) against the AAV capsid in the human population. They could show that between 30 and 96% are positive for AAV specific Ab and 18 to 67.5% of them have additionally neutralizing antibodies, depending on age and ethnic group (Blacklow et al. 1968b; Chirmule et al. 1999; Erles et al. 1999; Moskalenko et al. 2000). These neutralizing Ab can cause considerable problems, especially when readministration of the vector is required. In animal experiments, neutralizing Ab have been shown to eliminate (Fisher et al. 1997; Xiao et al. 1996) or greatly reduce (Chirmule et al. 2000; Xiao et al. 2000) the levels of transgene expression after readministration of the vector. Responsible for this block of readministration seems to be a humoral response associated with a T-cell dependent B-cell activation against the virion but not the transgene as seen with other viral vectors (Chirmule et al. 2000; Hernandez et al. 1999). Several studies have shown that transient immunosuppression (anti-CD40-ligand Ab and CTLA4, anti CD4) during the first administration helps to prevent generation of neutralizing Ab and allows readministration of a rAAV vector (Chirmule et al. 1999; Halbert et al. 1998; Manning et al. 1998). Acute inflammation due to activation of the innate immune system, i.e. neutrophils, natural killer cells, macrophages, and expression of chemokines and cytokines which has been strongly observed for Ad does not seem to take place after AAV transduction or is only very short lived (Zaiss et al. 2002). Therefore, AAV vectors seem to have markedly reduced inflammatory properties.

For many viral vectors, e.g. adenovirus, a strong cellular immune response against the vector and the delivered transgene, which can cause severe complications for the treated patient, has been observed, as was probably the case for Jesse Gelsinger, who died in a Phase I gene therapy trial after application of an adenoviral vector (for further information see Teichler Zallen 2000). In contrast, after *in vivo* gene transfer by rAAV vectors, apparently no evidence for a cellular immune response to the transgene product has been reported (Chirmule et al. 1999; Hernandez et al. 1999; Jooss et al. 1998). This may be due to the fact that rAAV fails to infect mature dendritic cells capable of stimulating antigen-specific T-cell responses and therefore presentation of neoantigen might be inefficient (Jooss et al. 1998). One study described *in vitro* transduction of immature dendritic cells by AAV which initiated subsequently a CD40-ligand dependent T-cell response to transduced cells (Zhang et al. 2000). The role of such immature dendritic cells for eliciting a cellular immune response after AAV transduction *in vivo* has to be further elucidated. All these observations point towards a

humoral response against the AAV capsid being the major immune response in animal studies, while a cellular immune response to the virion or the delivered gene product is rare. Some exceptions, however, have been observed in animal studies. Generation of cytotoxic T-lymphocytes (CTL) and upregulation of major histocompatibility complex (MHC) class I molecules was reported after i.m. application of rAAV coding for β -galactosidase (Yuasa et al. 2002). In other studies a humoral and cell mediated immune response to AAV vectors expressing foreign viral proteins, i.e. herpes simplex virus glycoproteins or influenza virus hemagglutinin, and foreign secreted protein, has been described (Brockstedt et al. 1999; Manning et al. 1997; Sarukhan et al. 2001). However, one should note that these studies intended to exploit AAV for vaccination and therefore an immune response against the transgene was desired in these studies.

The conflicting data presented by several studies indicate that the CTL as well as the humoral response to the delivered gene depends on a number of variables, including the nature of the transgene, the route and site of injection, the age, health and immunological background of the subject, the degree of contamination with helper virus proteins, and even the maturation state of antigen presenting cells exposed to rAAV administration. This implies the need for a better understanding of the immune response against AAV. Moreover, new strategies to circumvent neutralization by antibodies and to overcome the limitations of a potential humoral and cellular immune response have to be developed.

3 AAV as Gene Therapy Vector: Pros and Cons

AAV has received a significant amount of interest as a potential vector for gene therapy. There are a number of characteristics that contribute to the potential utility of the virus for this purpose.

- rAAV vectors can efficiently transduce a wide variety of dividing and also non-dividing, terminally differentiated tissues *in vivo* including cells of the central nervous system, eye, muscle, liver, lung, and hematopoietic system (Fisher et al. 1997; Fisher-Adams et al. 1996; Flannery et al. 1997; Flotte et al. 1993; Kaplitt et al. 1994; Snyder et al. 1997).

- The vector genome persists for extended periods (up to 2 years in muscle, brain, liver, and eye of rodents) with no apparent decrease in expression (McCown et al. 1996; Snyder et al. 1999; Xiao et al. 1996).
- No inflammatory response is generated by *in vivo* injections of the vector which is in part the reason for the long term gene expression. The CTL response also appears to be lower than that seen with most other viral vectors, as well as the humoral immune response to the transgene product. This may be due in part to the absence of viral genes in the vector, and to the observation that AAV only inefficiently infects antigen-presenting cells like dendritic cells (Jooss et al. 1998).
- No apparent pathogenicity has been contributed by AAV so far (Berns & Linden 1995; Blacklow 1988; Blacklow et al. 1968b; Blacklow et al. 1971), which argues for the safety of this vector system. What has to be clarified, nevertheless, is the potential germ-line transduction which was described after acute wtAAV infection (Burguete et al. 1999; Erles et al. 2001).
- AAV vectors have the potential to specifically integrate into the host genome. This would minimize the risk of insertional mutagenesis, a problem that afflicts retroviral vectors (development of a leukemia-like blood disorder after treatment of X-linked severe combined immunodeficiency by a retroviral vector in October 2002, see Hacein-Bey-Abina et al. 2003). Additionally, readministration of the vector would be redundant. Currently available rAAV vectors, however, have lost this favorable characteristic due to the lack of the viral *rep* gene.

The rAAV vector system has also suffered from several disadvantages, some of which have now been addressed.

- The broad host tropism, initially considered as an advantage, has now turned out to be a disadvantage. Specific and selective transduction of the target tissue is highly desirable for *in vivo* gene therapy. This is not only important because of safety aspects but would also help to reduce the amount of delivered virus particles. First steps towards specific re-targeting vectors have been done but require further improvements (Bartlett et al. 1999; Girod et al. 1999; Nicklin et al. 2001).
- The coding capacity of AAV is a limiting factor for some transgene-promoter combinations. The optimal size for AAV vectors lies between 4.1. and 4.9 kb (Dong et al.

1996). Recent publications demonstrated that this problem can be overcome by the use of split genes that are cloned into two separate vectors (Duan et al. 2000; Nakai et al. 2000; Sun et al. 2000; Yan et al. 2000). These are expressed *in vivo* from head-to-tail concatamers of the vector with the use of appropriate splice signals. Still, a drawback in this strategy is the requirement for double transduction of the cell with complementing vectors and the low transduction efficiencies.

- A delayed onset of transgene expression (4 to 6 weeks after injection) has been observed in most animal experiments and represents a problem for acute clinical applications. Publications have shown that second-strand synthesis may be the rate limiting step for *in vivo* expression (Ferrari et al. 1996; Fisher et al. 1996). Furthermore, they demonstrated that helper virus and genotoxic stress not only help wtAAV to initiate productive infection, but also enhance rAAV transduction. Self-complementary rAAV vectors containing double-stranded replication intermediates could be a means towards overcoming this limitation (McCarty et al. 2001).
- The high prevalence of antibodies against the viral capsid and especially neutralizing antibodies represents a further hurdle for *in vivo* gene therapy. Several groups demonstrated that neutralizing antibodies can reduce or even eliminate transgene expression, which would make a readministration but also an initial therapy in many cases impossible (see above). Therefore, the development of rAAV vectors with the potential to escape the humoral response is crucial.

Despite the potential drawbacks, rAAV vectors have proven to be a useful tool for many applications in gene therapy, some of which will be given here as examples. Several publications have demonstrated efficient transduction of the brain with rAAV in animal models and have explored the possibility of rAAV mediated therapy of Alzheimer's (delivery of GABA receptor antisense constructs) and Parkinson's disease (delivery of enzymes for dopamine synthesis) (Kaplitt et al. 1994; Klein et al. 1998; Mandel et al. 1997; Xiao et al. 1997a). Other possible applications are inherited retinopathies. Mainly two groups have shown efficient photoreceptor-targeted gene transfer and functional recovery of photoreceptors after subretinal injections of AAV vectors in transgenic rodents (Flannery et al. 1997; Jomary et al. 1997; Lewin et al. 1998). Skeletal muscles and liver transduction with rAAV have been used as platforms for the secretion of several factors which are absent or reduced in certain diseases, including factor IX in hemophilia B (Kay et al. 2000; Snyder et

al. 1999; Wang et al. 1999), leptin for therapy of genetic obesity and noninsulin-dependent diabetes mellitus (Murphy et al. 1997), and erythropoietin (Kessler et al. 1996; Zhou et al. 1998). Attempts to develop gene therapy for Duchenne muscular dystrophy have been complicated by the enormous size of the dystrophin gene. Harper et al. (2002) recently generated functional mini- and micro-dystrophins that could be efficiently packaged into AAV virions and demonstrated efficient transfer in mice. The development of AAV vectors for gene therapy of lung diseases, focusing on cystic fibrosis also seems to be very promising. Flotte et al. (1993) were among the first to demonstrate successful and stable *in vivo* gene transfer to the airway epithelium with an AAV vector expressing the cystic fibrosis transmembrane conductance regulator cDNA. Actually, most clinical trials involving AAV vectors deal with the treatment of cystic fibrosis (Griesenbach et al. 2002). Finally, several studies demonstrated the potential of AAV in cancer gene therapy. Currently, various approaches are being used for the therapy of malignancies, including the delivery of a combination of genes and prodrugs that exhibit cytotoxicity on tumor cells, modulation of oncogenes and tumor suppressor genes, inhibition of tumor vascularization and enhancement of the host immunity against tumor cells. Interestingly, AAV itself seems to have antitumor properties which were initially attributed to the down-regulation of proto-oncogene promoters by the large Rep proteins and induction of cell cycle arrest (Hermonat 1994; Saudan et al. 2000). The nature of the single-stranded AAV genome also seems to be tumor protective by inducing apoptosis in cells lacking active p53, an important tumor suppressor found to be switched off in many human cancers (Raj et al. 2001). Moreover, rAAV vectors have proven their potential in various cancer gene therapy approaches, e.g. cancer immunotherapy using cytokines and co-stimulatory molecules to induce an antitumor T-cell response (Anderson et al. 1997; Chiorini et al. 1995; Wendtner et al. 2002), and transfer of antiangiogenic molecules to inhibit growth of tumor neovasculature (Nguyen et al. 1998).

Overall, adeno-associated viruses are very promising gene transfer vehicles for treatment of multiple diseases. The increasing interest in AAV as vector system and the rising amount of gene therapy trials which are currently under investigation argue for its potential as human gene therapy vector. Hurdles, however, still exist and have to be overcome, including specific and selective transduction of the target tissue, potential immune response to the vector and/or transgene, and loss of specific integration of recombinant AAV vectors. Some of these limitations have been addressed in the studies presented here: the requirements for targeted integration of recombinant vectors were investigated and an AAV vector construct

with the potential for site-specific integration was developed. Antigenic determinants of the AAV capsid were characterized in binding studies with human serum samples. Moreover, an AAV capsid mutant with the ability to escape neutralization by human antisera was identified. These results represent further steps towards an improved generation of AAV vectors for human gene therapy.

CHAPTER II

Analysis of site-specific transgene integration following co-transduction with recombinant adeno-associated virus and a Rep encoding plasmid

published as:

Huttner NA, Girod A, Schnittger S, Schoch C, Hallek M, and Büning H. (2003)

Analysis of site-specific transgene integration following co-transduction with recombinant adeno-associated virus and a Rep encoding plasmid. *J Gene Med* **5**: 120-129.

Abstract

Background. Recombinant adeno-associated virus (rAAV) has many advantages for gene therapeutic applications in comparison to other vector systems. One of the most promising features is the ability of wild-type (wt) AAV to integrate site-specifically into human chromosome 19. However, this feature is lost in rAAV vectors due to the removal of the Rep coding sequences.

Methods. HeLa cells were transfected with a Rep expression plasmid, infected by rAAV and grown with or without selection pressure. Single cell clones were generated and genomic DNA was analyzed for site-specific integration by Southern blotting analysis and fluorescence *in situ* hybridization (FISH).

Results. Transfection of HeLa cells with a Rep expression plasmid followed by the transduction with a rAAV vector resulted in site-specific integration of the transgene at AAVS1 on human chromosome 19 in 7 of 10 cell clones analyzed. In marked contrast, transduction of cells with rAAV alone did not result in any site-specific integration of the transgene.

Conclusions. The high frequency with which the site-specific integration took place in the presence of Rep protein is comparable to the results observed with wtAAV. These results offer opportunities for the development of specifically integrating rAAV vectors.

Introduction

The development of safe, stable and efficient gene transfer vehicles is one of the most critical steps for the success of gene therapy. One of the most promising vectors is derived from the adeno-associated virus type 2 (AAV), a member of the parvovirus family. AAV has many advantages in comparison to other vector systems, e.g. its ability to transduce both dividing and non-dividing cells, its low immunogenicity and the apparent lack of pathogenicity. One of the most encouraging features of AAV is its ability to integrate site-specifically into the distal portion of the q arm of human chromosome 19. For this integration step only two viral elements are necessary, namely, the Rep proteins and the inverted terminal repeats (ITR) (Giraud et al. 1994; Kotin et al. 1992; Kotin et al. 1990; Lamartina et al. 2000; Samulski et al. 1987).

The viral genome is a single stranded DNA of 4.7 kb, containing the palindromic ITR sequences at both ends. These ITRs are not only required for the integration process, but serve also as origin of replication, are required for rescue of the provirus after integration and for encapsidation of the viral genome. In between these ITR structures two open reading frames, *rep* and *cap*, are found. *rep* encodes four overlapping, multifunctional proteins (Rep78, Rep68, Rep52 and Rep40) controlled by two different promoters (Balague et al. 1997). The transcription of the large Rep proteins (Rep78 and its splice variant Rep68) is controlled by the p5 promoter. They are necessary for viral DNA replication, transcriptional control and site-specific integration. Rep52 and its splice variant Rep40 are known as small Rep proteins. They are transcribed from the p19 promoter and play an essential role in the accumulation of single-stranded progeny genomes used for packaging. The 3' ORF *cap* accommodates the three capsid proteins VP1, VP2 and VP3. They are transcribed from the p40 promoter and form the viral capsid, which is an icosahedron of 20 to 25 nm in diameter.

After entry into the cell AAV depends on a helper virus, such as adenovirus or herpesvirus, for efficient replication and reproduction. In the absence of the helper virus, AAV latently infects cells by integrating into the host genome. In most cases (70-80%) this integration was found at AAVS1 (Kotin et al. 1990; Shelling & Smith 1994), which is located in the human chromosome 19 within 19q13.4 (Dutheil et al. 2000). Subsequent super infection of AAV latently infected cells with the helper virus results in the rescue of the provirus, in the replication of the AAV genome and the production of new viral particles (Kotin 1994).

The ability to integrate site-specifically into a distinct region of the human genome, resulting in stable and efficient gene expression without adverse effects on the host cell, would be an ideal situation for the development of viral vectors designed for long-term gene expression in human cells. However, commonly used rAAV vectors do not target to AAVS1, because they do not express the *rep* genes (Flotte & Carter 1995; Linden et al. 1996a). As it is known that supplying the Rep protein *in trans* can help to overcome this limitation (Surosky et al. 1997), we wanted to define the conditions and develop appropriate methods for the analysis of site-specific transgene integration following transduction with rAAV vectors *in vitro*.

Materials and Methods

Plasmids. The pRC plasmid was constructed as previously described (Girod et al. 1999). Briefly, the 4.5 kb Xba I-fragment of psub201(+)(Samulski et al. 1987), containing the *rep* and *cap* ORFs of AAV was subcloned into the Pst I and BamH I sites of pSV40oriAAV (Chiorini et al. 1995). The pGFP plasmid is an AAV-based vector plasmid in which the AAV ITR sequences are flanking the hygromycin selectable marker gene controlled by the thymidine kinase promoter and the *Aequorea victoria* Green Fluorescence Protein (GFP) gene regulated by the cytomegalovirus promoter. pGFP was generated by inserting the Asp718-Not I fragment of pEGFP-N1 (Clontech) into the Asp718-Not I sites of psub/CEP4(Sal invers). psub/Cep4(Sal invers) is a derivative of psub201(+) (Samulski et al. 1987), which was digested with Xba I, blunt ended and ligated to blunt ended 3923 bp Sal I-Nru I-Fragment of pCEP4(Sal inverse). pCEP4(Sal inverse) differs from pCEP4 (Invitrogen) by inversion of the Sal I (8)-Sal I (1316)-fragment.

Cell culture. The human cervix epitheloid carcinoma cell line HeLa (ATCC CCL 2; American Type Culture Collection, Rockville, Maryland) was maintained as monolayer culture at 37°C and 5% CO₂ in Dulbecco's modified Eagle's medium (DMEM), supplemented with 10% fetal calf serum (FCS), 100 U/ml penicillin, 100 mg/ml streptomycin and 2 mM L-glutamine.

Production of rAAV vector particles. The rAAV vectors were generated as described (Girod et al. 1999). Briefly, HeLa cells were seeded at 10% confluency in 15 cm dishes and transfected with 17.5 µg of vector plasmid pGFP and 17.5 µg of helper plasmid pRC by adding a 1:1 mixture of 2x BBS (50 mM BES (N,N-bis(2-hydroxyethyl)-2-aminoethanesulfonic acid), pH 6.95, containing 280 mM NaCl, 0.75 mM Na₂HPO₄ and 0.75 mM NaH₂PO₄) and 260 mM CaCl₂ and subsequently incubated 18-22 hours at 35°C and 3% CO₂. At 48 hours after transfection, cells were incubated with adenovirus type 5 (MOI 5) for 1 hour in 10 ml of serum-free medium and then supplemented with 10 ml of medium containing 20% FCS. At 72 hrs after adenovirus type 5 infection the rAAV vector particles were purified and concentrated by two cycles of ultracentrifugation on CsCl gradients ($\rho = 1.4$ g/ml) as described (Chiorini et al. 1995). After dialysis against 1x PBS the concentration of DNA containing viral particles and of transducing rAAV viral particles was determined by standard procedures (Girod et al. 1999).

Immunofluorescence assay. HeLa cells were seeded at 10% confluency on slides in 15 cm dishes and transfected with 35 µg of helper plasmid pRC as described for the rAAV vector production. 12, 24, 36 and 45 hours after transfection Rep protein synthesis was analyzed in an immunofluorescence assay (Wistuba et al. 1997). As a control, HeLa cells were infected with wtAAV (MOI 3) in an adenovirus type 5 (MOI 5) containing medium, incubated for 16 hours and then analyzed for Rep expression.

Cotransfection. 1.5×10^5 HeLa cells were seeded in 6-well-plates and transfected with the 2.5 µg pRC as described for rAAV vector production. After 24 hours, the cells were infected with rAAV-GFP/Hygro at a MOI 4. One part of the cotransfected cells was grown in the presence of hygromycin (350 µg/ml), whereas the other part was cultivated without selection pressure. As a control, HeLa cells were only infected with rAAV-

GFP/Hygro and not transfected with pRC, and treated in the same manner. Single cell clones were generated from the GFP expressing cells by limiting dilution and cultivated for Southern blot and FISH analysis.

Southern blot analysis. Genomic DNA was isolated by standard methods. Briefly, cells were harvested, lysed with 1% Sarcosyl in 75 mM Tris-HCl, pH 8.0, 25 mM EDTA and incubated with Proteinase K (100 µg/ml) at 50°C overnight. After phenol/chloroform extraction RNA was removed by incubation with RNase (100 µg/ml). The genomic DNA solution was dialyzed against TE buffer (10 mM Tris-HCl pH 7.5, 1 mM EDTA) and digested with EcoR I. EcoR I cuts twice in rAAV-GFP/Hygro (Fig. 1a) and at position 2 in AAVS1 (S51329). Another EcoR I site is found approximately 8.2 kb upstream, outside the AAVS1. The DNA was then separated by agarose gel electrophoresis (0.8%) and blotted to a nylon membrane. The membrane was hybridized with a random-primed transgene probe by standard methods, an autoradiogram was taken, the membrane was stripped and then hybridized with a random-primed AAVS1-specific probe and exposed again. The transgene probe encompasses the GFP and the hygromycin resistance sequences of pGFP (Fig. 1a) and was generated by a Pst I digest. The AAVS1-specific probe includes position 1439-2527 of AAVS1 cloned into pRIA-N3 and was also generated by Pst I digest. pRIA-N3 was kindly provided by R. Kotin.

Chromosomal fluorescence *in situ* hybridization (FISH). After fixation in methanol:acetic acid 3:1, the cells were air dried on glass slides and frozen at -20°C for at least one day. The pGFP was digested with Spe I and then labeled with biotin-11-dUTP using a nick translation labeling kit (Roche Diagnostics, Mannheim, Germany). 10 ng of labeled and precipitated DNA was dissolved in 10 µl hybridization solution consisting of 50% formamide, 10% dextran sulfate, 1x SSC, 5 µg sonicated salmon sperm DNA, and then denatured at 95°C for 5 min. Slides with metaphase spreads were first dehydrated by passing through a graded ethanol series. Then they were denatured in 70% formamide/2x SSC at 72°C for 2 min on a heating plate and subsequently passed through a graded ethanol series. Hybridization was performed in 10 µl hybridization solution/4cm² at 37°C overnight under a cover slip sealed with rubber cement. Post-hybridization washes were performed in 0.4x SSC at 72°C for 2 min and 2x SSC at room temperature for 2 min, followed by 30 min incubation with 5% nonfat dry milk/4x SSC at room temperature. Immunochemical detection of the biotin labeled probe was carried out with fluorescein isothiocyanate (FITC)-conjugated avidin (Vector, Burlingame, CA) as described (Lichter et al. 1988). The signal was amplified by using biotinylated goat anti-avidin immunoglobulins (Vector). The slides were counterstained with 4,6-diamino-2-phenylindol (DAPI) (2mg/mL) and mounted in anti-fade solution (90% glycerol, 10% PBS, 1 mg/ml phenylenediamine). After microscopy the cover slips and anti-fade solution was removed by incubation in 2x SSC for at least 2 hrs. The whole chromosome 19 painting probe labeled with Spectrum Orange was purchased from Vysis (Bergisch Gladbach, Germany) and hybridization was carried out according to the manufacturers instructions. Metaphases were analyzed using a Zeiss Axioskop epifluorescence microscope equipped with filter combinations according to Pinkel (AHF Analysentechnik, Tübingen, Germany) and a cooled charge-coupled device camera. FITC, Spectrum Orange, and DAPI fluorescence were recorded separately as gray-scale images by only changing the excitation wave length while the beam splitter and emission filter remained in position. The images were then pseudocoloured and were merged using a digital image analysis software program (ISIS, Metasystem, Altflusheim).

Results

Construction of the plasmids and functional testing

A unique characteristic of wild-type (wt) AAV is its ability to integrate site-specifically into the human chromosome 19 (AAVS1). Although rAAV can integrate into the genome, the specificity for AAVS1 is lost due to the absence of the large Rep proteins. Therefore, we have initiated studies to determine if Rep proteins expressed in *trans* from a suitable co-transfected plasmid could promote site-specific integration of rAAV.

For these studies two plasmids, pGFP and pRC, were generated. pGFP was cloned as described in Material and Methods. It was used as the vector plasmid in the packaging process of rAAV-GFP/Hygro. pGFP encodes the transgenes for Green Fluorescence Protein (GFP) and hygromycin resistance, controlled by the cytomegalovirus and the thymidine kinase promoter, respectively (Fig. 1a). GFP was chosen as transgene, because its expression facilitates the determination of transfection efficiency and stability of gene expression. To study the influence of antibiotic selection pressure on the site-specific integration process, the hygromycin resistance gene was included in the vector plasmid. The two genes were flanked by the viral inverted terminal repeats (ITR), the sole *cis* elements required for packaging AAV.

The plasmid pRC encodes the Rep and Cap proteins of wtAAV controlled by their natural promoters (Fig. 1b). This plasmid was employed as helper plasmid for packaging rAAV (Material and Method) and, furthermore, to express Rep in *trans* in the genomic targeting approach described in this article. Providing Rep in *trans* by a Rep expressing plasmid lacking the ITR of AAV and other integration promoting signals was expected to have the following advantages: (i) integration of rAAV vectors in a site-specific manner, (ii) preservation of the full transgene coding capacity of the rAAV vectors, and (iii) transient expression of the potentially cytotoxic Rep proteins.

In the first experiments we intended to determine whether the Rep proteins controlled by their natural promoter were expressed in HeLa cells in the absence of helper virus co-infection. For this purpose HeLa cells were transfected with the plasmid pRC by calcium phosphate precipitation and the transfection was stopped by fixation of the cells at different time points (12, 24, 36 and 45 hours after transfection). Immunostaining techniques were used to determine the expression of Rep proteins. As a positive control HeLa cells were cotransfected with wtAAV and adenovirus type 5, cultivated for 16 hours, and analyzed for

Rep expression. In this experiment, Rep expression could easily be detected at 24 hours post transfection (Fig. 2a). Expression increased and reached a plateau at 36 hours post transfection (Fig. 2b), and declined thereafter (Fig. 2c). Although after co-infection of wtAAV and adenovirus expression of Rep was visible at an earlier time point (Fig. 2d), these results clearly demonstrated that Rep was synthesized in significant quantities from the Rep expressing plasmid pRC in the absence of adenovirus type 5.

Production of stable GFP expression cell lines

Since Rep was expressed after transfection of pRC in the absence of helper virus in HeLa cells (Fig. 2), we next examined whether this Rep expression was able to mediate the site-specific integration of rAAV. Moreover, we wanted to determine whether antibiotic selection pressure negatively influenced site-specific integration. Together, 25 single cell clones generated under four different experimental conditions (Table 1) were investigated. Groups 1 and 2 were obtained by transfecting HeLa cells with pRC 24 hours before rAAV-GFP/Hygro infection. Half of these co-transfected cells were then grown in the presence of hygromycin (350 µg/ml) starting 48 hours after infection (group 2), while the other half was cultivated without selection pressure (group 1). 14 days later, single cell clones were obtained by limiting dilution and expansion of the GFP expressing cell clones, resulting in 4 clones in group 1, and 6 clones in group 2. As controls (groups 3 and 4), single cell clones were obtained by infecting HeLa cells with rAAV-GFP/Hygro followed by cultivation in the absence (group 3) or presence (group 4) of hygromycin. By this approach, 9 cell clones were obtained in group 3, and 6 clones in group 4, respectively. All 25 single cell clones stably expressed GFP for more than eight months in culture, although the initial high levels of GFP expression started to decrease slowly after week 4.

To estimate of the overall integration frequency of rAAV-GFP/Hygro, the polyclonal cell population of group 1 and 3, which were kept without selection pressure after infection, was monitored for GFP expression for one month. Two days after infection, both cell populations showed a high number of GFP positive cells, indicating a transduction efficiency of more than 70%. After one month, 45 % of the cells infected with rAAV-GFP/Hygro after pRC transfection remained positive for GFP fluorescence. In marked contrast, less than 2% of the cells transduced with rAAV-GFP/Hygro but not transfected with pRC showed GFP expression. This indicated that transfection of a Rep expressing plasmid alone was able to

significantly increase the overall integration frequency in agreement with previous studies (Balague et al. 1997).

Table 1. AAVS1 specific integration after rAAV-GFP/Hygro infection and co-transfection with pRC

Experimental condition	Group 1	Group 2	Group 3	Group 4
<i>Transfection with pRC</i>	+	+	-	-
<i>Transduction with rAAV-GFP/Hygro</i>	+	+	+	+
<i>Selection with hygromycin</i>	-	+	-	+
Results				
GFP positive clones	4/4	6/6	9/9	6/6
AAVS1 integration (Southern blot with EcoR I)	1/4	6/6	0/9	0/6
Transgene signal on chromosome 19 (FISH) ¹	1/1	4/4	n.d.	0/1

Four experimental groups with a total of 25 single cell clones were established. In groups 1 and 2 Rep was provided by transfection of pRC 24 hours before rAAV-GFP/Hygro infection. The cells were subsequently grown in the absence (group 1: clones B6, D6, F3 and H6) or presence (group 2: clones A3, B12, C2, C10, D4 and F4) of hygromycin (350 µg/ml). The clones belonging to groups 3 and 4 were generated by infection with rAAV-GFP/Hygro without prior transfection of pRC and then growing in the absence (group 3: clones 1B11, 1D11, 2D10, 4A7, 4G1, 5B10, 5F2, 6B2 and 6B11) or presence (group 4: clones B9, C4, C11.5, C11.7, G5 and H11) of hygromycin (350 µg/ml). (n.d.: not determined; ¹of the clones analyzed by this method)

Site-specific integration of the transgene occurs only in the co-transfected cells

To test whether site-specific integration of rAAV-GFP/Hygro in AAVS1 occurred in any of the 25 GFP expressing single cell clones, Southern blot analysis of EcoR I digested genomic DNA was performed. This restriction enzyme cuts twice within rAAV-GFP/Hygro (Fig. 1a) and at position 2 of the GenBank deposited sequence of AAVS1 (S51329) (Kotin et al. 1992). A site-specific integration event was expected to result in at least one up shifted band with respect to the normal AAVS1 site present in the parental HeLa cell line, and the transgene should also be detectable at this site. Therefore, the Southern blot membrane was first hybridized with a transgene specific probe and then, after removal of the first probe, with an AAVS1 specific probe. The hybridization pattern⁹ obtained with the two different probes was then compared.

Figure 3 shows the Southern blot results of the 10 independent clones generated by cotransfection of the Rep expression plasmid pRC and rAAV-GFP/Hygro. Six of these clones (A3, B12, C2, C10, D4, F4) were grown in the presence of hygromycin (group 2), whereas the remaining were cultivated in the absence of hygromycin (group 1). In all clones (Fig. 3b) additional higher migrating AAVS1 specific fragments were detectable in comparison to the uninfected HeLa cell control (Fig. 3b), one criteria pointing towards a site-specific integration event. Moreover, the up shifted band co-hybridized with the transgene specific probe in 7 of 10 clones (H6, A3, B12, C2, C10, D4, F4) (compare Fig. 3a with 3b). This demonstrated that providing Rep in *trans* by cotransfection allowed to target the genomic integration of rAAV vectors to AAVS1. Integration of AAV as head-to-tail concatamers have been described previously (Yang et al. 1997). Such an integration would result in an additional transgene specific signal of 4.5 kb which could not be observed (Fig. 3). Other concatameric forms such as head-to-head and tail-to-tail integration can also be excluded on the basis of the banding pattern.

Similarly, clones obtained by rAAV-GFP/Hygro infection without pRC cotransfection, followed by culture in the absence (group 3) or presence (group 4) of hygromycin, were analyzed by EcoR I Southern blot. Figure 4 shows a representative blot of 10 out of a total of 15 clones obtained. None of the clones, including those not shown, displayed a banding pattern in which the transgene signal co-migrated with the AAVS1 specific signal (compare Fig. 4a with 4b). Furthermore, all clones showed the presence of a single AAVS1 specific signal (Fig. 4b). Both findings suggest that no site-specific transgene integration occurred in the absence of pRC transfection.

Taken together, the Southern blot analysis revealed that no site-specific integration event occurred in the absence of *rep* gene expression (0/15). In contrast, site-specific integration of rAAV-GFP/Hygro at AAVS1 was seen in the majority of the clones obtained by cotransfection of the *rep* gene (7/10).

FISH analysis of the HeLa cell clones confirms integration at chromosome 19 in the presence of Rep

To confirm the Southern blot results, fluorescence *in situ* hybridization analysis (FISH) of the five HeLa cell clones A3, B12, C10, D4 and H6 was performed. As controls, uninfected HeLa cells and clone G5 were analyzed. For this FISH analysis two probes were used, the 7.9 kb pGFP and a probe for chromosome 19 (see Material and Methods).

Before starting FISH analysis, the parental HeLa cell line was characterized by conventional chromosome banding analysis (Fig. 5a). In agreement with previous literature, numerous chromosomal aberrations were detected in this cell line. Regarding chromosome 19, one normal chromosome and two chromosomes with a translocation t(13;19) were detected (Fig. 5a), as described previously by Macville and colleagues (1999).

Thereafter, a FISH analysis of the metaphase chromosomes of the above cell clones was performed. The red dye shown in Figure 5b-h indicates chromosome 19, whereas the yellow spots show the hybridized transgene probe. The uninfected HeLa cell clone (Fig. 5b) hybridized only with the chromosome 19 specific probe, revealing one signal for each chromosome 19. Figure 5h shows the clone G5 (group 4). This clone was generated through infection with rAAV-GFP/Hygro in the absence of *rep* gene expression and did not show any evidence for site-specific transgene integration in Southern blots. In FISH analysis, the red signals specific for chromosome 19 were visible. In addition, rAAV-GFP/Hygro specific signals were detectable on one of the D group chromosomes (chromosome 13, 14 or 15), confirming that rAAV had integrated at a site different from AAVS1. Thus, the FISH analysis supported the Southern blot results for the clone G5. In marked contrast, clones A3, B12, C10, D4 and H6 resulting from cotransfection of pRC and rAAV-GFP/Hygro (groups 1 and 2) showed a site-specific integration by FISH analysis in each clone, as demonstrated by the co-localization of the rAAV specific probe with chromosome 19 (Fig. 5c-g). Moreover, this co-localization was consistently visible on the q arm. This result strongly suggested that a site-specific integration of the GFP gene at AAVS1 had occurred.

In summary, the FISH analysis confirmed the Southern blot results for every clone analyzed. The results suggest that providing Rep in *trans* by cotransfection of a plasmid vector is sufficient to achieve site-specific integration of an ITR flanked transgene carried by an AAV vector.

Discussion

Avoiding insertional mutations by random integration is a major concern when gene therapy needs long-term gene expression in normal tissue. Up to now AAV is the only known virus capable of site-specific integration into the human chromosome. For this specific integration process, the viral encoded Rep proteins and the ITR structures flanking the vector genome are required. However, in the commonly used rAAV vectors only the ITR structures are retained, which results in the loss of integration specificity. Not only safety concerns (in particular with regard to homologous recombination during rAAV packaging), but also the limited packaging capacity (Dong et al. 1996), reduce the possibility of constructing rAAV vectors which retain the *rep* gene in *cis* to mediate site-specific integration.

One potential approach to overcome this problem was described by Balagué et al. (1997). They could show that transfecting a plasmid containing both an ITR flanked transgene and a Rep expression cassette outside the ITRs into 293 cells resulted in the site-specific integration of the transgene into AAVS1. However, Tsunoda et al. (2000) and Surosky et al. (1997) observed that the entire plasmid backbone, not only the ITR flanked transgene, integrated into the AAVS1 at a high frequency, when the *rep* gene was provided on the same or on a co-transfected plasmid.

For this reason we chose a different approach. The Rep expression plasmid pRC was transfected independently of the transgene into HeLa cells. This approach allowed to express Rep in significant quantities in the absence of any helper virus such as adenovirus type 5. Subsequent infection of cells with a rAAV vector caused site-specific integration of the GFP transgene in 70% of the clones. Integration occurred regardless of whether the cells were grown under selection pressure with hygromycin or not. In marked contrast, no transgene integration at AAVS1 was obtained when cells were infected by rAAV-GFP/Hygro without prior pRC transfection (Fig. 3 and 5).

In contrast to Balagué et al. (1997) who assumed that selection pressure interfered with the site-specific integration event, we observed integration at AAVS1 also in the

presence of hygromycin selection at high frequency (6/6). Moreover, the GFP expression level was sustained at much higher levels in clones grown with selection than in those grown without selection. Since Balagué et al. (1997) did not provide a detailed description of their selection procedure, the explanation for this difference is not obvious. One reason might be the time point at which the selection pressure was started (in our experiments 48 hours after rAAV infection).

HeLa cells contain only one normal chromosome 19 and two t(13;19) translocations (Fig. 5). The translocation event occurs in both t(13;19) cases at the p arm of chromosome 19, i.e. far from AAVS1 (19q13.4) (Macville et al. 1999). A negative influence of the chromosomal translocation on the integration process could not be excluded at the beginning of our studies. However, our FISH results suggest that this is not the case. In two clones, H6 and C10, rAAV integrated into one of these translocated chromosomes. Integration into the normal chromosome 19 took place in the remaining three clones analyzed by FISH (A3, B12 and D4). In addition to this, none of the clones in which rAAV had integrated specifically at AAVS1, showed integration into an additional chromosome. This argues for a relatively high specificity of Rep mediated integration. The ITRs are integration promoting signals. This was demonstrated by Balagué and colleagues (1997) who compared the integration frequency of ITR containing plasmids with plasmids lacking the ITR sequence.

For directing the ITR containing sequence to the AAVS1 site, at least one of the large Rep proteins is necessary. One model for site-specific integration (Brister & Muzyczka 2000; Meneses et al. 2000) proposes that Rep78 and/or Rep68 bind as a multimeric complex both to the Rep binding site (RBS) on chromosome 19 and to the viral DNA. Rep then nicks at the chromosomal terminal resolution site (trs), possibly aided by cellular proteins (Costello et al. 1997; Dyall et al. 1999). Subsequently, Rep initiates a strand displacement DNA synthesis, during which DNA template switches occur linking viral with cellular DNA. Also other models for targeted integration are possible, e.g. integration could be mediated by ligase activity of the large Rep proteins (Smith & Kotin 2000). Meneses and colleagues (2000) showed that three parameters are necessary for the integration process: 1) RBS, 2) trs and 3) a spacer sequence, containing either a GCTC motif or two CTC triplets embedded in a pyrimidine-rich sequence. The specific combination of these three parameters can only be found once in the human genome, in AAVS1, which could explain the specificity of the integration process.

The clones C2, D4 and F4 were obtained by cotransfection of pRC and rAAV-GFP/Hygro (group 2) and showed site-specific integration by Southern blot analysis. In these clones an additional up shifted AAVS1-specific band was detected (Fig. 3b), which showed no co-hybridization with the transgene probe. The FISH analysis of D4 (Fig. 5f) confirmed the presence of an additional chromosome 19 specific signal. These results demonstrate Rep dependent rearrangements of AAVS1, since none of the control clones obtained by rAAV alone (groups 3 and 4) showed such a pattern (Fig. 4). However, such rearrangements did not occur consistently in all clones (Fig. 3b). Further studies on the function of Rep and the integration process will elucidate this event and hopefully the design of strategies to avoid these rearrangements.

The three clones B6, D6 and F3 were negative for the occurrence of site-specific integration in the EcoR I Southern blot analysis, although they were obtained by cotransfection of pRC and rAAV-GFP/Hygro (group 1) and although they all showed additional AAVS1-specific bands pointing towards Rep activity. One explanation for this might be that the level of Rep expression was lower than necessary (Young et al. 2000) or occurred too late to mediate the specific integration. Another explanation could be that these clones integrated site-specifically but the orientation of the integrated transgene was inverted. In this case it would not be possible to detect site specific integration using EcoR I as restriction enzyme (Fig. 1). To test this point, we performed a Southern blot using Bcl I, which cuts neither in the rAAV used nor in AAVS1. This resulted in an up shifted band in comparison to the parental cell line (data not shown). Moreover, this band co-hybridized with the transgene specific probe (data not shown). Both observations argue for the occurrence of site-specific integration of the transgene in these clones, detection of which failed when using EcoR I to digest the genomic DNA.

Another characteristic of AAV is the ability of the integrated viral genome to rescue from the latent state and reenter the lytic life cycle, when helper functions are provided. This was observed with wtAAV and rAAV preferentially when the viral genome had integrated as concatamer and/or when at least one ITR was still intact after integration (McLaughlin et al. 1988; Rutledge & Russell 1997). We therefore tested the specifically integrated clones for rescue and replication of the proviral genome after transduction with pRC and adenovirus. In our setting all clones were rescue deficient, although in control transfections virus production could be observed (data not shown). One explanation for the rescue deficiency could be that AAV had integrated as a monomer and that deletions and rearrangements in the ITRs had

occurred during the integration process. This is in agreement with our Southern blot results in which the banding pattern also points towards monomeric integration. Further studies are now ongoing to determine the molecular structure of the integration junctions.

In conclusion, our results show that providing Rep in *trans* by the described cotransfection approach is a very efficient method to achieve site-specific integration of the commonly used rAAV vectors *in vitro*. In particular for *ex vivo* gene therapy of diseases of the hematopoietic system, e.g. by gene transfer into CD34⁺ stem cells, it would be beneficial to use the described system to achieve efficient and specific integration of transgenes. On this promising basis we are now developing methods suitable for genomic *in vivo* targeting of rAAV vectors.

Acknowledgments

We thank Dr. Robert Kotin for helpful advice and discussion, and for providing the pRIA-N3. Furthermore we thank Kristin Leike for excellent technical help and Susan King and Franz Gerner for kindly reading this manuscript. This work was supported by the Bayerischer Forschungsverbund Grundlagen Gentechnischer Verfahren (FORGEN, VV5) and the German Research Council (DFG, SFB 455).

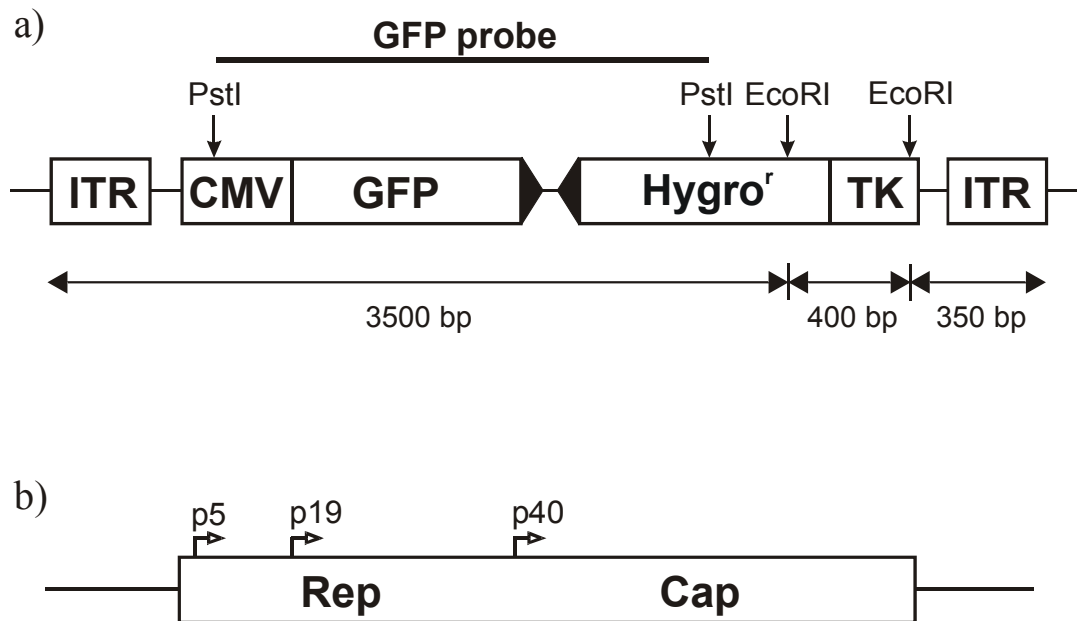


Figure 1. Schematic representation of the plasmid constructs used. (a) The plasmid pGFP encodes, flanked by the AAV ITR sequences, the genes for the *Aequorea victoria* Green Fluorescence Protein (GFP) and the hygromycin resistance gene controlled by the cytomegalovirus promoter and the thymidine kinase promoter, respectively. The important restriction sites and the size of the fragments obtained after digestion of the AAV genome with EcoR I are marked. The probe used to detect the transgene encompassed the region indicated. b) The plasmid pRC contains the *rep* and *cap* genes of wtAAV, controlled by its natural promoters p5, p19 and p40.

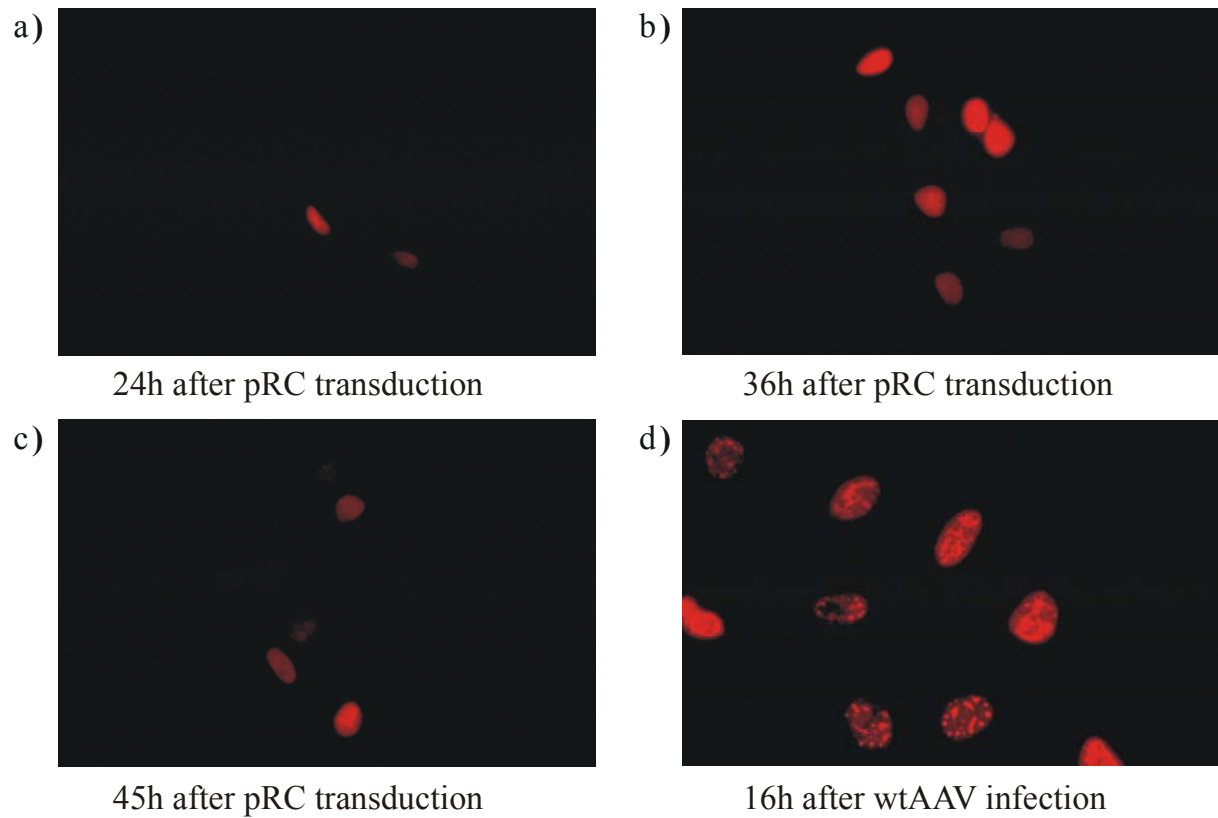


Figure 2. Rep protein synthesis in the absence of adenoviral gene products. HeLa cells were transfected with pRC by calcium phosphate precipitation. The transfection was stopped at different time points by fixation with methanol and acetone. Cells were then analyzed for Rep expression by immunostaining. Fig. 2a-c shows the Rep expression detected after 24, 36 and 45 hours. Fig. 2d shows the amount of Rep expression visible 16 hours after wtAAV and adenovirus co-infection of HeLa cells with an MOI 3 and 5, respectively.

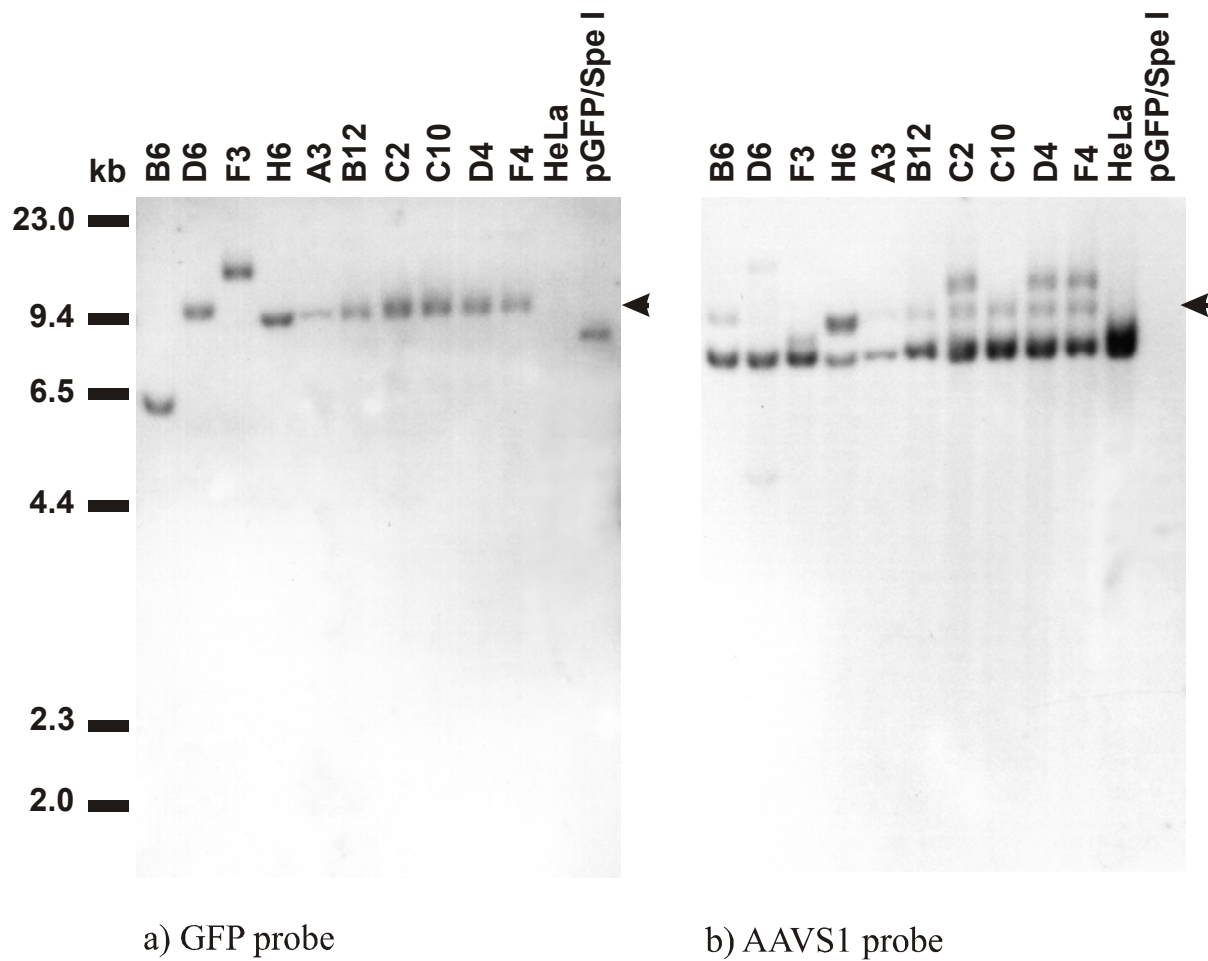


Figure 3. *EcoR* I Southern blot of the cell clones generated by pRC and rAAV-GFP/Hygro cotransfection. The genomic DNA was isolated from different cells. Clones B6, D6, F3 and H6 were grown without selection pressure (group 1), while clones A3, B12, C2, C10, D4 and F4 were grown in the presence of hygromycin (350 μ g/ml) (group 2). The genomic DNA was digested with the restriction enzyme *EcoR* I (for details see Material and Methods). After electrophoresis Southern hybridization with the transgene probe was performed (a). After exposure the membrane was stripped and hybridized with an AAVS1 probe (b). Arrows indicate bands which hybridized to the transgene probe as well as to the AAVS1 probe. The position of the molecular weight DNA marker is indicated on the left.

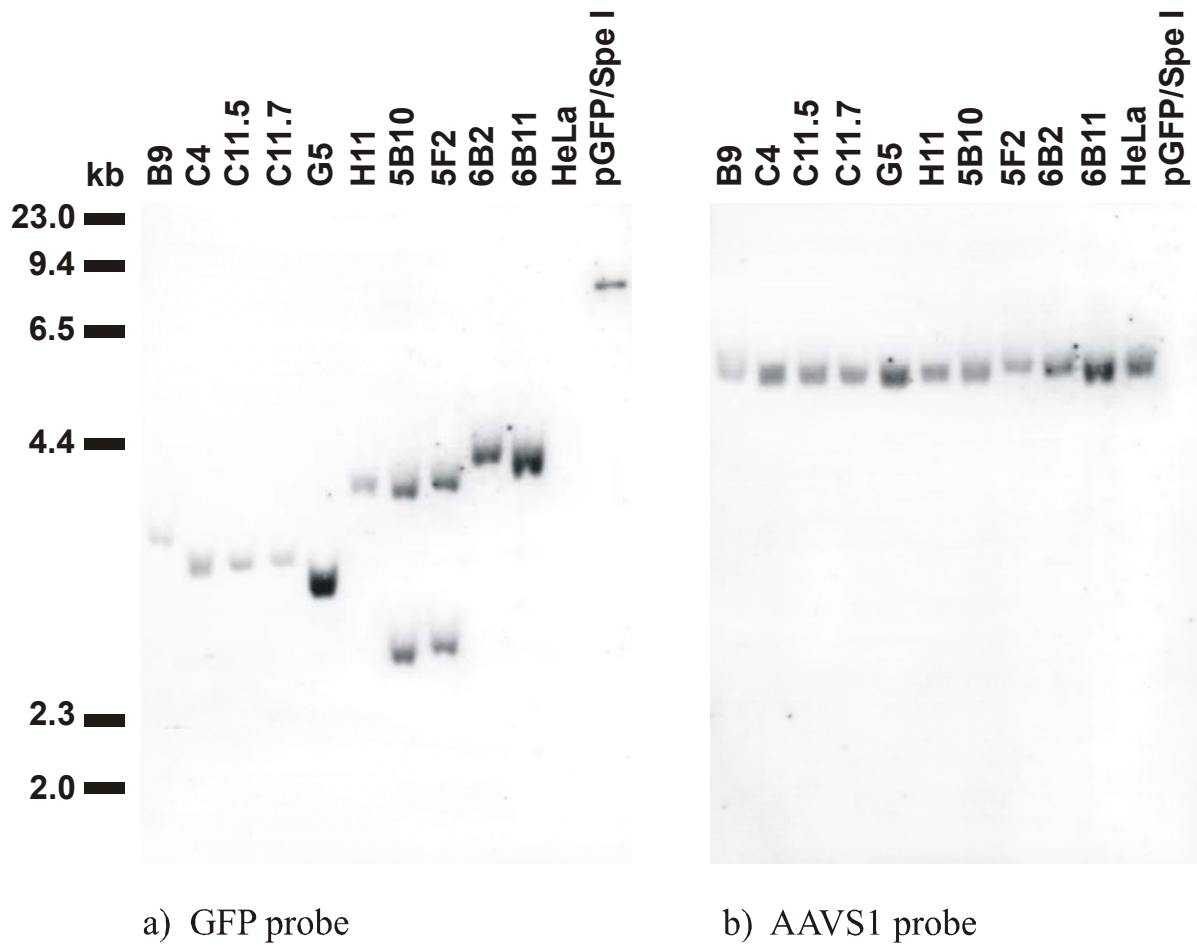
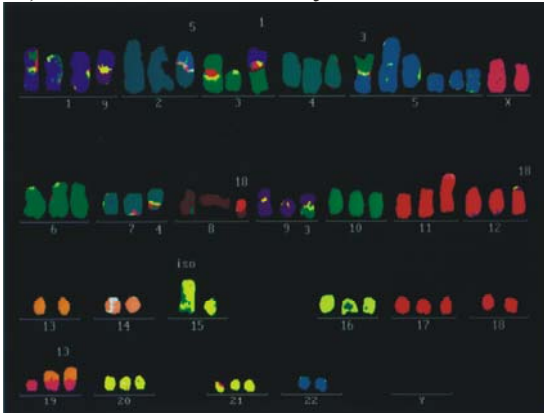
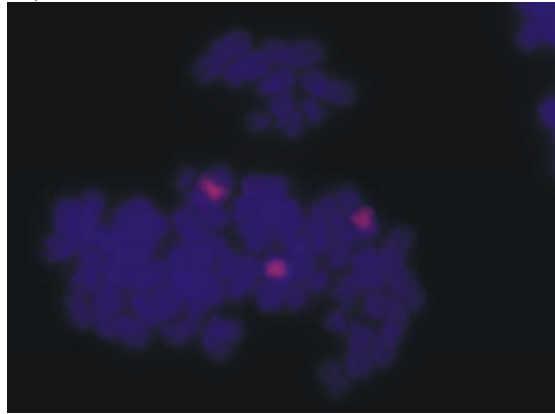


Figure 4. EcoR I Southern blot of cell clones generated by rAAV-GFP/Hygro infection *without* pRC cotransfection. The genomic DNA was isolated from different cell clones grown in the absence (group 3: 5B10, 5F2, 6B2, 6B11) or presence (group 4: B9, C4, C11.5, C11.7, G5, H11) of hygromycin (350 μ g/ml). The genomic DNA was digested with the restriction enzyme EcoR I and treated as described in Fig. 3 and in Materials and Methods. The position of the molecular weight DNA marker is indicated on the left.

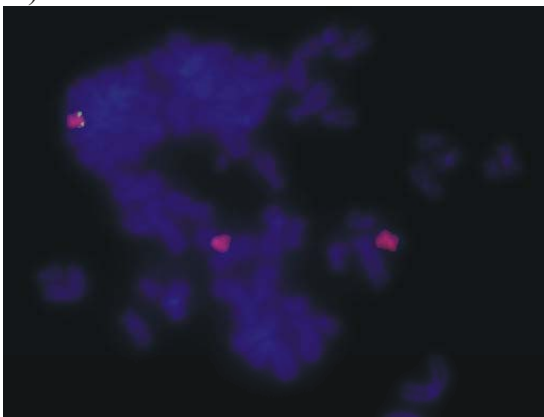
a) Chromosome analysis of HeLa



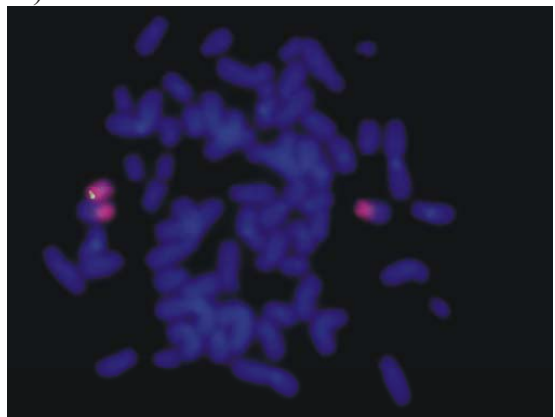
b) HeLa



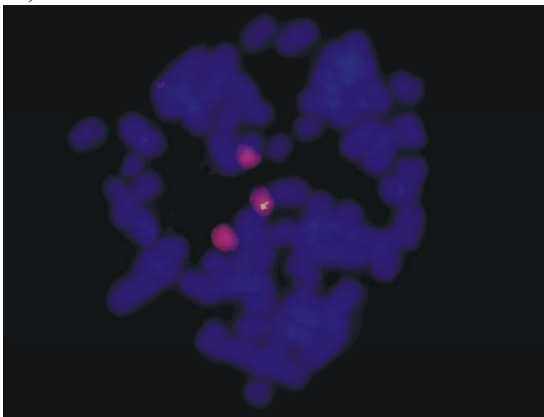
c) Clone A3



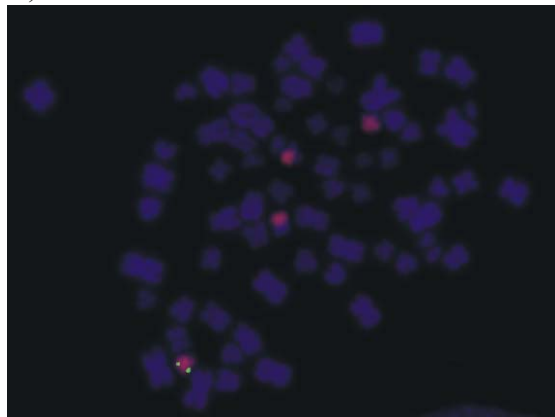
d) Clone B12



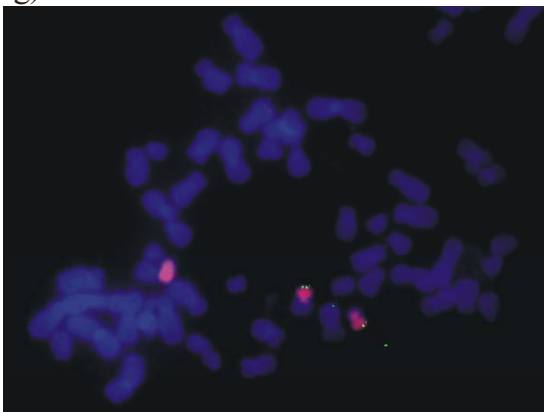
e) Clone C10



f) Clone D4



g) Clone H6



h) Clone G5

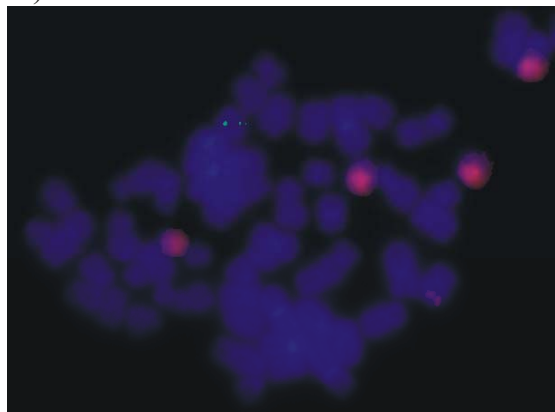


Figure 5. Chromosome banding analysis of the HeLa cell line used and FISH analysis. (a) Chromosome banding analysis of the HeLa cell line used. Numbers indicate the chromosome number. The colors help to associate the translocations with the corresponding "mother" chromosome. Three chromosome 19s could be detected (one normal and two t(13;19) translocations). (b-h) FISH analysis of the metaphase chromosomes of the HeLa cell line and of the cell clones A3, B12, C10, D4, H6 and G5. The red dye indicates the chromosome 19 specific signal, the yellow spots are the hybridization signals of the transgene probe.

CHAPTER III

PLL/DNA complexes coupled to adeno-associated virus vectors allow for simultaneous gene transfer of a Rep encoding plasmid

submitted for publication as:

Huttner NA, Endress T, Stark M, Girod A, Guckenberger R, Bräuchle C, Hallek M, Büning H.

PLL/DNA complexes coupled to adeno-associated virus vectors allow for simultaneous gene transfer of a Rep encoding plasmid.

Abstract

Adeno-associated virus type 2 (AAV) has many features that makes it an attractive vector for human gene therapy. A unique advantage of wild-type AAV is the ability to specifically integrate into the human genome at a distinct locus within chromosome 19 (AAVS1), especially with regard to stable transgene expression and avoiding the risk of insertional mutagenesis by random integration. However, recombinant AAV vectors have lost this ability due to the deletion of the viral *rep* gene. Previously we could show that targeted integration can be restored by providing *rep*-DNA in *trans* (Huttner et al. 2003). To design specifically integrating recombinant AAV vectors we decided to couple *rep* as polylysine/DNA complex via a biotin-streptavidin bridge directly to the AAV capsid. In this study we demonstrated that a Rep encoding plasmid can be efficiently packaged by polylysine (PLL) into small compact particles. These complexes could be coupled to biotinylated AAV particles via a biotin-streptavidin bridge. Moreover, we could show that the biotin labeling of AAV and the linkage of streptavidin did not interfere with the viral infection process. Interestingly, AAV-PLL/DNA complexes were able to infect HeLa cells and could be observed in the cytoplasm by single-molecule microscopy in real-time, while PLL/DNA complexes alone did not enter cells. These findings are an important step towards specifically integrating AAV vectors for the use in human gene therapy.

Introduction

Adeno-associated virus type 2 (AAV) is a small, replication defective, DNA virus that has promising features as a vector for human gene therapy. Both wild-type and recombinant AAV display a wide target cell tropism, transduce terminally differentiated and non-dividing cells, and show low immunogenicity and no pathogenicity (Monahan & Samulski 2000). One of the most promising features of AAV is its ability to integrate site-specifically into the human chromosome (Berns & Giraud 1996).

AAV is a member of the *Parvoviridae* family with a small icosahedral capsid harboring a single-stranded DNA genome of approximately 4.7 kb. The genome consists of two open reading frames (ORF), which comprise the *rep* and *cap* genes, and is flanked by the inverted terminal repeats (ITR). The ITRs serve as the origins of replication for viral DNA synthesis and are required for packaging and targeted integration. The 5' ORF encodes four non-structural proteins, Rep78, Rep68, Rep52, and Rep40. The large Rep proteins (Rep78 and

Rep68) are required for viral replication, transcriptional control and site-specific integration. The small Rep proteins (Rep52 and Rep40) play an essential role in the accumulation of viral DNA into preformed capsids. The three capsid proteins VP1, VP2, and VP3 are encoded in the 3' ORF. They form the icosahedral capsid, which has a diameter of 25 nm.

To persist in nature AAV utilizes a biphasic life cycle. In the presence of helper virus, adenovirus (Ad) or herpesvirus, wild-type AAV (wtAAV) undergoes a productive infection. Lacking a helper virus, wtAAV latently infects by integrating into the host genome preferentially (> 70%) into human chromosome 19 within 19q13.4 (AAVS1) (Berns & Giraud 1996). The ability of this virus to integrate site-specifically has made it an attractive candidate vector for human gene therapy. For targeted integration the non-structural proteins Rep78 and/or Rep68 are required; the ITRs flanking the vector genome are the essential *cis* components (McLaughlin et al. 1988; Samulski et al. 1989; Xiao et al. 1997b). In the absence of Rep proteins, the virus can still integrate through the ITR sequences but randomly into the host genome (Kearns et al. 1996; Walsh et al. 1992; Xiao et al. 1997b). However, commonly used recombinant AAV vectors (rAAV) lack the viral *rep* gene, only the ITRs are retained. Therefore rAAV vectors have lost the ability to integrate in a specific manner. Previously, we could show that this ability can be restored by providing Rep in *trans* by co-transducing a Rep encoding plasmid and a viral vector coding for a transgene (Huttner et al. 2003).

To develop specifically integrating rAAV vectors for gene therapy applications we decided to link *rep*-DNA as a polylysine/DNA complex directly to the AAV capsid. After infection with such a construct Rep proteins could be expressed and mediate targeted integration of the ITR flanked transgene encoded in rAAV in AAVS1 (see Fig. 1). Poly-L-lysine (PLL) has many advantages that makes it attractive for our approach. PLL is a biodegradable cationic polymer with the ability to condense linear, circular and supercoiled DNA to compact structures (Gao & Huang 1996). In these PLL/DNA complexes (PLL/DNA) the DNA is protected from degradation by nucleases. PLL/DNA have been previously used as vector systems for gene therapy applications. Since PLL/DNA alone are not able to transduce cells (Curiel et al. 1992; Gao & Huang 1996; Lee & Huang 1996) they had to be coupled to ligands, e.g. Ad or transferrin, which mediated receptor attachment, cell entry, and endosomal release (Curiel et al. 1992; Wagner et al. 1991; Wagner et al. 1992). After cell entry the PLL can be degraded and the DNA is released into the cytoplasm. Moreover, there have been reports that PLL might function as nuclear localization signal and transport the DNA directly to the nucleus (Gao & Huang 1996). In this study we analyzed the coupling of PLL/DNA

complexes to the AAV capsid via a biotin-streptavidin bridge, and studied transduction with these constructs. Our results will not only be useful to generate rAAV vectors with the potential to integrate site-specifically but also offer a possibility to overcome the limited coding capacity of conventional rAAV vectors.

Materials and Methods

Cell culture. The human cervix epitheloid carcinoma cell line HeLa (ATCC CCL 2; American Type Culture Collection, Rockville, Maryland) was maintained as monolayer culture at 37°C and 5% CO₂ in Dulbecco's modified Eagle's medium (DMEM), supplemented with 10% fetal calf serum (FCS), 100 U/ml penicillin, 100 mg/ml streptomycin and 2 mM L-glutamine.

Reagents. Poly-L-lysine (PLL) with a mean molecular weight of 1 kDa (PLL₆, P8954), 4 kDa (PLL₁₉, P0879), 9.8 kDa (PLL₄₇, P6516), 23 kDa (PLL₁₂₀, P7890), and 47 kDa (PLL₂₂₅, P2636) was obtained from Sigma-Aldrich. Steptavidin was purchased from Roche Diagnostics, and Sulfo-NHS-LC-Biotin and Sulfo-LC-SPDP from Pierce. Cy5-labeled streptavidin was obtained from Amersham Pharmacia and the Cy3-labeled biotin antibody from Jackson Immuno Research Laboratories.

Plasmids. The plasmid pUC-AV2 contains the full-length AAV2 genome and was constructed as described in Girod et al. (1999). The pRC plasmid was constructed as previously described (Girod et al. 1999). Briefly, the 4.5 kb Xba I-fragment of psub201(+) (Samulski et al. 1987), containing the *rep* and *cap* ORFs of AAV was subcloned into the Pst I and BamH I sites of pSV40oriAAV (Chiorini et al. 1995).

The pGFP plasmid is an AAV-based vector plasmid in which the AAV ITR sequences are flanking the hygromycin selectable marker gene controlled by the thymidine kinase promoter and the *Aequorea victoria* Green Fluorescence Protein (GFP) gene regulated by the cytomegalovirus promoter. pGFP was generated by inserting the Asp718-Not I fragment of pEGFP-N1 (Clontech) into the Asp718-Not I sites of psub/CEP4 (Sal invers). psub/Cep4 (Sal invers) is a derivative of psub201(+) (Samulski et al. 1987), which was digested with Xba I, blunt ended and ligated to blunt ended 3923 bp Sal I-Nru I-Fragment of pCEP4 (Sal inverse). pCEP4 (Sal inverse) differs from pCEP4 (Invitrogen) by inversion of the Sal I (8)-Sal I (1316)-fragment. The adenovirus helper plasmid pXX6 (Xiao et al. 1998) was kindly provided by R. Jude Samulski.

For the construction of pUCGFP the pUC18 plasmid (GenBank accession number L09136) was digested with Afl III and Ssp I, blunt ended, and the Sal I fragment of pGFP (containing the cytomegalovirus promoter, the GFP gene and the SV40 poly A) was inserted. Similarly, for construction of pRep the blunted Xba I-BsrB I fragment of pRC (corresponds to nt 2310 – 3812 of the AAV genome) was inserted into the Afl III/Ssp I digested pUC18 plasmid backbone.

Production of AAV particles. 293 cells were seeded in twenty culture dishes (150-mm diameter), each containing 7.5×10^6 293 cells, were cotransfected by calcium phosphate with a total of 37.5 µg of vector plasmid (pGFP), packaging plasmid pRC and adenoviral plasmid pXX6 at a 1:1:1 molar ratio. For viruses

containing an AAV *rep* and *cap* gene, the pUC-AV2 plasmid or mutated plasmid were transfected with pXX6 in a 2:1 molar ratio. After 24 hr the transfection medium was replaced by fresh DMEM culture medium containing 2% FCS and the cells were incubated for 24 h at 37°C and 5% CO₂. Thereafter cells were harvested and pelleted by low speed centrifugation at 3000xg. Viral particles in the supernatant were precipitated by addition of ammonium sulfate and centrifuged (pellet A). The cell pellet was resuspended in DMEM and sonicated. Cell debris was spun down at 3700xg for 20 min at 4°C. Supernatant was added to pellet A and further purified by ammonium sulfate precipitation. In detail, contaminations were precipitated with 35% ammonium sulfate, after centrifugation the viral particles in the supernatant were precipitated in 55% ammonium sulfate. The pellet was resuspended in CsCl solution ($\rho = 1.37$ g/ml) and purified by CsCl gradient centrifugation at 41000 rpm for 48 h. The main fractions were collected, pooled, dialyzed against HBS (150 mM NaCl, 50 mM Hepes), and further purified first by ion-exchange-chromatography and then by affinity-chromatography (heparin-column) as described previously (Zolotukhin et al. 1999).

Evaluation of AAV titers. Particle titers of virus stocks were quantified by dot-blot analysis as described (Girod et al. 1999). Briefly, serial dilutions of the AAV preparations were first incubated in 0.5 M NaOH, then blotted onto a nylon membrane, and finally hybridized with a random-primer probe specific for *gfp* or *rep* by standard methods. Infectious particle titers of AAV stocks carrying the *rep* and *cap* gene were determined by immunofluorescence. 3×10^3 HeLa cells were seeded on 6-well object slides, infected with serial dilutions of AAV stocks and co-infected with adenovirus 5 to provide helper functions. 48 h later expression of viral Rep proteins was detected with Cy3-labeled 76/3 monoclonal antibody (Cy3 mono-Reactive Dye Pack, Amersham, according to the manufacturer's protocol). Infectious particle titers of the GFP encoding virus stocks were determined by infecting irradiated HeLa cells (120 Gy from a ¹³⁷Cs gamma irradiation source) with serial dilutions of the AAV preparation in a 12-well plate. After 48 h cells were harvested and assayed for GFP expression by fluorescence-activated cell sorting (FACS).

Labeling Reactions. Labeling of the AAV capsid with Cy5 was carried out with Fluoro Link Cy5 monofunctional dye (Amersham Pharmacia, Freiburg). Cy5-labeling of the plasmid pRep was performed with Cy5 ULS labeling kit (Amersham Pharmacia, Freiburg) according to the manufacturer's protocols.

Biotinylation of AAV. AAV (1×10^{12} genomic particles) in PBS was treated with 180 nmol of NHS-LC-Biotin (sulfosuccinimidyl 6-(biotinamido) hexanoate). After incubation for 3 h at room temperature (RT), the virus was separated from unreacted biotin by gel-filtration. The biotinylated AAV stock was stored at 80°C. Efficiency of this labeling reaction was controlled by ELISA and Western blotting. For the ELISA purified A20 antibody (200 ng per well) was coated onto 96-well cell culture plates (Costar) in PBS. After blocking with 6% BSA in PBS/0.05% Tween wells were incubated with serial dilutions of biotinylated AAV, and after washing with PBS/0.05% Tween incubated with peroxidase-conjugated streptavidin (Dianova, Germany). Colorimetric detection was done as described previously (Girod et al. 1999). For Western blot analysis 3×10^3 genomic AAV particles were separated on a 10% SDS-PAGE and blotted on nitrocellulose membrane using standard protocols. Biotin labeled capsid proteins were visualized with alkaline phosphatase-coupled streptavidin following established protocols (Harlow & Lane 1988).

Streptavidinylation of polylysine. Streptavidinylation of PLL was carried out as described previously (Wagner et al. 1992; Wagner et al. 1990). Briefly, 336 nmol SPDP (heterobifunctional reagent) dissolved in 100% ethanol was added to 5 mg streptavidin (Stav) dissolved in HBS (20 mM Hepes, 150 mM NaCl, pH 7.3), incubated at RT, and purified by gel-filtration (Sephadex G-25, Pharmazia). 78 nmol of Stav modified with 192 nmol of dithiopyridine linker was obtained. PLL₂₂₅ (average chain length of 225 residues) was also incubated with SPDP at RT. Then β -Mercaptoethanol was added to reduce the disulfide group, and after gel-filtration (Sephadex G-25) 60 nmol PLL₂₂₅ modified with 211 nmol of mercaptopropionate linker was obtained (3.5 linkers for each PLL₂₂₅ chain). The modified Stav was added and reaction was carried out in HBS at RT overnight. The Stav-PLL₂₂₅ conjugate (Stpl₂₂₅) was recovered by chromatography on a Mono 2 column (Pharmazia) by salt-gradient elution, and extensively dialyzed against HBS pH 7.3.

Generation of virus-PLL/DNA conjugates. Virus-PLL/DNA conjugates were generated as follows. Biotinylated wtAAV (5×10^{10} physical particles) or Ad (5×10^8 physical particles) were treated with 30 ng of Stpl₂₂₅ or Stpl₂₅₀ in HBS. After a 15 min incubation at RT 300 ng plasmid DNA in 15 μ l HBS was added and incubated at RT for 15 min. Then 300 or 600 ng PLL (PLL₁₉, PLL₄₇, or PLL₁₂₀) in 15 μ l HBS was added and again incubated for 15 min before the solution was used for transfection of HeLa cells (4×10^4 cells per well in 48-well plates). GFP expression was analyzed 24 or 48 h post infection by fluorescence microscopy and FACS.

Atomic force microscopy (AFM) of PLL/DNA complexes. For generation of PLL/DNA for AFM indicated amounts of poly-L-lysine (PLL₆, PLL₁₉, PLL₄₇, or PLL₁₂₀) were added to 50 μ l plasmid DNA (40 μ g/ml of pUCGFP, pRC, or pXX6) in a total reaction volume of 100 μ l 20 mM HEPES and incubated at RT for 30 min. All buffer solutions were prepared with ultra-pure water and adjusted to pH 7.3. For samples preparation for AFM, freshly cleaved Muscovite mica (Bal-Tec AG, Balzers, Lichtenstein) was used as support, glued to a Teflon-laminated mounting. 7 μ l of PLL/DNA and 7 μ l adsorption buffer (20 mM Hepes / 300 mM KCl) were placed on the mica. After 15 min of adsorption, the samples were first gently rinsed with buffer (20 mM Hepes / 150 mM KCl) and then with ultra-pure water to remove weakly adsorbed particles, and blown dried with nitrogen gas. A commercial AFM (Nanoscope Multimode IIIa, Digital Instruments, Santa Barbara, CA) equipped with a 12- μ m piezo scanner was operated in standard tapping mode under ambient conditions. V-shaped silicon nitride cantilevers with normal spring constants around 48 N/m (90 μ m length; type NSCH 11, Silicon-MDT, Moscow) and resonance frequencies in air of $f_0 = 420$ kHz, and etched silicon probes with cantilever length of 125 μ m (type di TESP-I, Digital Instruments, Santa Barbara, CA, USA) and resonance frequencies between 311 and 393 kHz were used. Images were recorded with a slow scan rate of 1.1 Hz and below, and a resolution of 512 \times 512 pixels per image was chosen.

Single molecule imaging (single virus tracing, SVT). Single molecule imaging was performed in collaboration with Prof. Bräuchle at the Center for Nanoscience (LMU München). HeLa cells (3×10^3 per well) were seeded on 6-well object slides and infected with AAV constructs as described in the text. Measurements were performed as described previously (Seisenberger et al. 2001).

Results and Discussion

Generation of PLL/DNA complexes

PLL/DNA complexes have been previously used as vector systems for gene therapy, after coupling to ligand molecules or viruses like Ad which mediate cellular uptake. PLL/DNA coupled to Ad had a size of 100 to 200 nm in diameter. However, AAV has a small capsid of only 25 nm in diameter. Therefore, we had to minimize the size of the PLL/DNA, to reduce the risk of interference with receptor attachment and cell entry.

First, we analyzed the impact of plasmid size and PLL molecular weight (chain length) on complex formation and size of the PLL/DNA complexes. We therefore used PLL of varying chain length ($n = 6 - 120$) to complex plasmid DNA of various sizes (pUCGFP 3.8 kb, pRC 8.2 kb, and pXX6 23.0 kb). PLL/DNA-ratios between 0.5 and 3.0 were tested. All reactions were carried out in HEPES buffer without the addition of NaCl, because PLL/DNA tend to aggregate in saline buffers (personal communication). The dimensions of the polyelectrolyte complexes were analyzed by atomic force microscopy (AFM). The AFM images of PLL/DNA conjugates formed in HEPES buffer are shown in Figure 2. PLL₄₇ and PLL₁₂₀ efficiently condensed DNA to compact particles even at low PLL/DNA-ratios (ratio 1.0). In these complexes DNA was protected against DNase I degradation (data not shown). The shorter PLL₁₉ also yielded small particles, but there was still free DNA visible. Moreover, a high access of PLL₁₉ was necessary to complex DNA and render it resistant to DNase degradation. The smallest PLL with a chain length of 6 lysine residues was not able to complex plasmid DNA at any PLL/DNA-ratio tested. These results indicate that a minimal PLL chain length is needed in order to completely condense plasmid DNA to compact structures and render it resistant to nuclease activity. These results are supported by studies of Kwoh and colleagues (1999), who also made the observation that shorter PLL (e.g. PLL₁₉) did not complex DNA as efficiently as PLL₄₇ or PLL₁₂₀. In most cases the complexes were spherical particles with a size around 30 to 40 nm (Table 1). Only in a few cases, e.g. when PLL₁₂₀ was used for complex formation, could small rods (15 nm width and 80 nm length) also be detected. This is in contrast to other studies which observed besides spheres and rods mainly donut shaped structures (Kwoh et al. 1999; Wagner et al. 1991). Interestingly, the size of the PLL/DNA did not increase significantly with increasing PLL chain length and the plasmid size also did not have an apparent influence on particle diameter. Moreover, the larger plasmid pRC seemed to form complexes more easily than pUCGFP. In contrast to our

findings are the results of Wolfert and Seymour (1996) which have reported a larger difference in the average size of PLL/DNA with increasing PLL chain length. This discrepancy may reflect differences in the concentration of reactants during complex formation. Also the high PLL/DNA-ratio of 5 used in that study may attribute to their observation.

Table 1. Size of PLL/DNA complexes

	PLL/DNA ratio	pUCGFP	pRC	pXX6
PLL₆	no complex formation at any ratio		n.d.	n.d.
	2.0	25 – 45 nm	n.d.	n.d.
PLL₁₉	2.4	30 – 45 nm	n.d.	15 – 25 nm
	3.0	20 – 30 nm	n.d.	20 – 25 nm
PLL₄₇	1.0	25 – 50 nm	20 – 40 nm	15 – 30 nm
	2.0	25 – 40 nm	15 – 25 nm	20 – 30 nm
PLL₁₂₀	1.0	30 – 50 nm	30 – 45 nm	30 – 50 nm
	2.0	20 – 45 nm	15 – 25 nm	30 – 60 nm

n.d., not determined

Taken together PLL₄₇ and PLL₁₂₀ were able to efficiently complex plasmid DNA to small spherical particles of approx. 20–45 nm in diameter. At a PLL/DNA-ratio of 1 and 2 DNA was completely condensed and protected from endonucleases. Such complexes have a suitable size for coupling to the AAV capsid.

Coupling of PLL/DNA complexes to AAV

For coupling of PLL/DNA complexes to viral capsids especially adenovirus different methods have been described in literature (Wagner et al. 1992). In these settings a biotin-streptavidin bridge seemed to work most efficiently. We therefore decided to couple PLL/DNA to the AAV capsid also via a biotin-streptavidin bridge. Biotin and streptavidin (Stav) have a strong binding affinity ($K_d \sim 10^{-15}$ mol/l), comparable to a covalent linkage.

Biotin was covalently linked to AAV and the efficiency of this labeling reaction was analyzed by ELISA (data not shown). Western blotting (Fig. 3A) demonstrated that all three capsid proteins are accessible for biotinylation. Moreover, this assay also demonstrated that the AAV-linked biotin is still able to efficiently bind Stav which is essential for successful coupling. To estimate how many biotin molecules are bound per virion, analogous labeling reactions were done with Cy5 and AAV, and the Cy5-labeled virus was analyzed by single molecule spectroscopy (single virus tracing, SVT) (Seisenberger et al. 2001). These experiments revealed that 1 to 2 dye molecules are attached to a single virion in agreement with previous observations (Bartlett & Samulski 1998). We therefore assumed that the same amount of biotin molecules are bound. Next we tested whether biotinylation interferes with AAV infection. HeLa cells were infected with biotinylated AAV and internalized virus was detected with an antibody directed against biotin. As figure 3B shows, biotinylated AAV efficiently transduces HeLa cells, indicating that this labeling reaction does not interfere with the viral infection process. Additionally, infectious titer assays were performed to confirm these data. Also in these assays only a minor influence on the transduction efficiency was observed, namely a reduction of factor 2 as compared with unmodified virus (data not shown).

For coupling of PLL/DNA to AAV and efficient transduction of these conjugates it is essential that the cellular uptake of AAV is not hindered by binding of Stav to the biotinylated virus. We therefore analyzed the transduction efficiency of the AAV-biotin/Stav construct (AAV-Stav) by SVT. With this method single labeled molecules can be detected on living cells in real time. This has the advantage that the fate of single virions can be followed and information over unusual behavior compared to unmodified virus can be easily obtained. For these experiments biotinylated wtAAV was incubated with a 100 fold molar excess of Cy5-labeled Stav (Stav^{Cy5}), the conjugate was purified by gel-filtration (Sephadex G100) to remove unbound Stav^{Cy5}, and HeLa cells were infected (Fig. 4). 380 trajectories were measured. In solution, complexes moved with a diffusion coefficient of $D = 2.61 \mu\text{m}^2/\text{s}$. This

is significantly slower than expected when compared with unmodified wtAAV ($D = 11.2 \mu\text{m}^2/\text{s}$). Two explanations are possible. First, Stav tends to stick to surfaces like glass slides. This could mimic a slower diffusion coefficient in these measurements. On the other hand, as Stav has four binding sites for biotin, it is possible that more than one biotinylated AAV is bound to Stav. In this case the analyzed particles would be bigger and therefore also move with a slower diffusion coefficient in solutions than a single virion. From the 380 analyzed trajectories 261 had no membrane contact at all. In 96 of the trajectories the AAV-Stav complex had membrane contact without entering the cell, and 23 trajectories were observed inside the cell. This gives an uptake efficiency of 19%, which is in the range of the uptake efficiency observed for wtAAV without Stav (penetration efficiency of 13%) (Seisenberger et al. 2001). Two examples of trajectories are given in figure 4A. The images in the top row show a Stav-linked virion in contact with the cellular membrane. In the bottom row an AAV-Stav^{Cy5} that has entered the cell and moves through the cytoplasm is depicted. As control Stav^{Cy5} without AAV was also analyzed to test whether the observed trajectories might have been caused by Stav^{Cy5}, which possibly had detached from the virion after gel-filtration. As expected Stav^{Cy5} alone was not able to enter the HeLa cells. Additionally, we analyzed trajectories of Stav linked to an AAV that carried a Cy3-labeled viral DNA (Fig. 4B). Similarly, conjugates in contact with the membrane and inside the cell were observed. Based on these findings we conclude that AAV-Stav complexes enter the cell as intact conjugate with AAV mediating the uptake by interacting with its cellular receptors.

Taken together, AAV could be easily labeled with biotin without negative effects on the viability of the virus. After biotinylation AAV was accessible for Stav binding and the AAV-Stav conjugate was able to transduce HeLa cells with an efficiency comparable to the unmodified virus. These results provided the basis to couple PLL/DNA complexes to AAV via biotin-streptavidin linkage.

Analysis of transduction with AAV-PLL/DNA conjugates

After the successful linkage between Stav and the biotinylated AAV we set out to analyze the coupling of PLL/DNA complexes to virus particles to study transduction. First, we analyzed the coupling of PLL/DNA to adenovirus to optimize the reaction parameters in an established system. Biotinylated Ad was incubated with streptavidinylated PLL₂₂₅ (Stpl₂₂₅), pUCGFP plasmid was added and finally PLL₄₇ or PLL₁₂₀ in a PLL/DNA-ratio of 1 or 2 was added to complex the plasmid DNA to compact structures. HeLa cells were infected with these

Ad-PLL/DNA conjugates and GFP expression was assayed by FACS analysis 24 h later. As a control PLL/DNA complexes alone and virus conjugates generated without Stpl₂₂₅ were used to test for unspecific coupling and/or transduction. The results of this transduction assay are given in figure 5. As expected, transduction with PLL/DNA alone was not detectable at any ratio tested in agreement with previously published data (Curiel et al. 1991; Curiel et al. 1992; Zenke et al. 1990). In contrast, when Ad was incorporated into the virus-PLL/DNA conjugates (PLL/DNA-ratio of 1) 31% and 36% of the cells were positive for GFP expression when using PLL₄₇ or PLL₁₂₀, respectively. Unspecific linkage of the PLL/DNA to the virion (Fig. 5, w/o Stpl) due to charge interactions showed only a minor effect (5% and 7 %). The situation was different when Ad-PLL/DNA were generated with PLL₄₇ or PLL₁₂₀ at a PLL/DNA-ratio of 2. The transduction rate with 16% for PLL₄₇ and 13% for PLL₁₂₀ was significantly lower. Moreover, transduction of conjugates generated without Stpl yielded with 21% (PLL₄₇) and 16% (PLL₁₂₀) positive cells even higher transduction rates (Fig. 5). This suggests that at a PLL/DNA-ratio of 2 the linkage between the PLL/DNA and the Ad virion might be achieved by electrostatic interactions between the positively charged PLL/DNA and the negatively charged Ad capsid surface and not exclusively by biotin-streptavidin binding. In addition, transduction with Ad-PLL/DNA formed with PLL₁₉ was analyzed. These conjugates were not able to transduce HeLa cells at any ratio tested (data not shown) which confirmed our observations made in the AFM analysis that PLL₁₉ only insufficiently complexes DNA.

For coupling of PLL/DNA to AAV particles we therefore employed complexes generated with PLL₁₂₀, since virus conjugates generated with PLL₁₂₀ yielded the highest transduction rates. Although PLL/DNA-ratios of 2 resulted in unspecific linkage of PLL/DNA complexes to Ad, we decided to use both, ratio 1 and 2, for formation of AAV-PLL/DNA conjugates. In contrast to Ad AAV has clusters of positive charges on its capsid surface (Xie et al. 2002), therefore these unspecific interactions should be rather unlikely to occur with AAV.

First, properties of AAV-PLL/DNA conjugates were analyzed by SVT. Complexes were generated as described above and PLL₁₂₀ was used to complex Cy5-labeled pRep plasmid at a ratio of 1 or 2. These complexes were analyzed for diffusion properties and particle size. In solution AAV-PLL/DNA moved with a diffusion coefficient of $D = 4.58 \mu\text{m}^2/\text{s} \pm 0.03$ (ratio 1) and $D = 4.56 \mu\text{m}^2/\text{s} \pm 0.4$ (ratio 2). Based thereon the size of the measured complexes was calculated to be approx. 60nm for both ratios. We therefore assume that these

conjugates consist of one PLL/DNA complex (approx. 30 nm) linked to one AAV particle (25 nm) rather than a multimeric aggregate. In a next step HeLa cells were transduced with AAV-PLL/DNA and the traces of the conjugates were monitored by SVT. For AAV-PLL₁₂₀/DNA (ratio 1) 123 trajectories and for AAV-PLL₁₂₀/DNA (ratio 2) 108 trajectories were analyzed. Several membrane contacts as well as cellular entry of both AAV-PLL/DNA were observed (Fig. 6A). Uptake efficiencies, however, were significantly lower than measured for AAV-Stav alone, possibly due to steric hindrance of the interaction of AAV with its cellular receptor. Nonetheless, these measurements indicate that transduction with AAV-PLL/DNA is feasible, although transduction efficiencies need further improvement. To confirm these observations transduction by AAV-PLL/DNA containing wtAAV and pUCGFP was analyzed by convectional fluorescence microscopy and FACS analysis. For complex formation PLL₁₂₀ was applied in a PLL/DNA-ratio of 1 or 2. HeLa cells were infected and 48 h later analyzed for GFP expression. As a negative control PLL/DNA complexes alone were used. One representative experiment of this transduction assay is given in figure 6B. As seen in the FACS image, cells were clearly positive for GFP expression after transduction with AAV-PLL₁₂₀/pUCGFP (ratio 1), while the control transfections were completely negative. Thus, it is reasonable to assume that the PLL/DNA have entered cells conjugated to AAV, confirming the observations from the SVT experiments. Transduction efficiencies, however, were rather low (4% GFP positive cells), and need further improvement before the system can be applied in an *in vivo* model. Studies are therefore currently ongoing to improve the transduction efficiency. Additionally, SVT experiments with double labeled AAV-PLL/DNA, Cy3-labeled viral DNA and Cy5-labeled exterior DNA, are under investigation to get a more detailed insight in the uptake route of these constructs.

Taken together, our study demonstrates for the first time that co-transduction of an AAV vector and a transgene cassette attached to the viral capsid is possible. This provides the basis for specifically integrating rAAV vectors for the use in human gene therapy. Targeted integration of virus vectors is of striking importance for gene therapy applications, especially with regard to the risk of insertional mutagenesis of randomly integrating vectors (retroviral vector systems). Moreover such vector constructs give the opportunity for many other applications: simultaneous gene transfer of regulating factors or more than one therapeutic gene would be conceivable. Hence, these vector constructs should develop to become useful tools not only to restore site-specific integration of rAAV but also to expand the limited coding capacity of commonly used AAV vectors for human gene therapy.

Acknowledgments

We are grateful to Christian Plank for helping to generate AAV-PLL/DNA conjugates. Furthermore we thank Kristin Leike for excellent technical assistance and Susan King for kindly reading this manuscript. This work was supported by the Bayerischer Forschungsverbund Grundlagen Gentechnischer Verfahren (FORGEN) and the Deutsche Forschungsgemeinschaft (SFB 455).

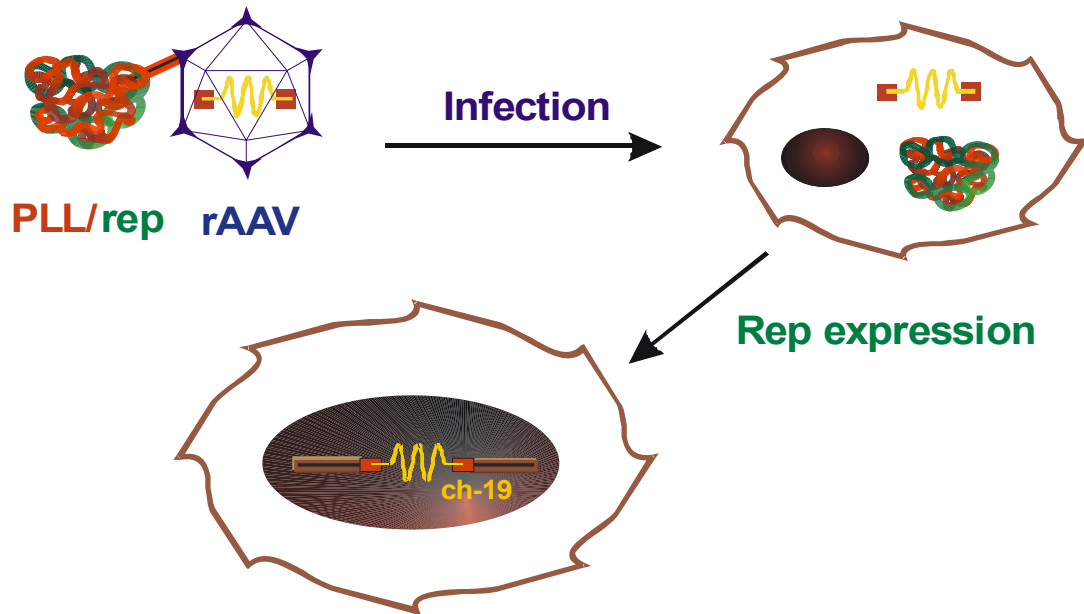


Figure 1. Model for specific integration of AAV-PLL/DNA conjugates. Plasmid DNA coding for the viral Rep protein is condensed by PLL to compact particles which can be directly linked to the AAV capsid. After transduction with these AAV-PLL/DNA conjugates PLL is degraded and the DNA transported to the nucleus. After expression of the AAV Rep proteins targeted integration of the ITR flanked transgene cassette takes place.

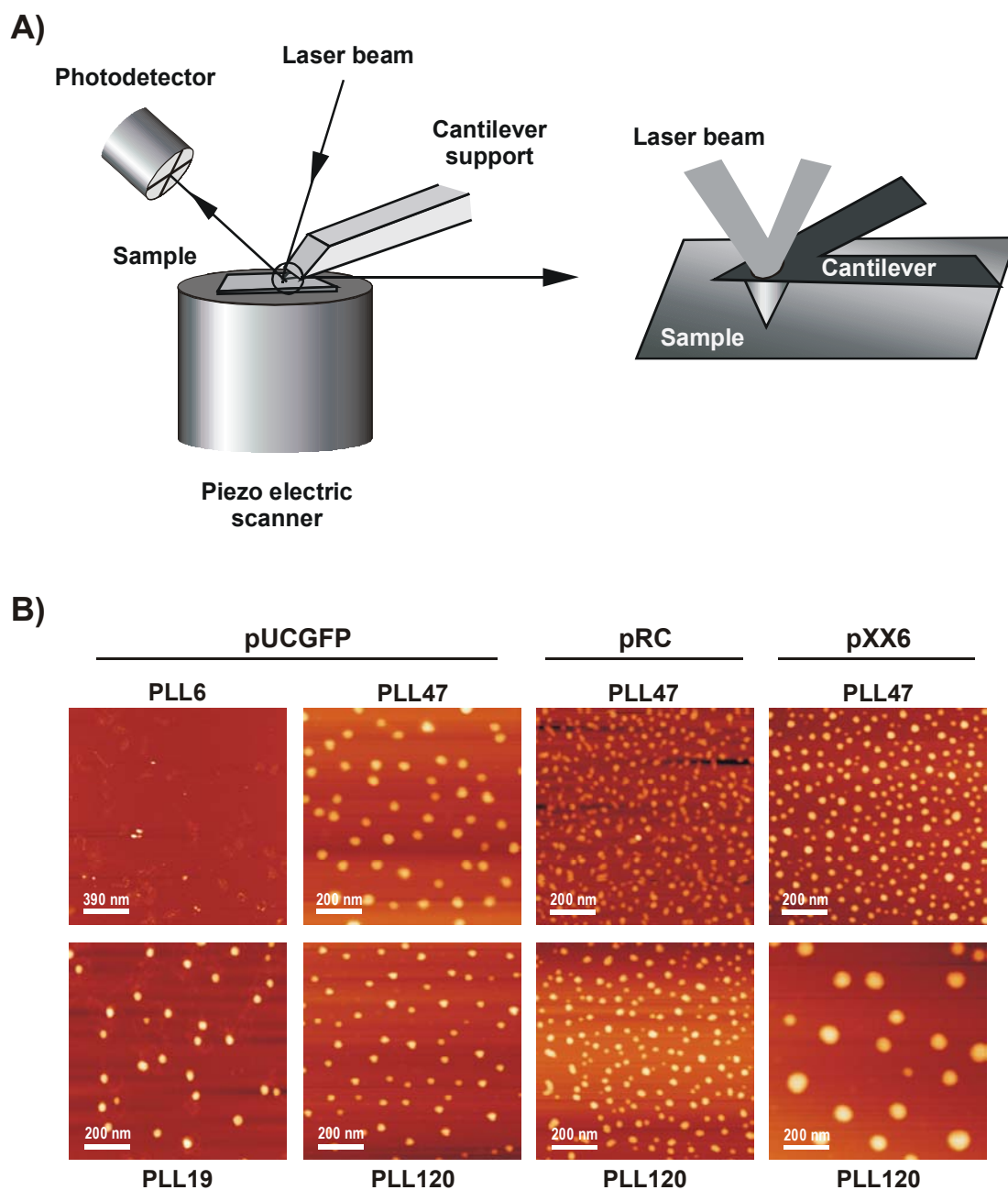


Figure 2. Analysis of PLL/DNA by atomic force microscopy (AFM). (A) Setup of an atomic force microscope for tapping mode measurements under ambient conditions. The sample is placed on a piezo-electric scanner, a laser beam is focused on the cantilever which is fixed to a cantilever support, and the reflected light of the laser beam is captured by a photodetector. The tapping mode operates by scanning a tip, attached to the end of a vibrating cantilever, across the sample surface, so that it is in intermittent contact with the surface; the cantilever amplitude is maintained constant by altering the vertical position of the piezo-electric scanner. The height image is computed from the changes in vertical position. (B) AFM images of PLL/DNA complexes formed at a PLL/DNA ratio of 2.0. The height of the images is represented by a graded brown-white scale, with the white color indicating a height of more than 50 nm (PLL₁₉/pUCGFP), 40 nm (PLL₄₇/pUCGFP), 25 nm (PLL₁₂₀/pUCGFP), 35 nm (PLL₄₇/pRC), 25 nm (PLL₁₂₀/pRC), and 45 nm (PLL₄₇/pXX6 and PLL₁₂₀/pXX6) above the mica.

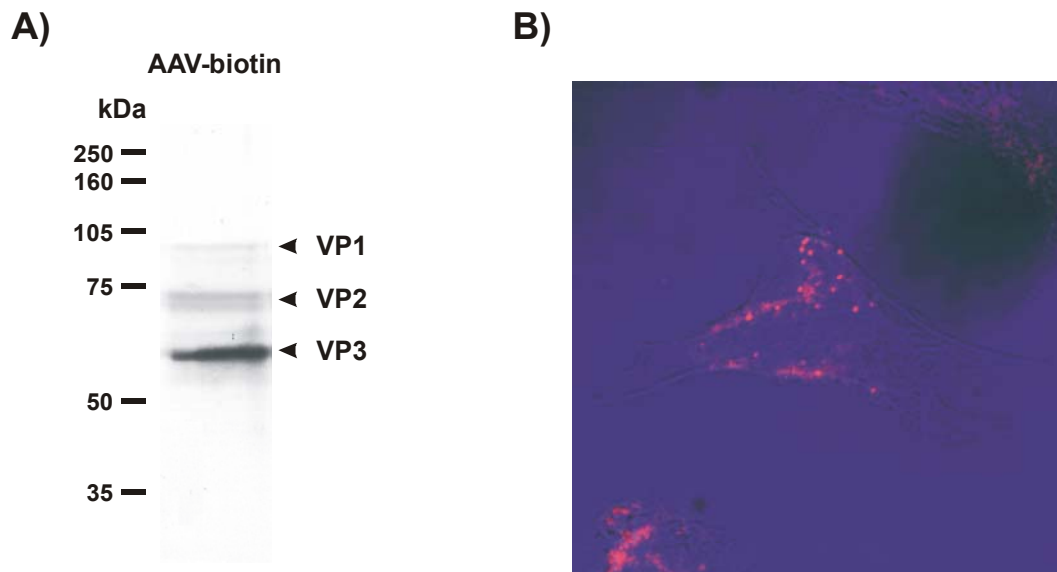


Figure 3. Biotinylation of AAV. (A) Western Blot analysis of AAV-biotin. Biotinylated capsid proteins (VP1, VP2, and VP3) were separated on a denaturing gel and detected by streptavidin labeled with alkaline phosphatase (indicated by arrow heads). (B) Fluorescence image of HeLa cells infected with biotinylated AAV. AAV-biotin was detected by a Cy3-labeled biotin-antibody 24 h after infection.

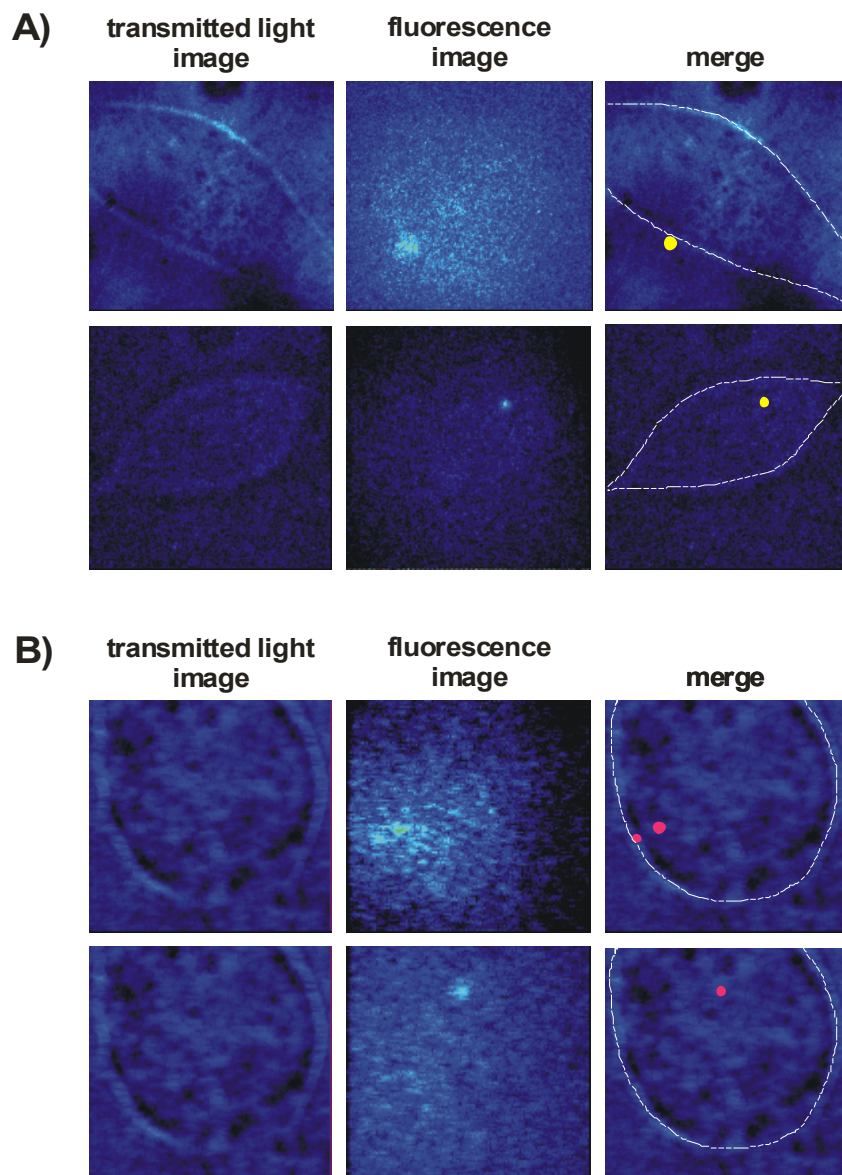


Figure 4. Analysis of AAV-Stav by single virus tracing. (A) AAV-biotin was coupled to Cy5-labeled Stav and HeLa cells were infected. Single AAV-Stav^{Cy5} particles were detected by excitation with red laser light of 633 nm. (B) Similarly, Stav was bound to AAV containing Cy3-labeled DNA and particles were detected by green light of 532 nm.

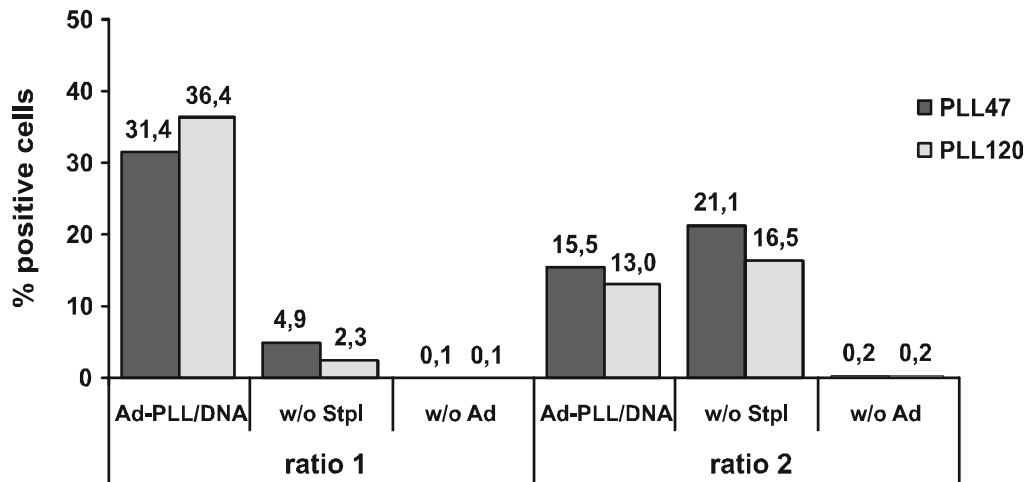


Figure 5. Transduction with Ad-PLL/DNA. pUCGFP was complexed with PLL₄₇ or PLL₁₂₀ at a PLL/DNA ratio of 1 or 2 and linked through Stav to biotinylated Ad. These conjugates were used to infect HeLa cells and the number of GFP expressing cells was determined by FACS analysis 48 h later. As control conjugates were formed without the addition of Stpl or Ad to test for unspecific linkage and transduction.

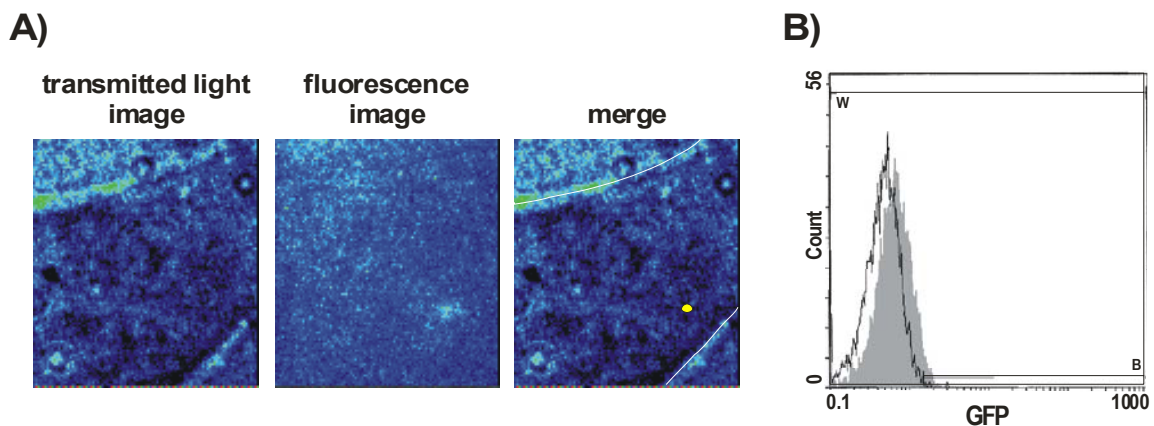


Figure 6. Transduction with AAV-PLL/DNA. (A) HeLa cells were infected with AAV-PLL₁₂₀/pRep^{Cys5} (ratio 1) and trajectories were monitored at 633 nm. (B) Infection of HeLa cells with AAV-PLL₁₂₀/pGFP (ratio 1) and analysis of GFP positive cells in comparison to the negative control by FACS.

CHAPTER IV

Genetic modifications of the adeno-associated virus type 2 capsid reduce the affinity and the neutralizing effects of human serum antibodies

published as:

Huttner NA, Girod A, Perabo L, Edbauer D, Kleinschmidt JA, Büning H, and Hallek M. (2003)

Genetic modifications of the adeno-associated virus type 2 capsid reduce the affinity and the neutralizing effects of human serum antibodies. *Gene Ther.* (in press)

Summary

The high prevalence of human serum antibodies against adeno-associated virus type 2 (AAV) vectors represents a potential limitation for *in vivo* applications. Consequently, the development of AAV vectors able to escape antibody binding and neutralization is of importance. To identify capsid domains which contain major immunogenic epitopes, six AAV capsid mutants carrying peptide insertions in surface exposed loop regions (I-261, I-381, I-447, I-534, I-573, I-587) were analyzed. Two of these mutants, I-534 and I-573, showed an up to 70% reduced affinity for AAV antibodies as compared to wild-type AAV in the majority of serum samples. In addition, AAV mutant I-587 but not wild-type AAV efficiently transduced cells despite the presence of neutralizing antisera. Taken together, the results show that major neutralizing effects of human AAV antisera might be overcome by the use of AAV capsid mutants.

Introduction

The human parvovirus adeno-associated virus type 2 (AAV) is a promising vector for human somatic gene therapy. Recombinant AAV vectors (rAAV) have many advantages in comparison to other vector systems, including the ability to transduce both dividing and non-dividing cells, long-term gene expression *in vitro* and *in vivo*, and the apparent lack of pathogenicity. AAV has a broad host range and transduces a wide variety of tissues, including muscle, lung, liver, brain, and hematopoietic cells (Fisher-Adams et al. 1996; Flotte et al. 1993; Halbert et al. 2000; Kaplitt et al. 1994; Russell & Kay 1999; Snyder et al. 1997; Xiao et al. 1996). In a potential model of the infection process, AAV first interacts with its primary receptor heparan sulfate proteoglycan (HSPG), mediating the attachment of the virions to the host cell membrane (Summerford & Samulski 1998). In addition, two types of co-receptors, $\alpha_v\beta_5$ integrin and fibroblast growth factor receptor 1 (FGFR), have been suggested, which seem to be involved in the subsequent internalization process (Qing et al. 1999; Summerford et al. 1999). However, conflicting results were reported about the contribution of these co-receptors (Qiu & Brown 1999; Qiu et al. 1999). Following receptor binding, AAV enters the cell via a dynamin-dependent endosomal pathway (Bartlett et al. 2000; Duan et al. 1999). After acidification of endosomes, viral particles are released into the cytoplasm and rapidly

transported to the nucleus, involving microfilaments and microtubules, before they enter the nucleus (Douar et al. 2001; Sanlioglu et al. 2000; Seisenberger et al. 2001).

The capsid of wild-type AAV (wtAAV) harbors a linear, single-stranded DNA genome of 4.7 kb, which contains two open reading frames (ORF), *rep* and *cap*, flanked by the inverted terminal repeats (ITR). The 5' ORF encodes the four nonstructural proteins (Rep78, Rep68, Rep52, and Rep40), which are required for replication, transcriptional control and site-specific integration. The three structural proteins, designated VP1, VP2, and VP3, are encoded in the 3' ORF and transcribed from the same promoter (p40) using alternate splicing and different translational initiation codons. The small icosahedral capsid, which is only 25 nm in diameter, is composed of 60 subunits with a relative stoichiometry of about 1:1:8 for VP1, VP2, and VP3 (Kronenberg et al. 2001). Recently the atomic structure of AAV has been determined (Xie et al. 2002). Each subunit has a β -barrel motif, which is highly conserved among parvoviruses. Between the strands of the β -barrel core large loop insertions are found that constitute the majority of the capsid surface. These loop insertions seem to interact with antibodies and cellular receptors and are highly variable among related parvoviruses. The most prominent features of the capsid are the threefold-proximal peaks, which cluster around the threefold axis (Xie et al. 2002). Positions on the AAV capsid where interaction with HSPG takes place have been determined (Rabinowitz et al. 1999; Wu et al. 2000). They map to a positively charged region on the side of the threefold-proximal peaks (Xie et al. 2002). Moreover, epitopes of monoclonal antibodies (mAb) which interfere with the AAV infection process (A20 and C37-B) have also been mapped to this threefold axis (Wobus et al. 2000; Xie et al. 2002).

Although knowledge is rising about basic AAV biology, there are still obstacles for the application of AAV as vector system for somatic gene therapy. One major problem is the high prevalence of AAV specific antibodies (Ab) in the human population. 50 to 96% are seropositive for AAV Ab, and 18 to 67.5% of them have neutralizing Ab, depending on age and ethnic group (Chirmule et al. 1999; Erles et al. 1999; Moskalenko et al. 2000). Especially these preexisting neutralizing Ab have profound implications for the application of AAV in human gene therapy. Animal experiments have shown that neutralizing Ab greatly reduce or even prevent transgene expression after readministration of the vector (Fisher et al. 1997; Xiao et al. 2000; Xiao et al. 1996). Different mechanisms for neutralization of viral infections have been described (Smith 2001): (i) aggregation of viral particles, (ii) induction of conformational changes in the capsid, (iii) interference with receptor attachment, and

(iv) inhibition of uncoating due to virion stabilization. In related parvoviruses immunogenic sites are formed by highly variable and accessible domains on the capsid surface, which can be generally found in the threefold spike region (Fig. 1): on the tip and the shoulder of the spike, and between the twofold dimple and the spike (Chapman & Rossmann 1993). In canine parvovirus (CPV) two dominant neutralizing epitopes, which are both conformational epitopes, are found on the shoulder of the threefold spike (epitope A: residues 93, 222, 224, 426 and epitope B: residues 299, 300, 302 of VP2) (Strassheim et al. 1994). Similarly, the epitopes of two monoclonal neutralizing Ab of B19 parvovirus have also been mapped to the threefold spike region (Chipman et al. 1996). Therefore it is possible that immunogenic sites of AAV are also located in variable regions of the threefold spike region.

In a previous study we had generated six AAV capsid mutants bearing an integrin specific peptide ligand (L14) insertion at position 261, 381, 447, 534, 573, or 587 of the AAV VP1 protein (Girod et al. 1999). These positions were originally selected based on structural alignments with the related parvoviruses CPV, B19 and feline panleukopenia virus (FPV), with regard to flexible, highly variable, and immunogenic domains of these viruses (see Fig. 1; Girod et al., 1999). Indeed, we and others could show that the insertion sites are displayed on the capsid surface (Girod et al. 1999; Grifman et al. 2001; Nicklin et al. 2001; Wu et al. 2000) and the recently published atomic structure of AAV confirmed the localization of the selected positions in surface exposed loop regions (Xie et al. 2002). Moreover, binding studies with the neutralizing mAb A20 and C37-B demonstrated that the mutations impaired their affinities for the AAV capsid. This indicated that immunogenic domains had been affected by the capsid mutations (see Fig. 2a; Wobus et al., 2000). In this paper we analyzed these six AAV capsid mutants with polyclonal human serum samples in binding and neutralization assays. This allowed us to characterize immunogenic and neutralizing regions on the AAV capsid.

Results

AAV antibodies from human serum samples have a reduced affinity for AAV insertion mutants

To determine major antigenic domains involved in the humoral immune response of humans against the capsid of AAV, we analyzed the ability of human antisera to recognize AAV capsid mutants carrying a 14 amino acid (aa) peptide (L14, QAGTFALRGDNPQG) of the laminin fragment P1 inserted at positions 261, 381, 447, 534, 573, or 587 (Girod et al. 1999).

In a first step, the capsid morphology of the six different VP3 mutants was characterized by electron microscopy (EM). All viral preparations showed an EM morphology similar to wtAAV and contained predominantly intact particles (data not shown).

Table1. Titers of AAV stocks

Virus stocks	Physical particles/ml ¹	Infectious particles/ml ²
wtAAV	4.9 x 10 ¹²	7 x 10 ⁹
I-261	1.0 x 10 ¹²	1 x 10 ⁴
I-381	1.0 x 10 ¹²	<1 x 10 ²
I-447	2.2 x 10 ¹²	1 x 10 ⁶
I-534	3.5 x 10 ¹²	<1 x 10 ²
I-573	3.1 x 10 ¹²	<1 x 10 ²
I-587	2.5 x 10 ¹²	6 x 10 ⁶
rAAV	2.5 x 10 ¹²	3 x 10 ⁹
rAAV-587/L14	3.0 x 10 ¹¹	4 x 10 ⁶
rAAV-587/MecA	1.3 x 10 ¹²	2 x 10 ⁸

¹ Physical particle titers were determined by EM for *rep/cap*-containing particles and by dot-blot analysis for recombinant vectors

² Determined on HeLa cells by immunofluorescence for preparations containing a *rep* gene, and by FACS analysis for GFP encoding particles

The presence of antibodies against wtAAV was then analyzed in 65 human serum samples. In an ELISA, 43 out of 65 serum samples (66%) were positive for AAV antibodies. Out of these 43 seropositive samples, 29 sera with a high titer of AAV specific antibodies (OD>0.6 after subtraction of background) were selected for further analysis. The binding affinity of these 29 serum samples to the six AAV insertion mutants (I-261, I-381, I-447, I-534, I-573, and I-587) was analyzed in an ELISA and compared to wtAAV. Identical numbers of particles of the respective insertion mutants and of wtAAV, as determined by EM (Table 1) and confirmed by Western blotting, were coated on the ELISA plates. Binding of serum Ab to wtAAV was set as 100%, and the change in serum binding to the AAV mutants was determined. Several patterns of interaction of human sera with AAV mutants could be distinguished (Table 2). One group of serum samples, designated *class A*, reacted with all six AAV mutants in a way similar to wtAAV (e.g. serum P17, Fig. 2b). This was the case for 10 out of 29 sera (34%). A second group of serum samples (12 out of 29, 42%), designated *class B*, displayed a reduced binding affinity only to mutants I-534 and I-573 (e.g. serum P37, Fig. 2b). The average reduction for both, I-534 and I-573, was 31% as compared with wtAAV. A third and smaller group of serum samples (7 out of 29, 21%), *class C*, additionally showed a reduced affinity for the other 4 capsid mutants (e.g. serum P26, Fig. 2b). On average, binding to these 4 mutants was decreased by 7% (I-381) to 26% (I-447) (Table 2). Nevertheless, insertions at positions 534 and 573 reduced binding of serum antibodies to the capsid more than insertions at other positions, i.e. by 51% and 45%, respectively (Table 2). Interestingly, binding of *class C* sera to these two capsid mutants was more affected than binding of *class B* serum samples. The observed differences in binding affinity did not significantly change when using various serum dilutions.

Strikingly, mutations at positions 534 or 573 had an effect on the affinity of human antisera in 19 of 29 cases. In some cases, serum binding was reduced up to 70%. In 7 serum samples, mutations at position 261, 381, 447, or 587 also resulted in a reduced binding affinity, albeit to a smaller extent. Based on these findings, we conclude that insertions in positions 534 or 573 affected major antigenic determinants of the humoral immune response against the AAV capsid.

Table 2.
Binding of seropositive human sera to AAV insertion mutants compared to wtAAV

Class¹	Serum	I-261	I-381	I-447	I-534	I-573	I-587
A	P1	—	—	—	—	—	—
	P2	—	—	—	—	—	—
	P6	—	—	—	—	—	—
	P14	—	—	—	—	—	—
	P17	—	—	—	—	—	—
	P19	—	—	—	—	—	—
	P24	—	—	—	—	—	—
	P31	—	—	—	—	—	—
	P47	—	—	—	—	—	—
	P60	—	—	—	—	—	—
	Reduction²	0.3% ± 6.6%	0.2% ± 4.7%	7.5% ± 5.5%	0.0% ± 7.4%	3.9% ± 8.3%	- 2.3% ± 5.4%
B	P5	—	—	—	↓	↓↓	—
	P7	—	—	—	↓↓↓	↓↓	—
	P16	—	—	—	↓↓	↓	—
	P27	—	—	—	↓↓↓	↓↓	—
	P29	—	—	—	↓	↓	—
	P32	—	—	—	—	↓	—
	P33	—	—	—	↓	↓	—
	P37	—	—	—	↓↓	↓↓	—
	P48	—	—	—	↓↓	↓↓	—
	P51	—	—	—	↓	↓↓	—
	P53	—	—	—	↓	↓↓	—
	P59	—	—	—	↓	↓	—
		Reduction	3.4% ± 5.8%	1.8% ± 8.9%	9.2% ± 5.5%	30.9% ± 13.5%	30.7% ± 7.2%
C	P3	↓	—	↓↓	↓↓↓	↓↓↓	—
	P26	↓	—	↓	↓↓↓	↓↓↓	↓
	P35	—	—	↓↓	↓↓	↓↓	—
	P40	—	↓↓	—	↓↓	↓↓	—
	P54	—	—	↓	↓↓↓	↓↓	—
	P57	↓	↓	↓↓	↓↓	↓↓	↓
	P65	↓	—	↓	↓↓↓	↓↓↓	↓
		Reduction	12.5% ± 10.6%	6.8% ± 9.9%	25.8% ± 11.7%	51.3% ± 10.9%	44.8% ± 5.0%
mAb	A20	↓↓↓↓↓	↓↓↓↓↓	—	↓↓↓	↓↓↓	—
	C37-B	↓↓↓↓↓	—	↓↓↓	↓↓↓↓↓	↓↓↓↓↓	↓↓↓↓↓

The symbols —, ↓, ↓↓, ↓↓↓ and ↓↓↓↓ illustrate a reduction in affinity in comparison to wtAAV of 0-14%, ≥15%, ≥25%, ≥50% and 100%, respectively.

¹ Classification of the serum samples: A, affinity to insertions mutants like to wtAAV; B, reduced affinity to I-534 and I-573; C, reduced binding with I-534, I-573 and other capsid mutants

² The mean reduction and standard deviation are given

Transduction of HeLa cells by rAAV-587/L14 is not inhibited by preexisting neutralizing antibodies in human serum samples

A detailed understanding of major immunogenic domains on the AAV capsid is not only important with regard to the binding of serum antibodies to the virus and its subsequent neutralization by the immune system, but also with regard to the existence of neutralizing antibodies that directly inhibit infection of the target cells by AAV vectors. To analyze the interference of different human antisera with AAV transduction, we used a recombinant AAV vector carrying the L14 ligand at position 587 (rAAV-587/L14) to determine whether this modification would block the neutralizing ability of human antisera. Unfortunately, only rAAV-587/L14 could be purified to sufficiently high titers to perform these studies, therefore the other insertion mutants were not further tested (Table 1).

First, we determined the presence of neutralizing Ab in human serum samples. The 43 positive serum samples were tested in a neutralization assay with an AAV vector coding for GFP, which carried the wild-type capsid (rAAV). rAAV was incubated with serial dilutions of serum samples prior to transduction of HeLa cells. Thereafter, the number of GFP expressing cells was assessed by FACS analysis. Neutralizing titers were defined as the serum dilution where transduction was reduced by 50% (N_{50}). Serum samples were considered as neutralizing when the N_{50} was 1:320 or higher. 31 of these 43 serum samples (72%) contained neutralizing Ab against AAV, in agreement with previously published data (Erles et al. 1999).

15 of these 31 serum samples, equally distributed over the above mentioned three classes (5 class A, 6 class B, and 4 class C), were selected for further analysis. The effect of these serum samples on the transduction of HeLa cells by rAAV-587/L14 as compared with rAAV was determined (Fig. 3a). In addition, the neutralizing mAb C37-B and an anti-L14 serum (see Materials and Methods) were tested. For these experiments identical transducing particle numbers of rAAV-587/L14 and rAAV were used. Both vectors were incubated with serial dilutions of neutralizing serum samples prior to transduction of HeLa cells. For all serum samples tested, transduction by rAAV-587/L14 was 8 up to 64 fold less reduced than transduction by rAAV (mean 15 fold). In 13 out of 15 serum samples, transduction by rAAV-587/L14 was only slightly impaired, with neutralizing titers of 1:80 or lower, demonstrating the ability of rAAV-587/L14 to escape the effects of neutralizing Ab (Fig. 3a). Strikingly, rAAV-587/L14 was able to escape the neutralizing Ab in serum P47 at any dilution tested, and serum samples P17, P31 and P37 reduced transduction only at a dilution of 1:20, where unspecific interactions could not be excluded. Figures 3b and 3c show one

representative experiment with serum P35, which completely inhibited transduction by rAAV at a 1:80 dilution (Fig. 3b). In marked contrast, transduction by rAAV-587/L14 was not affected (Fig. 3c). Only two serum samples (P16 and P48) were able to neutralize rAAV-587/L14 transduction efficiently, with a N_{50} of 1:320. We assume that this was due to the high neutralizing Ab content in these serum samples, because transduction by rAAV-587/L14 still remained less affected than transduction by rAAV. As an additional control, the mAb C37-B was tested. C37-B is a neutralizing Ab that inhibits binding of AAV to the host cell (Wobus et al. 2000). It failed to bind I-587 in an ELISA, therefore it should not interfere with rAAV-587/L14 transduction. As expected, rAAV-587/L14 transduction was not neutralized by C37-B, while rAAV transduction could be totally inhibited by this antibody (data not shown). In marked contrast, anti-L14 serum, which was generated against the L14 ligand, neutralized rAAV-587/L14 transduction completely at a 1:160 dilution, while rAAV transduction remained unaffected (Fig. 3a). To rule out the possibility that these observations were due to different numbers of physical particles used for rAAV and rAAV-587/L14, we performed additional control experiments, where neutralization assays were performed with identical numbers of physical particles for both AAV vectors. For these experiments empty capsids were added to the rAAV preparation and neutralization assays were performed with three selected serum samples (P16, P17, P35). As seen in figure 3d these experiments yielded identical results. Taken together, these results demonstrate that the mutant rAAV-587/L14 is able to escape preexisting neutralizing Ab in human serum samples.

Neutralizing sera do not interfere with the L14 mediated tropism of rAAV-587/L14 on B16F10 cells

Insertion of the integrin specific L14 peptide in 587 expands the tropism of AAV to non-permissive B16F10 cells (Girod et al. 1999). To determine if rAAV-587/L14 was able to retain its ability to infect the target cell line B16F10 via the inserted ligand L14 in the presence of neutralizing antisera, we performed additional experiments with selected serum samples. rAAV-587/L14 was incubated with serial dilutions of P35 serum before transduction of irradiated B16F10 cells. After 72 hours GFP expression was measured. rAAV-587/L14 efficiently transduced B16F10 cells despite incubation with P35 at a 1:80 dilution, whereas anti-L14 serum completely inhibited transduction at this dilution (Fig. 4b and c). When testing P37 and P26, the same neutralizing titers as determined on HeLa cells were obtained

(data not shown). These findings showed that the AAV L14 targeting vector could escape neutralizing antibodies in human sera while retaining its retargeting ability.

The ability of rAAV-587 to escape neutralizing sera does not depend on the inserted L14 ligand

To exclude that the escape from neutralizing antisera was caused by a specific ligand, we tested another insertion mutant, rAAV-587/MecA that carries a 7 aa ligand (GENQARS) at position 587. This mutant has been selected by AAV-display on Mec1 cells and efficiently transduces Mec1 cells and primary B-cells from chronic lymphocytic leukemia patients in a receptor specific manner (Perabo et al. 2003). rAAV-587/MecA and rAAV were incubated with the serum P35 before Mec1 cells were infected. Transduction of Mec1 cells by rAAV-587/MecA was not affected by the neutralizing Ab of serum P35 (1:80 dilution). In contrast, rAAV transduction was almost completely inhibited by this serum (Fig. 5). Experiments with other neutralizing serum samples provided identical results (data not shown). In additional control experiments the neutralizing Ab A20 was able to inhibit transduction by rAAV-587/MecA, while C37-B had no effect (data not shown).

Taken together, the results demonstrate that the insertion of different heterologous ligands at position 587 allows escape from preexisting neutralizing antibodies. Targeting properties of these vectors are retained in these capsid mutants, even in the presence of neutralizing antisera.

Discussion

Because of the high prevalence of antibodies against AAV in the population, it is essential in gene therapy approaches to understand the immunogenic determinants of the AAV capsid and to develop strategies to circumvent antibody binding and neutralization of AAV vectors. In this study, we analyzed six AAV capsid mutants (I-261, I-381, I-447, I-534, I-573, and I-587) with a 14 aa peptide ligand inserted into the VP3 part of the capsid protein to identify immunogenic domains on the AAV capsid. We showed that peptide insertions at position 534 or 573 reduced binding of human antisera in 66% of the analyzed samples, indicating that these regions might be preferentially recognized by human AAV antibodies. In addition, we analyzed AAV vectors modified at position 587 to study the potential of AAV capsid mutants

to escape the neutralizing effects of human antisera with regard to the transduction efficiency. We demonstrated that these modified vectors were able to escape neutralizing Ab in human antisera without losing their ability to infect cells via the targeted receptors. In marked contrast, transduction of AAV carrying the unmodified capsid was significantly reduced or inhibited. These findings demonstrate that the insertion of peptide ligands at site 587 reduces the ability of AAV antibodies in human blood to neutralize the transduction by rAAV vectors.

The atomic structures of related parvoviruses like CPV, FPV and B19 have been resolved during the past decade and antigenic sites have been determined (see Fig. 1) (Agbandje et al. 1994; Chang et al. 1992; Chapman & Rossmann 1993; Chipman et al. 1996; Strassheim et al. 1994 ; Tsao et al. 1991). At the beginning of our studies the capsid structure of AAV was still unknown. Alignments of these related parvoviruses with AAV led to hypothetical models of the AAV capsid, and systematic mutagenesis helped to map functional sites on the capsid (Girod et al. 1999; Rabinowitz et al. 1999; Wu et al. 2000). Based on our structural alignments, six sites on the AAV capsid, selected with regard to flexible, highly variable loops and immunogenic domains of related parvoviruses (Fig. 1), were identified to accept the insertion of an integrin specific RGD ligand (L14, QAGTFALRGDNPQG) (Girod et al. 1999). Immunological analysis demonstrated the surface localization of the inserted L14 peptide (Girod et al. 1999). Characterization of other AAV serotypes revealed that the selected positions are also within highly variable regions amongst these serotypes (Chiorini et al. 1999). The recent unveiling of the atomic structure of AAV (Xie et al. 2002) broadly confirmed the flexible loop regions predicted by our initial structural model (Girod et al. 1999). When mapping the six insertion sites used in this report on the three-dimensional structure of AAV, they can all be found on the capsid surface within the threefold spike region (Fig. 6).

The high prevalence of AAV specific Ab causes substantial problems for human gene therapy. Different approaches have been pursued to map epitopes on the AAV capsid. Moskalenko et al. (2000) used small overlapping peptides (15aa) spanning the VP1 protein and human antisera to screen the AAV capsid protein by peptide scan. They identified several linear epitopes presented on the capsid surface, amongst them sites mapping to I-261 and I-447. However, some of the identified peptides might block Ab binding unspecifically or might not be displayed on the capsid surface (Wobus et al. 2000; Xie et al. 2002). Moreover, conformational epitopes cannot be identified by this method. Wobus et al. (2000) used murine mAb, which recognize conformational epitopes (D3, C37-B, C24-B, and A20), to identify

epitopes on the AAV capsid. Immunological analysis of these mAb with our six AAV insertion mutants helped mapping the epitopes of these antibodies on the AAV capsid and provided information about regions involved in receptor attachment. However, murine mAb cannot mimic the polyclonal Ab repertoire after an infection in humans. We therefore analyzed the ability of human antisera to recognize the six AAV insertion mutants in order to determine major antigenic domains of AAV involved in the humoral immune response. By using an ELISA we could demonstrate that the majority of the serum samples had a reduced affinity towards two insertion mutants, I-534 and I-573. Although at 39 aa distance from each other on the primary sequence, these sites are found in close proximity in the assembled capsid, on the side of the peaks at the threefold rotation axis (Xie et al. 2002). These data indicate the importance of the threefold-proximal peak region in the recognition by the humoral immune response, as it has been already shown for B19 or CPV (Chapman & Rossmann 1993; Chipman et al. 1996; Strassheim et al. 1994). It remains to be elucidated whether these mutations interfere with Ab binding directly or indirectly due to structural changes in adjacent regions.

Insertions at sites 261, 381, 447, and 587 affected binding of serum Ab only in a minority of serum samples. This was surprising, because mutations at position 261, 381 and 587 abolished binding of murine mAb A20 and C37-B, respectively (Fig. 2a). Moreover, amino acids corresponding to positions 261, 381, and 447 are part of major antigenic determinants in CPV (Strassheim et al. 1994). Different explanations are conceivable for this minor effect of these mutations on human Ab binding. (i) It is possible that epitopes, especially linear epitopes, which are adjacent to these insertion sites, have not been affected and that they are responsible for the remaining reactivity of serum Ab towards these mutants. (ii) In contrast to CPV, AAV residues 261 and 381 are located in the valley between two peaks of the threefold symmetry axis and this region might be less accessible for Ab binding, or less relevant for inducing a humoral immune response. (iii) Serum samples consist of a polyclonal Ab population. Thus, epitopes which only induce a weak Ab response might not have been detected in this binding assay, although they were affected by the mutations. For the same reason, we also did not expect a complete inhibition of binding of the polyclonal Ab, as observed with the monoclonal Ab A20 with I-261, I-381 and C37-B with I-534, I-573, and I-587. (iv) In addition, the specificity of Ab for a given antigen is dependent on the B-cell repertoire, T-cell repertoire and the major histocompatibility complex (MHC), and is therefore different at the species and individual level. Murine Ab generated against viral

antigens may differ in their targeted sequences to those generated in humans. All six insertions are directly at or close to the spike region. It is likely that in individuals the positions of the major antigenic determinants of AAV are different. In this case differences in human serum Ab binding were only seen if the major antigenic determinants were close to the spike region. This might also explain why serum samples of *class A* displayed no reduced affinity for any of the six insertion mutants, but this does not exclude that different mutants would impair binding of these sera. Consequently, it is reasonable to assume that other immunogenic determinants exist which have not been identified so far.

For the *in vivo* application of AAV, epitopes which interact with neutralizing antibodies are of particular importance. We therefore investigated the ability of AAV vectors with insertion of different peptide ligands at 587 to escape the preexisting neutralizing Ab in human antisera. Such vectors have previously been shown to efficiently retarget infection to wtAAV resistant cells (Girod et al. 1999; Nicklin et al. 2001). Moreover, Wu and colleagues (2000) demonstrated that this 587 region is involved in binding to the primary attachment receptor HSPG. 15 neutralizing serum samples were analyzed for their ability to neutralize rAAV-587/L14 transduction in comparison to rAAV. Strikingly, rAAV-587/L14 could escape the neutralizing effects exerted by 13 of the 15 neutralizing serum samples and efficiently transduced various cell lines. The targeting properties of rAAV-587/L14 were not affected, and escape could also be observed with a second ligand (MecA) that differed in size and sequence, demonstrating that the escape did not depend on the particular L14 insertion. Unfortunately, infectious titers of the other insertion mutants were not sufficient to perform neutralization assays. However, it is possible that insertion of different peptide ligands yield higher infectious titers, as they strongly depend on the peptide size and sequence (compare MecA with L14, and see also Shi et al. 2001). Nevertheless, our results do not allow the conclusion that insertions at position 587 are the only site to generate mutants, which are able to escape the neutralizing effects of human antisera.

It seems contradictory that I-587 only slightly impaired binding of serum samples in the ELISA, while it had such strong effects on the neutralizing capacity of human antisera. At least two explanations are possible: Human sera consist of a polyclonal Ab population directed against various epitopes on the AAV surface, but only a small amount of these Ab are capable of neutralizing AAV transduction. Therefore, in an ELISA these neutralizing Ab may not have a noticeable effect on the overall Ab binding, whereas they inhibit virus transduction in a neutralization assay. The three dimensional structure of AAV shows that the

sites for interaction with the viral receptor HSPG are located within the peaks of the threefold axis, proximate to residue 587 (Wu et al. 2000; Xie et al. 2002). Furthermore, the neutralizing Ab C37-B, which inhibits binding of wtAAV to the host cell, has its epitope adjacent to this site in the assembled capsid. Therefore this region seems to be critical for receptor binding. It is very likely that neutralizing Ab are preferentially directed against this region and explains why the action of these Ab is affected by insertions at this region (Wobus et al. 2000; Xie et al. 2002). Whether these modifications directly interfere with neutralizing epitopes at position 587 or antigenic determinants on neighboring loops within the threefold proximal peaks are affected due to conformational changes remains to be elucidated. Additional experiments with point mutations or small deletions at 587, for example, could help to map such epitopes in the 587 region more precisely. Another explanation is that neutralizing Ab, which have been generated against the wtAAV capsid, only block the wt capsid mediated transduction. After insertion of a targeting ligand at position 587 the virus mutant can use a different uptake route than wtAAV, which does no longer depend on HSPG binding (rAAV-587/L14 via the integrin receptor) (Girod et al. 1999; Nicklin et al. 2001). Therefore it is supposable that these neutralizing Ab cannot block the interaction of these AAV mutants with alternative cell surface receptors. Of course, these explanations are not mutually exclusive, and due to the complexity and various mechanisms of the neutralization process other explanations are also possible. However, it is reasonable to assume that capsid modifications at position 587 might not only allow to alter the tropism of AAV but also to generate immune escape variants. All data presented here were generated *in vitro*. Animal experiments are now needed to corroborate the utility of this concept, not only with regard to neutralization by antibodies, but also with regard to transduction efficiency and tropism of these genetically modified vectors. In addition, *in vivo* studies could help to clarify if insertion of such peptide ligands possibly promotes the generation of new epitopes, e.g. the fusion region where the peptide is inserted.

Taken together the results indicate that the threefold-proximal peaks on the AAV capsid are major antigenic determinants for antibody binding as well as for neutralization of AAV transduction. Moreover, our results demonstrate that modifications at site 587 could allow to generate AAV vectors with the ability to escape neutralization by human antisera. Importantly, these modified vectors retain their ability to transduce specific target cells. These findings might be useful for the production of AAV vectors suitable for repeated administration in human gene therapy.

Materials and Methods

Cell culture. HeLa, 293 and B16F10 cells were grown in Dulbecco's modified Eagle's medium (DMEM) supplemented with 10% heat-inactivated fetal calf serum (FCS), penicillin (100 U/ml), streptomycin (100 µg/ml), and L-glutamine (2 mM). Mec1 cells were cultivated in Iscove's modified DMEM supplemented with 10% FCS, penicillin-streptomycin and L-glutamine. Cells were maintained at 37°C in a 5% CO₂ humidified incubator.

Antibodies and human serum samples. B1, A20 and C37-B were generated by immunization of mice with purified AAV capsid proteins and synthetic peptides, respectively, followed injection with AAV empty particles (Wistuba et al. 1995; Wobus et al. 2000). 76/3 was generated by immunization with purified Rep protein as described (Wistuba et al. 1995). Serum against the L14 ligand was obtained after immunization of a rabbit with L14 peptide (Girod et al. 1999). Serum samples from human patients were kindly provided by the Klinikum Großhadern in Munich, Germany.

Plasmids. The plasmid pUC-AV2 contains the full-length AAV2 genome and was constructed as described in Girod et al. (1999). The plasmids pI-261, pI-381, pI-447, pI-534, pI-573, pI-587 are derived from pUC-AV2, with the L14-encoding sequence inserted in the *cap* gene. The AAV2-based helper plasmids pRC, pRC(I-587) and pRC(587/MecA) contain the AAV2 Rep and Cap encoding regions but lack the viral ITRs (Girod et al. 1999; Perabo et al. 2003). pRC(587/MecA) contains a DNA fragment coding for the MecA ligand inserted between amino acid position 587 and 588. The pGFP plasmid is an AAV2-based vector plasmid in which the AAV ITR sequences flank the hygromycin selectable marker gene controlled by the thymidine kinase promoter and the enhanced GFP gene regulated by the cytomegalovirus promoter (Ried et al. 2002). The adenovirus helper plasmid pXX6 (Xiao et al. 1998) was kindly provided by R. J. Samulski.

Preparation of virus stocks. The AAV stocks were generated as described previously (Ried et al. 2002) with the following modifications. 293 cells seeded at 80% confluence in plates with 15 cm of diameter were transfected with a total of 37.5 µg of vector plasmid (pGFP) and packaging plasmid (pRC for wt capsid, pRC(I-587) for L14 carrying capsid, and pRC(587/MecA) for MecA carrying capsid) and adenoviral plasmid (pXX6) at a 1:1:1 molar ratio. For viruses containing an AAV *rep* and *cap* gene, the pUC-AV2 plasmid or mutated plasmids were transfected with pXX6 in a 2:1 molar ratio. After 48 h cells were collected and pelleted by centrifugation. Cells were resuspended in 150 mM NaCl, 50 mM Tris-HCl (pH 8.5), lysed by repeated freeze-thaw cycles, and treated with Benzonase (50 U/ml) for 30 min at 37°C. Cell debris was removed by centrifugation and the supernatant was loaded onto an iodixanol gradient as described (Zolotukhin et al. 1999). After centrifugation at 69,000 rpm for 1 h at 18°C the AAV containing iodixanol phase was harvested.

Evaluation of AAV titers. Particle titers of virus stocks containing *rep/cap* were determined by electron microscopy and confirmed by Western blotting. Electron microscopy was performed at the DKFZ (Heidelberg). Iodixanol gradient purified viral particles were adsorbed onto Formvar-carbon-coated copper grids and negatively stained with uranyl acetate. Titers were calculated in comparison to a known viral standard (Grimm et al. 1999). Western blot analysis was performed to confirm the titers obtained by electron microscopy. Equal

numbers of AAV particles were separated on a 10% SDS-PAGE and blotted on nitrocellulose membrane using standard protocols. Capsid proteins were detected by B1 hybridoma supernatant, followed by incubation with a peroxidase-coupled secondary antibody (Sigma) and visualized by enhanced chemiluminescence (Pierce). For recombinant vectors encoding the GFP protein genomic titers were quantified by dot-blot analysis as described (Girod et al. 1999). Briefly, serial dilutions of the AAV preparations were first incubated in 2 M NaOH, then blotted onto a nylon membrane, and finally hybridized with a random-primed *gfp* probe by standard methods. Infectious particle titers of the GFP encoding virus stocks were determined by infecting irradiated HeLa cells (100 Gy from a ^{137}Cs gamma irradiation source) with serial dilutions of the AAV preparation in a 12-well plate. After 48 h cells were harvested and assayed for GFP expression by fluorescence-activated cell sorting (FACS). Infectious titers on B16F10 and Mec1 cells were performed accordingly by co-infection with adenovirus 5 (AdV). Titers of AAV stocks carrying the *rep* and *cap* gene were determined by infection of HeLa cells after AdV co-infection and detection of the viral Rep proteins with Cy3-labeled 76/3 monoclonal antibody (Cy3 mono-Reactive Dye Pack, Amersham, according to the manufacturer's protocol).

ELISA. Identical particle amounts (5×10^8 per well) as determined by electron microscopy of wtAAV and AAV insertion mutants were coated onto microtiter plates (MaxiSorp; Nunc Nalgene International) in PBS overnight at 4°C. After blocking with 3% BSA / 5% sucrose in washing buffer (PBS/0,05% Tween 20) wells were incubated with A20- or C37-B-hybridoma supernatant or human serum diluted 1:50 to 1:400 in blocking buffer for 1h at room temperature. After washing wells were incubated with a biotin-conjugated anti-human or anti-mouse secondary antibody (Dianova) diluted in washing buffer for one hour. Detection and quantification was performed as described previously (Girod et al. 1999). Serum samples were considered as seropositive for AAV antibodies when the measured OD was 0.2 or higher at a 1:300 dilution after subtraction of background.

Neutralization Assay: HeLa cells or B16F10 cells were seeded in 96-well plates (5×10^3 cells per well) and infected with AdV (MOI 5) or irradiated 2 h prior to infection with AAV, respectively. Identical transducing particle numbers (MOI 5) of rAAV (wt capsid) and rAAV-587/L14 were incubated with serial dilutions (1:10 to 1:1200) of human serum in PBS for 2 h at 4°C in a total volume of 30 μl . Before addition of the AAV/serum-mixture medium was replaced by 100 μl of fresh medium. 48 h (HeLa) or 72 h (B16F10) after infection GFP-positive cells were detected by FACS analysis and fluorescence microscopy. Similarly, Mec1 cells were seeded at 5×10^4 cells per well, infected with AdV followed by infection with rAAV or rAAV-587/MecA, which had been incubated with serial dilutions of human serum as described above. The neutralizing titers are expressed as the dilution at which transduction was 50% reduced compared to the positive control (N_{50}). Serum samples were considered as neutralizing when the N_{50} was 1:320 or higher.

Acknowledgments

We are grateful to Birgit Hub (DKFZ, Heidelberg) for performing electron microscopy of AAV stocks and Dr. Peter Lohse from the Klinikum Großhadern for providing human serum samples. Furthermore we thank Susan King and Knut Hennecke for helpful discussion and for kindly reading the manuscript, and Kristin Leike for excellent technical assistance. This work was supported by the Deutsche Forschungsgemeinschaft, Sonderforschungsbereich 455 (to M.H.) and the Bayerische Forschungstiftung (FORGEN II, to M.H. and H.B.).

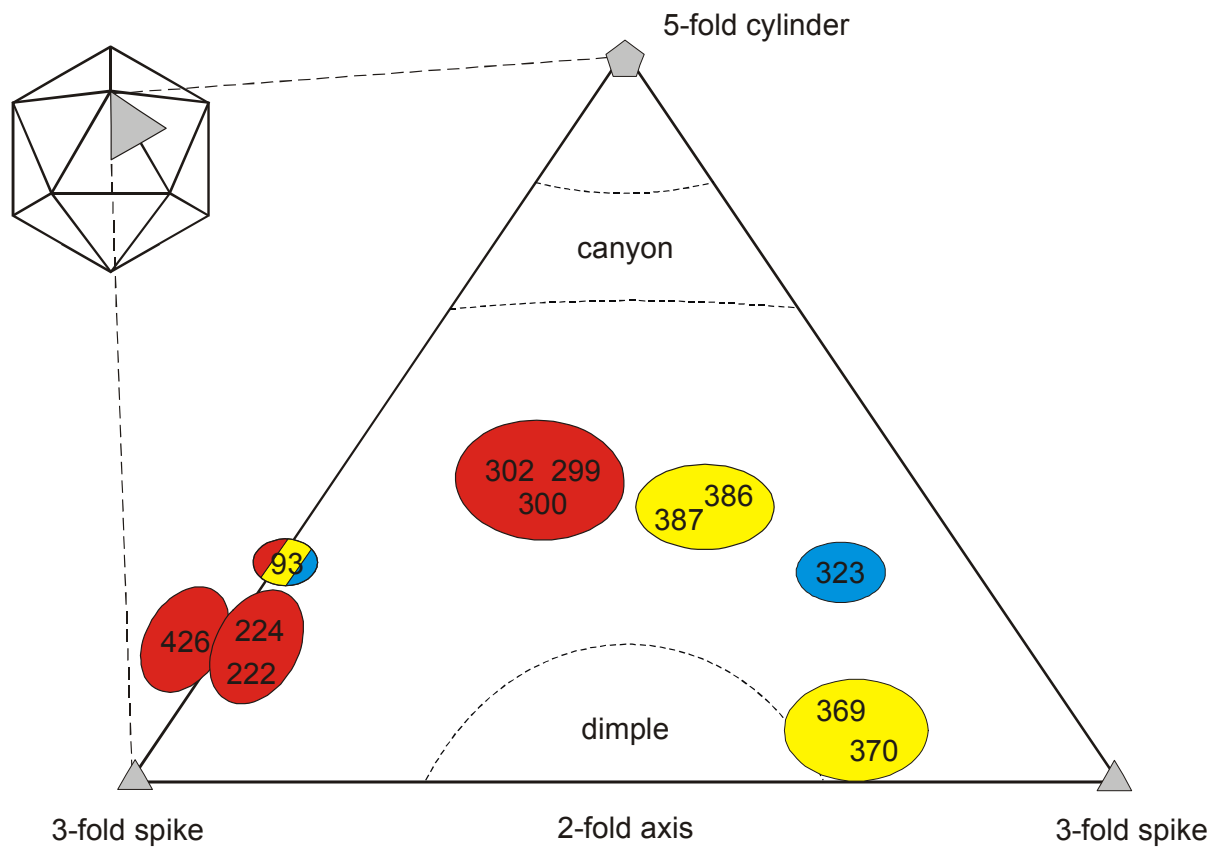


Figure 1. Map of major antigenic regions in CPV, FPV and B19. The triangle represents one asymmetric subunit of the CPV major capsid protein. The positions of the 5-fold, 3-fold and 2-fold symmetry axis are indicated. The amino acid positions of major antigenic determinants in CPV (red), B19 (yellow) and FPV (blue) are given (aligned to the CPV capsid protein) (Chapman & Rossmann 1993).

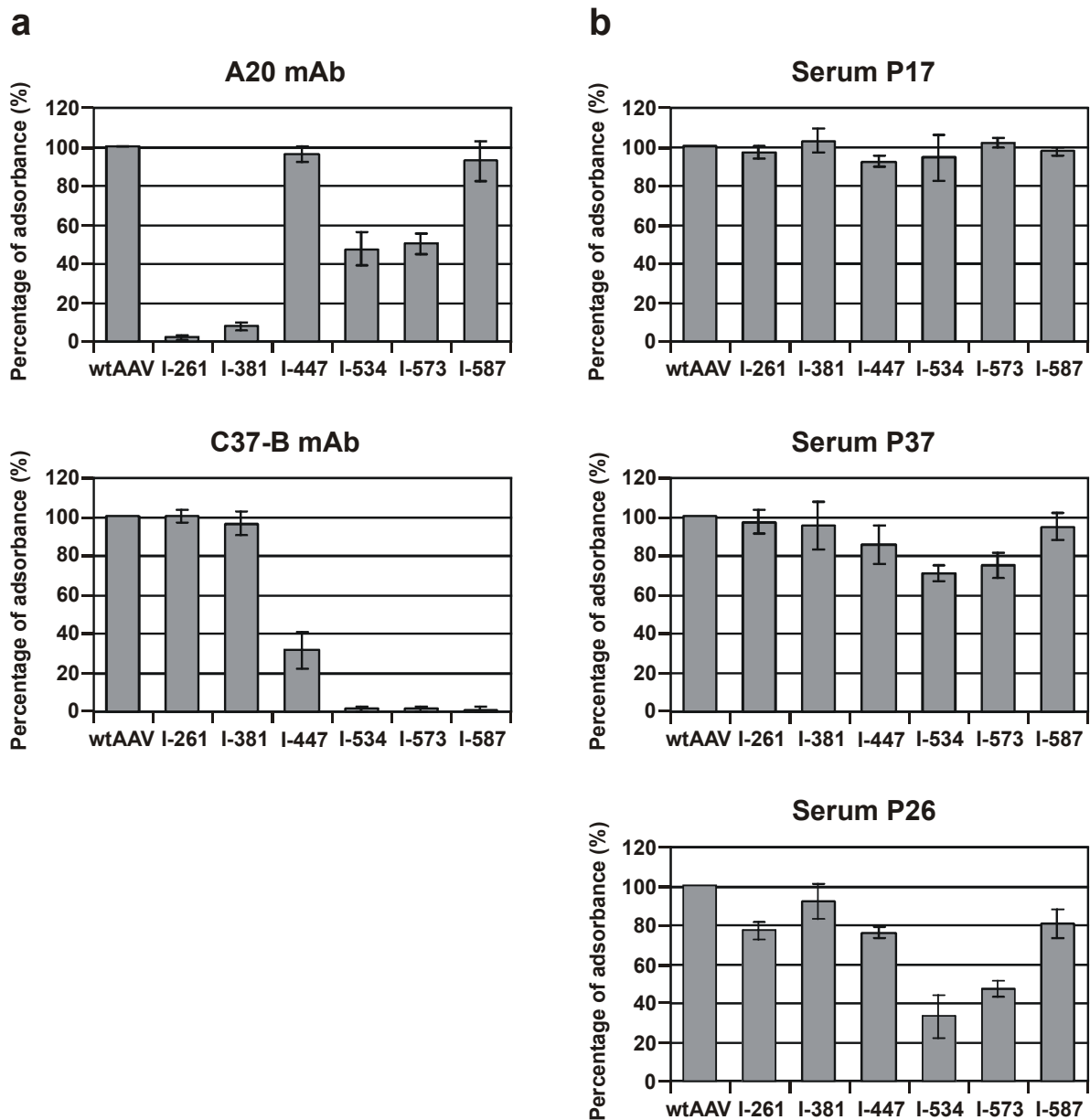


Figure 2. Binding of A20 and C37-B monoclonal antibody (a) and human serum samples (b) to wtAAV and AAV capsid mutants as determined by ELISA. Microtiter plates were coated with identical particle amounts of wtAAV and AAV insertion mutants and incubated with hybridoma supernatants of either A20 or C37-B mAb or with serum samples of human patients as described in Materials and Methods. Binding of antibodies to wtAAV was set at 100% (y axis). Each experiment was repeated independently at least three times; the figure shows the mean values and standard deviations (indicated by the error bars).

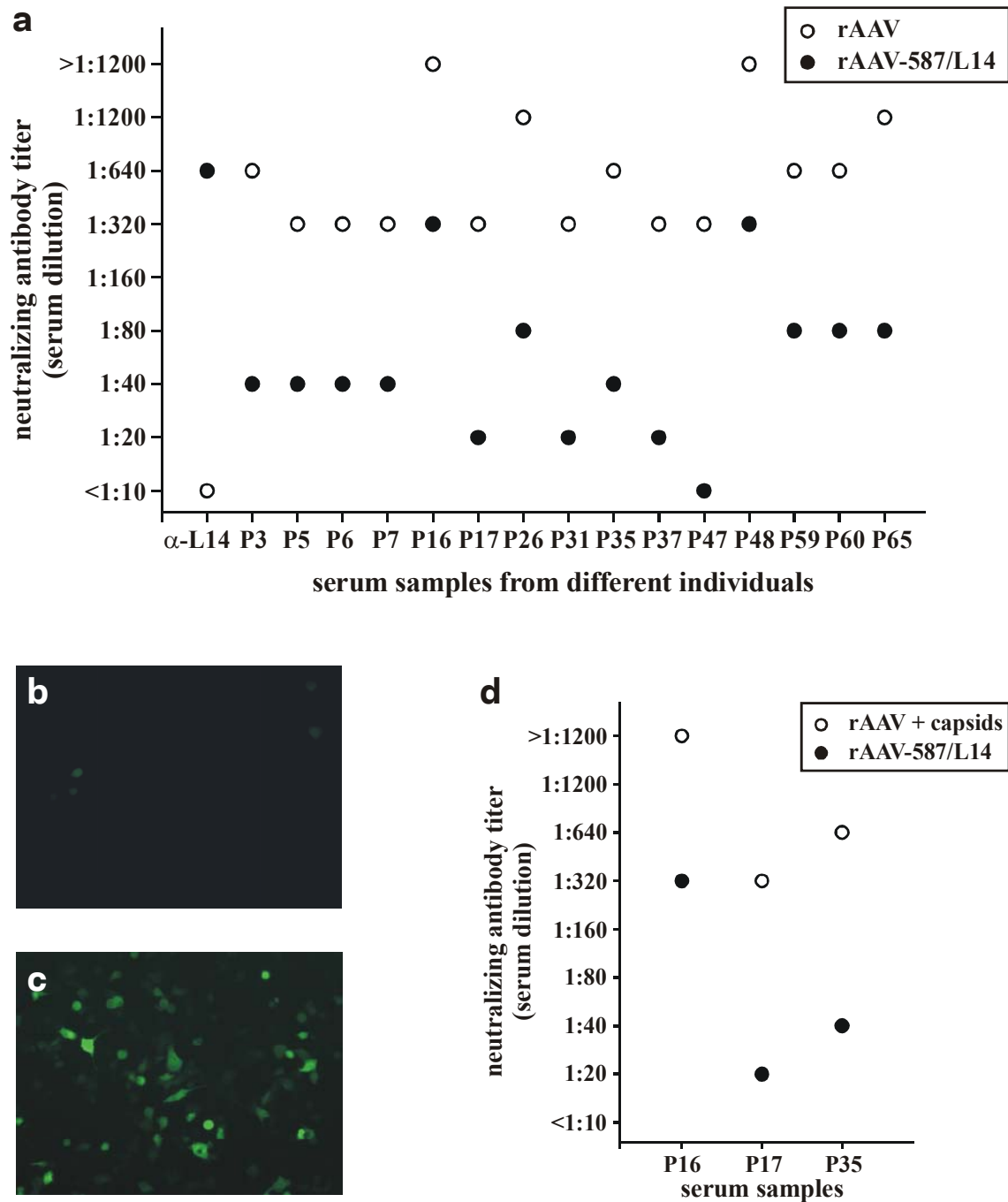


Figure 3. Neutralization assay on HeLa cells. (a) Neutralizing antibody titers against rAAV and rAAV-587/L14. Serial dilutions (1:10 – 1:1200) of 15 neutralizing human serum samples were analyzed on HeLa cells. As control, rabbit serum directed against the inserted L14-ligand (α -L14) was tested. The neutralizing titers (N_{50}) are expressed as the dilution at which transduction was 50% reduced compared to the positive control. rAAV (b) and rAAV-587/L14 (c) were incubated with serum P35 (1:80) prior infection of HeLa cells. GFP expression was monitored 48 hours post infection. (d) Empty capsids were added to rAAV to adjust physical particle numbers. The N_{50} was determined as described above.

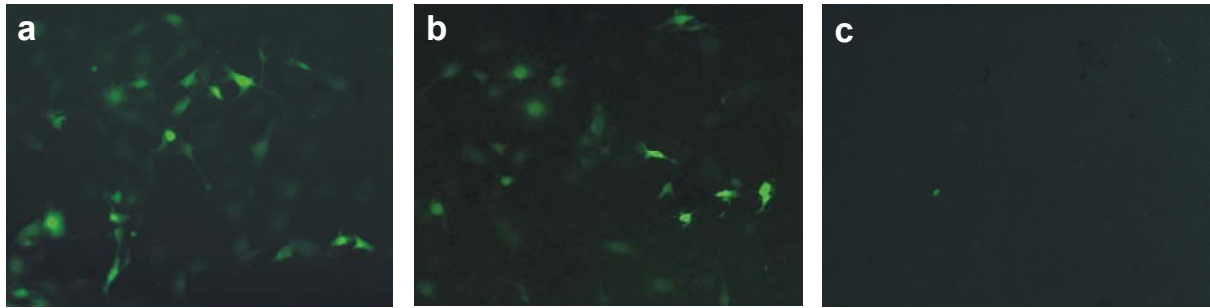


Figure 4. Neutralization assay on B16F10 cells. Infection of irradiated B16F10 cells with rAAV-587/L14 alone (a) or after co-incubation with P35 serum (b) or anti-L14 serum (c) at a 1:80 serum dilution. Cells were analyzed for GFP expression after 72 hours.

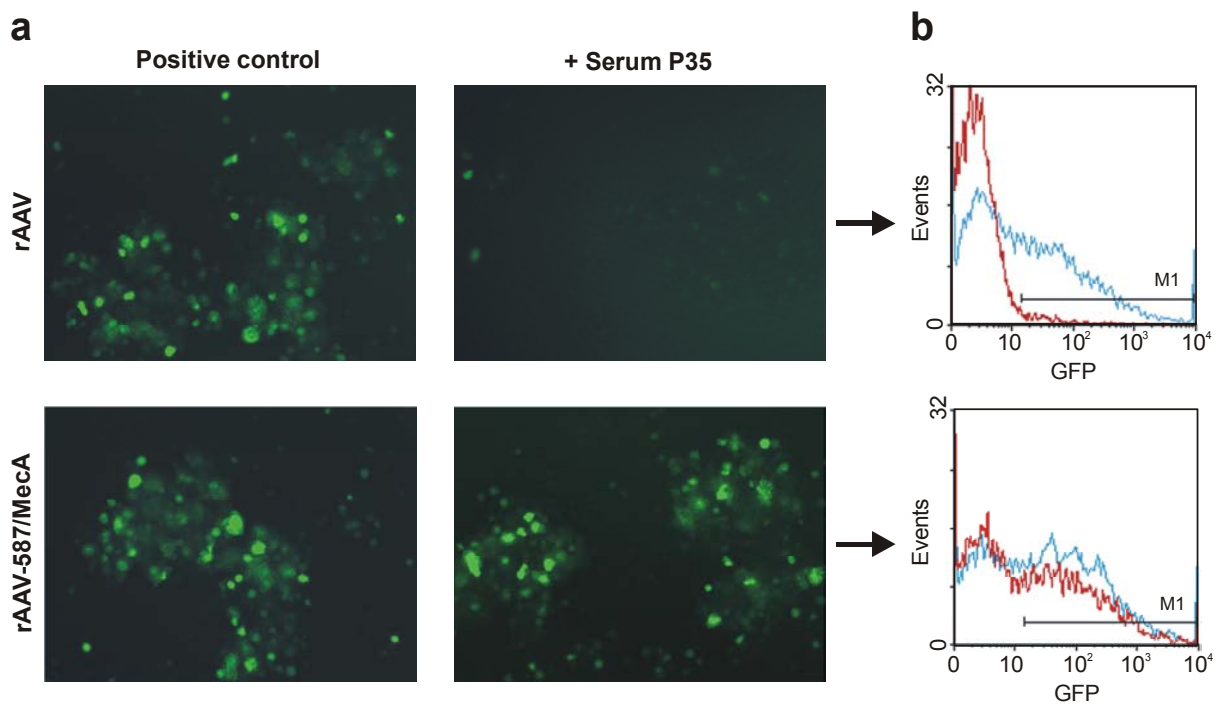


Figure 5. Effect of neutralizing antisera on rAAV-587/MecA transduction. (a) After infection with adenovirus, Mec1 cells were infected with rAAV (top row) and rAAV-587/MecA (bottom row) alone (positive control) or after co-incubation with serum P35 at a 1:80 dilution (+ serum P35). Note that more physical particles were used for rAAV to achieve similar transduction. (b) FACS analysis of rAAV (top row) and rAAV-587/MecA (bottom row) incubated with serum P35 (red line) in comparison to their positive controls (blue line). GFP expression was determined 48 hours post infection.

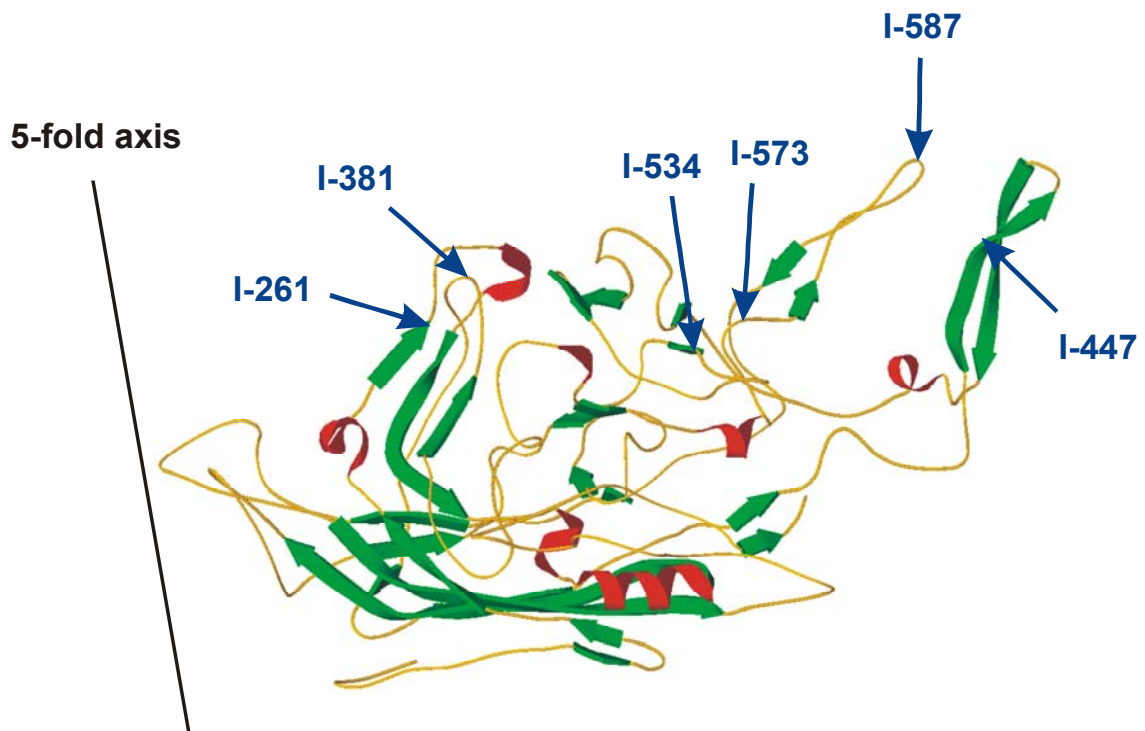


Figure 6. Model of the AAV major capsid protein according to the atomic structure by Xie et al. (2002) (taken from The Protein Data Bank). The sites of insertion are marked with arrows.

CHAPTER V

Receptor Targeting of Adeno-Associated Virus Vectors

published as:

Büning H, Ried MU, Perabo L, Gerner FM, Huttner NA, Enssle J, and Hallek M. (2003)
Retargeting of Adeno-Associated Virus Vectors. *Gene Ther* **10**: 1142-1151

Summary

Adeno-associated virus (AAV) is a promising vector for human somatic gene therapy. However, its broad host range is a disadvantage for *in vivo* gene therapy, because it does not allow the selective tissue- or organ-restricted transduction required to increase the safety and efficiency of the gene transfer. Therefore, increasing efforts are being made to target AAV-2 based vectors to specific receptors. The studies summarized in this review show that it is possible to target AAV-2 to a specific cell or organ. So far, the most promising approach is the genetic modification of the viral capsid. However, the currently available AAV-2 targeting vectors need to be improved with regard to the elimination of the wild type AAV-2 tropism and the improvement of infectious titers. The creation of highly efficient AAV-2 targeting vectors will also require a better understanding of the transmembrane and intracellular processing of this virus.

Introduction

The development of safe and efficient gene transfer vehicles is critical for the success of gene therapy. One of the most promising viral vectors is based on adeno-associated virus type 2 (AAV-2), a member of the parvovirus family. AAV-2 was discovered as a co-infecting agent during an adenovirus outbreak, without any apparent pathogenicity contributed by AAV-2 (Blacklow 1988; Blacklow et al. 1968a; Blacklow et al. 1971). Until now, no human disease caused by AAV-2 has been detected. Moreover, AAV-2 seems to be protective against bovine papillomavirus and adenovirus mediated cellular transformation (Hermonat 1989; Khleif et al. 1991; Mayor et al. 1973). AAV-2 does not induce cytotoxic effects and does not elicit a cellular immune response as commonly seen with other viral vectors (Carter & Samulski 2000). Finally, AAV-2 has the unique potential to integrate site specifically into the q-arm of human chromosome 19 (Kotin et al. 1990; Samulski et al. 1991).

AAV-2 has a broad tissue tropism infecting diverse organs such as brain, liver, muscle, lung, retina and heart muscle. This makes AAV-2 attractive for *in vitro* gene transfer into various tissues (Carter & Samulski 2000). AAV-2 vectors are now successfully used for *in vivo* gene transfer (Monahan & Samulski 2000; Tal 2000). However, the studies reported so far clearly demonstrate that clinically relevant gene expression can be reached only in the liver, unless vectors are administered directly into the target tissue or organ. These results emphasize the need for a targeting of AAV vectors in order to overcome the apparent

limitations of a broad tissue tropism. In addition, the targeting of AAV vectors would also enhance the safety and efficiency of AAV-mediated gene transfer *in vivo*. Therefore, increasing efforts are being made to retarget AAV-2 based vectors to specific receptors and to generate selective, tissue- or organ-restricted vectors. The studies summarized in this review show that it might become possible to target AAV-2 to a specific cell type or organ. However, the targeting vectors still need to be optimized by a further reduction of the wild type AAV-2 tropism, or with an increase in infectious titer. With the rapidly increasing knowledge about the functional domains on the AAV-2 capsid involved in receptor binding and subsequent steps of transmembrane and intracellular processing of the virion, we feel justified to predict that the creation of highly efficient AAV-2 targeting vectors will become possible in the near future.

Organization of the AAV-2 genome

AAV-2 is a single stranded, replication deficient non-enveloped DNA virus (Rivadeneira et al. 1998) composed of an icosahedral protein capsid and a viral genome of 4680 nucleotides. The AAV-2 genome encodes the two large open reading frames *rep* and *cap*. It is flanked at both ends by the 145 bp inverted terminal repeat sequences (ITR). The ITRs are required for encapsidation of the viral genome and seem to have enhancer and/or weak promoter activity. They are besides the viral Rep proteins necessary for the site specific integration of wild type AAV-2 and for the rescue of proviruses. The 5' open reading frame *rep* encodes four overlapping, multifunctional proteins (Rep78, Rep68, Rep52 and Rep40) controlled by two different promoters (Balague et al. 1997). The large Rep proteins (Rep78 and its splice variant Rep68) are controlled by the p5 promoter and are necessary for viral DNA replication, transcriptional control and site-specific integration. Rep52 and its splice variant Rep40 are known as small Rep proteins. They are transcribed from the p19 promoter and play an essential role in the accumulation of single-stranded progeny genomes used for packaging. The 3' ORF *cap* accommodates the three capsid proteins VP1 (90 kDa), VP2 (72 kDa) and VP3 (60 kDa), which form the 60 subunits of the AAV-2 viral capsid at a 1:1:20 ratio (Rabinowitz & Samulski 2000). They are controlled by the p40 promoter, share the same stop codon, but differ due to alternative splicing and different initiation codons resulting in progressively shorter proteins from VP1 to VP3. All three capsid proteins are necessary for the generation of infectious particles, although capsids are formed in the absence of VP1

(Hermonat et al. 1984; Smuda & Carter 1991; Tratschin et al. 1984). The capsid assembly itself occurs in the nucleus (Wistuba et al. 1997; Wistuba et al. 1995). The N-terminus of VP2 contains a nuclear localization sequence by which it transports VP3 into the nucleus (Hoque et al. 1999; Ruffing et al. 1992). The encapsidation of the AAV-2 genome probably takes place in the nucleoplasm and Rep-tagged DNA seems to initiate packaging by interaction with capsid proteins (Dubielzig et al. 1999).

If *rep* and *cap* are provided in *trans* on a helper plasmid, 96% of the wild type AAV genome can be removed and replaced by a transgene, because the ITRs are the only *cis* elements necessary for the generation of recombinant AAV (rAAV) (Carter & Samulski 2000). The protocols to generate high-titer and highly purified viral preparations have undergone continuous improvements (Hermens et al. 1999; Summerford & Samulski 1999). Until now, rAAV is commonly produced by transfection of a vector plasmid (containing the ITR flanked transgene) and a helper plasmid (encoding Rep and Cap) into HeLa or 293 cells, followed by superinfection with adenovirus type 5. Alternatively, a triple transfection of vector-, helper- and an adenovirus helper plasmid can be used (Ferrari et al. 1997; Girod et al. 1999; Grimm & Kleinschmidt 1999; Xiao et al. 1998). After harvesting, AAV is purified using iodixanol or CsCl gradient ultracentrifugation and/or chromatography (Chiorini et al. 1995; Hermens et al. 1999; Summerford & Samulski 1999; Zolotukhin et al. 1999). After purification, *infectious* particle titers of AAV-2 of $>10^9$ /ml are easily reached, which is sufficient for most *in vitro* and *in vivo* experiments, at least in smaller rodents. However, when it comes to larger animals or human beings in clinical applications, it is strongly desirable to enhance the target specificity of AAV vectors by receptor retargeting in order to reduce the amount of vector particles to be administered.

Three-dimensional structure of AAV-2

Recently, Xie et al. (2002) were able to determine the atomic structure of AAV-2 to a 3-Å resolution by x-ray crystallography. Like Kronenberg et al. (2001), who investigated empty capsids by electron cryo-microscopy and icosahedral image reconstruction, Xie et al. (2002) observed substantial differences in the surface topology between AAV-2 and other parvoviruses. The inner surface of the AAV-2 capsid is composed of a jelly-roll β -barrel motif, comprising two antiparallel β -sheets. This motif is common in virus capsids and has also been described for other parvoviruses like canine parvovirus (CPV) (Tsao et al. 1991),

feline panleukopenia virus (Agbandje et al. 1993), minute virus of mice (Agbandje-McKenna et al. 1998), or the human parvovirus B19 (Agbandje et al. 1994). However, the interstrand loops located between the strands of the core β -barrel have quite different structures in the different parvoviruses and are the regions responsible for interactions with antibodies and cellular receptors. The most prominent features of the AAV-2 surface topology are the “threefold-proximal” peaks. These peaks cluster around each icosahedral three-fold rotation axis. Unique for AAV-2 is that neighboring subunits interact intimately at this threefold axis. Additional, but more modest interactions were also observed for residues in the HI, BC and EF loop of neighboring subunits. The threefold proximal peaks are mainly formed by a so called GH loop. This loop is missing in densovirus (insect parvovirus) and is structurally different in CPV. This loop is, as expected, mainly involved in binding to the primary receptor of AAV-2 (see below) and contains the epitope recognized by the neutralizing antibody C37-B. Moreover, the most promising position for the insertion of receptor specific peptides (amino acid position 587) is also located in this loop.

Before the characterization of the three-dimensional structure of the AAV-2 capsid, potential insertion sites as well as the determination of antibody and receptor binding regions were identified by epitope mapping, mutagenesis studies of capsid proteins, as well as sequence alignments of AAV-2 and related parvovirus including other serotypes. Although it was possible by these approaches to determine functional relevant regions of the AAV-2 capsid, the now solved three dimensional structure will accelerate this process by using a more rational, structure-based approach.

Infectious pathway of wild type AAV-2

A successful viral infection is a multistep process starting with the attachment of the virus to the cell surface, followed by viral uptake, intracellular trafficking and - in most of the cases - nuclear transport and deposition or replication of the viral genome in the cell nucleus. In the current model of infection of permissive cells by AAV-2 (Fig. 1A), AAV-2 first binds to heparan sulfate proteoglycans (HSPG), which act as primary or attachment receptors (Summerford & Samulski 1998). Since all adherent cells express glycosaminoglycans on their surface, this offers a simple explanation for the broad tropism of AAV-2. No distinct heparin binding motif was identified so far in the AAV-2 capsid. However, Wu et al. (2000) mapped two regions involved in HSPG binding by alanine substitution and insertion of the

hemagglutinin (HA) epitope YPVDVPDYA. These regions encompass amino acids 509 to 522 and 561 to 591 (in VP3) and are clustered around the threefold-proximal peaks (Xie et al. 2002). The alanine substitution mutant 585-RGNR-588 and the HA insertion mutant 591 for example are located on the side of the threefold-proximal peak facing the valley, which separates this peak from its neighbor, whereas the alanine insertion mutant 509 is on the floor of the valley. The other two mutants generated by Wu et al. were mapped at the base of (alanine substitution at 561-565) and underneath (HA insertion at 522) the peak facing the twofold axis. Xie et al. assume that mutations in the regions underneath the peak (insertion at 522 and 519; see (Rabinowitz et al. 1999) are not directly affecting the HSPG binding of AAV-2.

Two types of AAV-2 co-receptors have been identified, $\alpha_v\beta_5$ integrin and fibroblast growth factor receptor 1 (FGFR1) (Bartlett et al. 2000; Qing et al. 1999; Summerford et al. 1999). It is postulated that FGFR1 enhances the attachment process (Bartlett et al. 2000; Qing et al. 1999). Antibodies against $\alpha_v\beta_5$ integrin do not interfere with cell binding but inhibit endocytosis. Therefore, $\alpha_v\beta_5$ integrins seem to be required for endocytosis of AAV-2 (Sanlioglu et al. 2000), which is mediated mainly by clathrin-coated pits (Bartlett et al. 2000; Duan et al. 1999). This endocytotic process and the subsequent steps are still poorly understood. However, it is possible to assume that like for adenovirus α_v integrin clustering facilitates the localization of virus particles to coated pits (Wang et al. 1998). This could then activate the endocytosis in which Dynamin, a 100 kDa cytosolic GTPase, is involved. Although the precise function of Dynamin in vesicle formation remains controversial (Marks et al. 2001; Sever et al. 2000), it is known that it is essential for scission of newly formed vesicles from the plasma membrane (Marks et al. 2001). For AAV-2 it was shown that the introduction of a dynamin mutant results in the decrease of AAV mediated transduction (Bartlett et al. 2000; Duan et al. 1999), although it was not possible to abolish the AAV-2 infection. However, Sanlioglu et al. (2000) assumed that the binding to the integrin could have an additional effect, which is the activation of Rac1. They propose that Rac1 activation results in the stimulation of phosphoinositol-3 kinase (PI3K) which facilitates the rearrangements of microfilaments and microtubuli. These rearrangements are necessary to support the initiation of the intracellular movements of AAV-2 to the nucleus after endocytosis. The release of AAV-2 from the endosome at the early-to-late endosomal transition requires a low endosomal pH (Bartlett et al. 2000; Douar et al. 2001). As with other

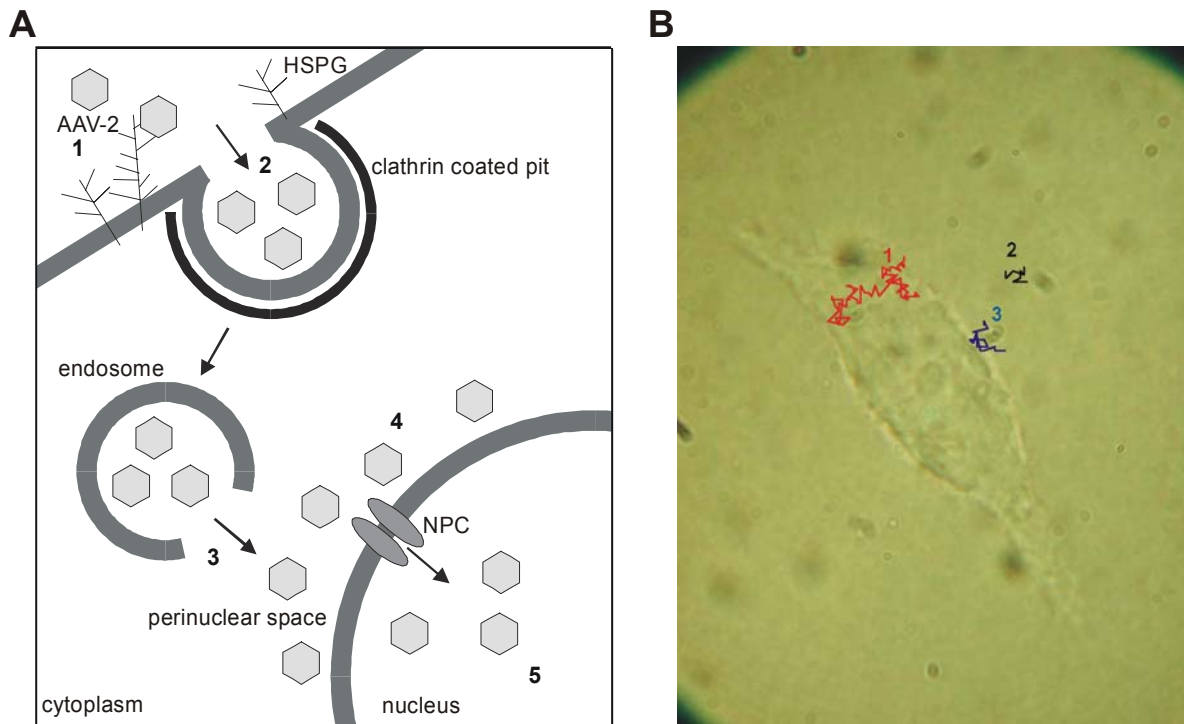


Figure 1. Infectious pathway of wild type AAV-2. (A) Schematic representation of AAV entry and endocytic trafficking in HeLa cells as seen by fluorescent and confocal laser microscopy. Following binding to heparan sulfate proteoglycans (HSPG) on the cell surface (1), AAV is rapidly internalized via clathrin-coated pits (2) through a process involving $\alpha_v\beta_5$ integrin, Dynamin and Rac1. Following endocytosis, the activation of phosphatidylinositol-3 kinase seems to support the initiation of the intracellular movement. After acidification AAV is released from the endosome into the cytoplasm (3), where it is found in a perinuclear localization (4). Then AAV slowly enters the nucleus (5) probably via nuclear pore complexes (NPC). (B) Trajectories of single AAV-Cy5 particles analyzed by single virus tracing (Seisenberger et al. 2001). The traces show single diffusion virus particles at different times. In this figure three examples of the various stages of the AAV-2 infection are visible (diffusion in the cytoplasm after cell entry (1), diffusion in solution (2) and touching at the cell membrane (3)). Normal diffusion with a diffusion coefficient of $D = 7.5 \mu\text{m}^2/\text{s}$ could be measured for AAV-2 outside the cell (2). A deceleration of AAV-2 near the cell could be observed. When approaching the cell, a repetitive touching of the cell membrane by AAV-2 occurred, which was interrupted by short diffusion path in the vicinity of the cell surface (3). Inside the cell AAV movements using direct motion, anomalous and normal diffusion were observed (1). This method also allowed to distinguish between free viruses and AAV inside endosomes by calculating the diffusion constants of the particles traced by SVT.

viruses (Marsh & Helenius 1989), the low pH is likely to induce conformational changes of key viral proteins necessary for a successful endosomal release or nuclear entry. Interestingly, the unique region of VP1 contains a potential phospholipase A2 (PLA2) domain (Girod et al. 2002), which might be involved in this process. PLA2 inactivating point mutations do not

influence the capsid assembly, packaging, cell binding or entry of AAV-2, but delay the onset and reduce the amount of early gene expression. Thus, the PLA2 activity in the N-terminus of VP1 may be required for the exit of AAV-2 from the endosome and the transfer of the viral genome to the nucleus. A PLA2 domain with similar function has been found in porcine parvovirus (Zadori et al. 2001). The destiny of AAV-2 after this endosomal release is mostly unclear. Some studies have observed a perinuclear accumulation of AAV-2 particles (Bartlett et al. 2000), before the virus slowly enters the nucleus, probably via nuclear pore complexes. However, the perinuclear accumulation of AAV-2 observed by conventional fluorescent and confocal laser microscopy may suffer from some methodological shortcomings such as interference effects and the cellular virus overload required for these conventional imaging studies (see next paragraph). These results need to be confirmed by independent methods.

The development of a novel technique, called single virus tracing (SVT), which allows the visualization of an individual virus in a living cell with high spatial and temporal resolution, may permit a more detailed analysis of specific steps of the cellular infection (Seisenberger et al. 2001) (Fig. 1B). Using this technique Seisenberger et al. observed AAV-2 movements towards the cell surface, which were followed by repetitive touching and short diffusion paths in the vicinity of the cell surface. The touching events were clearly visible as short periods of immobility at the cell surface, with a mean touching time of $t_t = 62$ ms. Inside the cell, three different kinds of AAV-2 movements were observed in the cytoplasm and the nuclear area, namely directed motion, anomalous diffusion and normal diffusion. In agreement with the current model of AAV-2 infection, most virions followed a normal diffusion in endo- or lysosomal particles. However, in marked contrast to the above findings with conventional microscopic techniques, neither a nuclear accumulation nor a slow penetration of the nuclear membrane was observed by SVT. Interestingly, the total time measured for membrane penetration, trafficking through the cytoplasm and entry into the nuclear area was much shorter than determined by other methods (Seisenberger et al. 2001). By this new method it was for example possible to detect at least one Cy5- labeled AAV-2 in the nucleus of 50% of the cells 15 minutes after adding virus to the cells.

AAV serotypes other than AAV-2

Most AAV vectors are based on the AAV-2 serotype, as it was the first serotype from which an infectious clone was available (Samulski et al. 1982). 50 to 96% of the population is seropositive for AAV-2. Five additional primate AAV serotypes (AAV-1, -3, -4, -5, and 6) have been characterized at the nucleotide level (Chiorini et al. 1999; Chiorini et al. 1997; Muramatsu et al. 1996; Rutledge et al. 1998). With the exception of AAV-6, which has a >99% amino acid homology with AAV-1, all serotypes show a significantly different amino acid sequence of the capsid proteins, which is most prominent in VP3 (Rabinowitz & Samulski 2000) and most obvious for AAV-4 and -5. It remains to be determined how these differences influence the binding of neutralizing antibodies, viral tropism and intracellular processing.

An investigation of the humoral immunity against AAV performed with a cohort of 85 human volunteers revealed that none of the sera contained neutralizing antibodies against AAV-5, although neutralizing antibodies against AAV-1 and AAV-2 were detected in 19 and 25% of the sera, respectively (Hildinger et al. 2001). Furthermore, neutralizing antibodies against AAV-4 or AAV-5 do not cross-react (Rabinowitz & Samulski 2000). Serum from mice immunized with AAV-2 vectors did not neutralize AAV-6 infection in tissue culture, neutralized AAV-3 only partially, but inhibited AAV-2 almost completely (Halbert et al. 2000). Similar results were obtained with AAV-3 used for immunization. Serum from AAV-6 immunized animals did not cross-react with AAV-2 or AAV-3 and neutralized the infection by AAV-6 only weakly.

In AAV-2, VP3 is responsible for receptor binding and therefore mainly determines the viral tropism. Differences in this region should result in a different receptor usage and viral tropism. Therefore it was not unexpected that AAV-4 and AAV-5, which show the lowest similarity to AAV-2, use α 2-3 O-linked (AAV-4) and N-linked (AAV-5) sialic acid for cell binding (Kaludov et al. 2001) instead of HSPG. AAV-6, which has a homology of about 60% to AAV-4 and -5 (Bantel-Schaal et al. 1999), also binds to sialic acid (Seiler et al. 2002), whereas AAV-3 binds to HSPG.

The various AAV serotypes show a different tissue or cell tropism (Halbert et al. 2000; Hildinger et al. 2001; Rabinowitz et al. 2002). AAV-1 is more efficient than AAV-2 for the transduction of skeletal muscle (Xiao et al. 1999). AAV-3 is superior for the transduction of megakaryocytes (Handa et al. 2000). Compared to AAV-2, AAV-5 and AAV-6 infect apical airway cells more efficiently (Halbert et al. 2001; Zabner et al. 2000).

AAV-2, -4 and -5 transduce cells of the central nervous system, but differences in the distribution and the target cell types exist (Davidson et al. 2000). It can be anticipated that further work on AAV serotypes will result in the identification of all domains involved in receptor binding and uptake. This knowledge will be very useful for the creation of AAV retargeting vectors.

Receptor Targeting of AAV

In principle, at least two different strategies are possible to achieve a receptor targeting of AAV (Cosset & Russell 1996):

1. **Indirect targeting:** In contrast to wild type (Fig. 2A) the interaction between the viral vector and the target cell is mediated by an associated molecule (e.g. a glycoside molecule or a bispecific antibody) which is bound to the viral surface and interacts with a specific cell surface molecule (Miller 1996) (Fig. 2B).
2. **Direct targeting:** The cell specific targeting of the vector is mediated by a ligand which is directly inserted into the viral capsid (Walter & Stein 1996) (Fig. 2C).

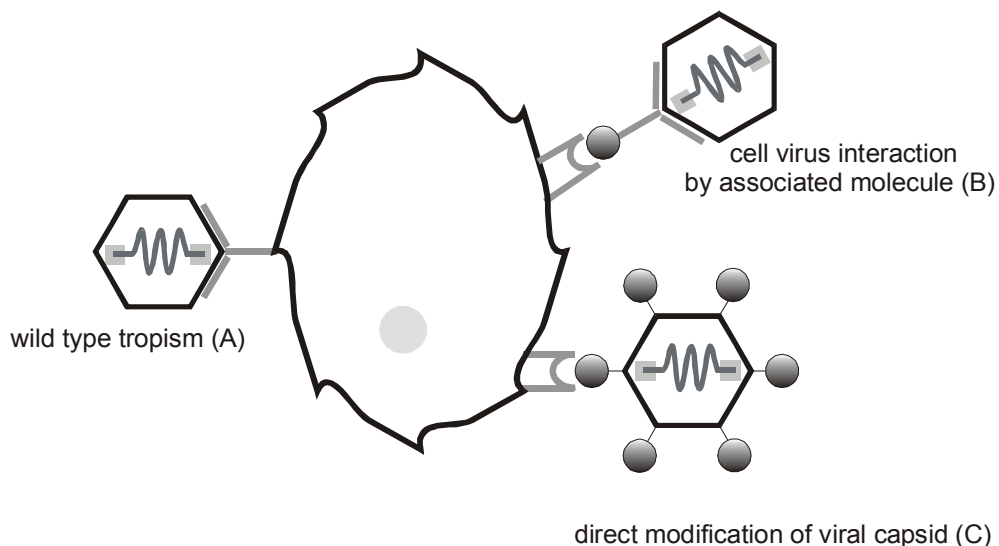


Figure 2. Possibilities of targeting viral vectors. Viral vectors with wild type tropism (A) show a direct binding of structural capsid components to the cell surface receptor. In targeting vectors, the virus-cell interaction is mediated by a molecule associated with the capsid (indirect targeting, B) or by a ligand directly inserted into the capsid (direct targeting, C).

For indirect targeting (Fig. 2B) it is not necessary to know the three-dimensional structure of the viral surface if high affinity viral surface binding molecules such as monoclonal antibodies are available. For this strategy, the stability of the interaction of the virus with the intermediate molecule and the efficiency by which the complex is generated are rate limiting. In addition, the intermediate molecules must bind to cell-specific receptors which allow the uptake and correct intracellular processing of the virus.

A combination of two important parameters is required for the successful generation of a targeting vector by direct modifications of the capsid (Fig. 2C). The first parameter is a good choice of the insertion site to ensure that packaging of the mutant remains efficient and the inserted ligand is exposed on the virus surface. Until now two alternative strategies have been used for AAV-2 to identify candidate positions for insertion of heterologous ligand: a) sequence alignment between AAV-2 and other parvoviruses for which the X-ray crystal structure is known (Girod et al. 1999; Grifman et al. 2001); b) a systematic, insertional mutagenesis of the whole AAV-2 capsid (Rabinowitz et al. 1999; Shi et al. 2001; Wu et al. 2000). The second important parameter is the choice of the targeting peptide. It is difficult to predict the secondary structure of the ligand inserted into the AAV capsid. Therefore, the ligand should be structure-independent and not too large to avoid the destabilization of the entire capsid. Moreover, the ligand should be cell type specific. Finally, the ligand-receptor complex should be internalized in a way that allows an efficient transport of the virus and the release of the viral DNA in the cell nucleus.

Both approaches and a combination thereof have been used to retarget AAV-2 and will be described in the following paragraphs (Bartlett et al. 1999; Girod et al. 1999; Grifman et al. 2001; Nicklin et al. 2001; Ried et al. 2002; Shi et al. 2001; Wu et al. 2000; Yang et al. 1998).

Targeting by bispecific antibodies

The feasibility to target AAV-2 using a bispecific antibody which mediates the interaction between virus and target cell (Fig. 2B) was first shown by Bartlett et al. (Bartlett et al. 1999). The antibody used was generated by a chemical cross-link of the Fab arms of monoclonal antibodies against the $\alpha_{IIb}\beta_3$ integrin (AP-2 antibody) and the intact AAV-2 capsid (A20 antibody, see (Wistuba et al. 1995)). The major ligand for $\alpha_{IIb}\beta_3$ is fibrinogen, which becomes internalized via endocytosis. Therefore, AAV-2 targeted to this integrin was expected to become internalized via receptor-mediated endocytosis, similar to wild type virus. This

targeting vector transduced MO7e and DAMI cells, which are not permissive for wild type AAV-2 infection (70-fold above background). In contrast, a 90% reduction in AAV-2 transduction was seen on cells negative for the targeting receptor. It remains to be determined whether this reduction was due to steric hindrance or some other mechanism. Another issue that remains to be resolved is the stability of the virus-bispecific antibody complexes *in vivo*.

Targeting by insertion of single chain antibodies or receptor specific ligands at the N-terminus of VP proteins

The first attempt to alter the tropism of AAV-2 was described by Yang et al. (Yang et al. 1998). They inserted a single-chain antibody against human CD34, a cell surface molecule expressed on hematopoietic progenitor cells, at the 5'-ends of VP1, VP2 and VP3. Using a transcription and translation assay, they could express all three different single-chain fragment variable region (scFv)-AAV-2 capsid fusion proteins. However, they failed to produce detectable rAAV-2 particles when using either all three scFv-VP fusion proteins or one scFv-VP fusion with two other unmodified capsid proteins. Therefore they had to use all three wild type AAV-2 capsid proteins for the packaging process in addition to one of the three single scFv-VP fusion proteins. Using this procedure, intact viral particles could be generated which were able to infect HeLa cells and showed an increased transduction of CD34 positive KG-1 cells. Although this approach provided the first demonstration that targeting of AAV-2 by direct modification of the capsid is possible, the virus titers (1.9×10^2 transducing units/ml on KG-1) were extremely low. Moreover, very heterogeneous viral preparations consisting of an unknown mixture of chimeric, targeting and wild type AAV-2 particles were produced.

Wu et al. (2000) inserted the hemagglutinin (HA) epitope YPVDVPDYA into the N-terminal regions of VP1, VP2 and VP3 and the C-terminus of the *cap* ORF. They observed that the insertion of this and other epitopes at the N termini of VP1 (VPN1) and VP3 (VPN3) and at the C-terminus of the *cap* ORF (VPC) resulted in either no detectable particles (VPN3 and VPC), or in a 2-3 log decrease of infectious and physical particle titers. In agreement with Yang et al. (1998), only the insertion at the N-terminus of VP2 (amino acid position 138) was tolerated (Wu et al. 2000). Moreover, exchanging the HA epitope by the serpin receptor ligand KFNKPFVFLI (Ziady et al. 1997) resulted in a 15-fold higher infection of the lung epithelial cell line IB3 than by wild type AAV-2. The fact that the N-terminal insertion of different peptides is tolerated in VP2 and allows targeting, albeit at low efficiency, probably

reflects the exposure of the N-terminus of VP2 at the viral surface analogous to CPV (Chapman & Rossmann 1993; Weichert et al. 1998). This assumption was further confirmed by the results of Shi et al. (2001), who inserted a 6 amino acid peptide (TPFYLK) from bovine papillomavirus (BPV) at position 139 and were able to detect this epitope on the capsid surface by monoclonal antibodies against BPV. In addition, the insertion of a 10 amino acid peptide (HCSTCYHKS) derived from the human luteinizing hormone (LH) increased the infection efficiency of a LH-receptor positive human ovarian adenocarcinoma cell line, OVCAR-3.

Targeting of rAAV-2 vectors by insertion of ligand coding sequences into the capsid genes

The first successful demonstration that a genetic capsid modification (direct targeting) can be used to retarget AAV-2 was described by Girod et al. (1999). A sequence alignment of AAV-2 and CPV identified 6 sites (amino acid positions 261, 381, 447, 534, 573, 587) that were expected to be exposed on the surface of the virus capsid and to accept the insertion of a ligand without disrupting functions essential for the viral life cycle (Fig. 3A).

At these positions the sequence for the 14 amino acid peptide L14 (QAGTFALRGDNPQG) was inserted into the capsid gene. The L14 peptide contains the RGD motif of the laminin fragment P1, is the target for several cellular integrin receptors, and can also serve as a viral receptor (Aumailley et al. 1990; White 1993). In addition no specific secondary structure is required for the recognition of the receptor (Aumailley et al. 1990). All six mutants could be packaged with an efficiency similar to wild type AAV-2 and showed an intact capsid structure in electron microscopy images (Grimm et al. 1999; Wistuba et al. 1997). Using an ELISA with an anti-L14 polyclonal antibody it was demonstrated that the L14 epitope was exposed at the viral surface when inserted at amino acid positions 261, 381, 447, 573 and 587. In a cell binding assay insertion mutants I-447 and I-587 were able to bind B16F10 (mouse melanoma) and RN22 (rat swannoma) cell lines, which did not bind to and were not infected by wild type AAV-2. An efficient transduction of B16F10 cells was observed using the AAV insertion mutant I-587 expressing Rep or β -galactosidase.

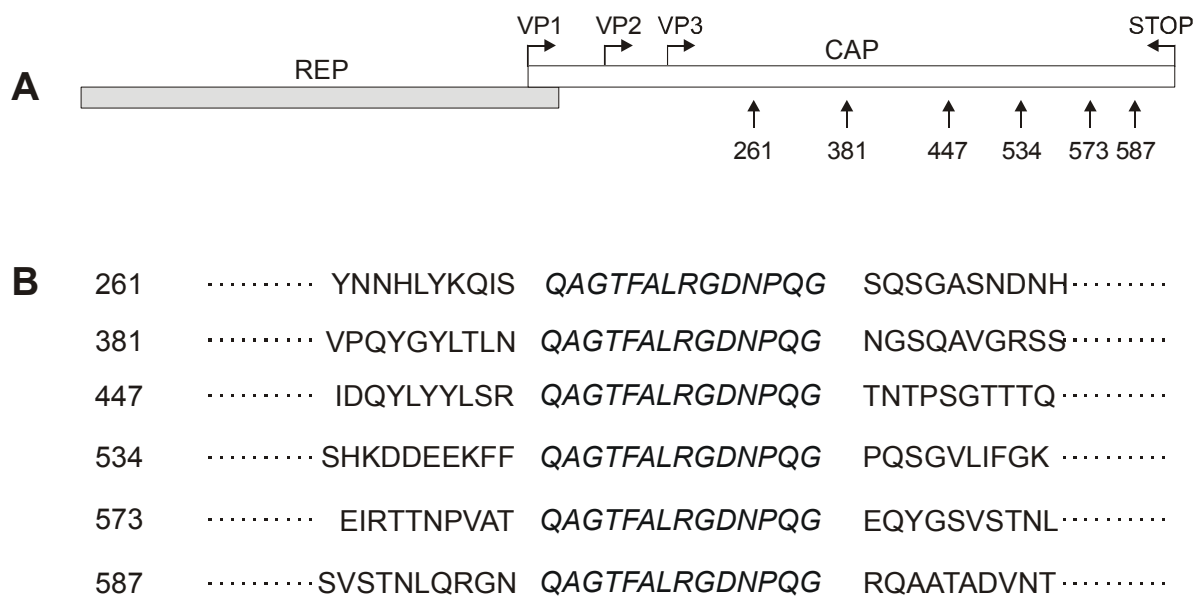


Figure 3. L14 peptide insertion sites in the AAV2 capsid. (A) Schematic diagram of the two open reading frames *rep* and *cap*. *Cap* encodes the three capsid protein VP1, VP2 and VP3. Sites of the L14 insertion described by Girod et al. (1999) are marked by arrows (numbers are the amino acid positions N-terminal of the insertion). (B) Sequence of L14 and flanking amino acids at the different insertion sites tested. The insertion mutant I-587 displayed the L14 peptide on the surface and was able to retarget the mutant to the mouse melanoma cell line B16F10 (Girod et al. 1999) (numbering starts at the start codon of VP1).

The same site, 587, was also successfully used for the insertion of an endothelial specific peptide isolated by phage display, and allowed the generation of an AAV-2 mutant able to infect endothelial cells such as human umbilical vein endothelial cells (HUVEC) and human saphenous vein endothelial cells (HSVEC) (Nicklin et al. 2001). In contrast to wild type AAV-2 infection, the infection of the endothelial specific cells by the mutant was not blocked by heparin, showing that the infection did not depend on HSPG. Moreover, heparin binding studies showed that the mutant was not retained in a heparin column, in contrast to wild type AAV-2. The specificity of the binding was shown by infection studies using different non-endothelial specific cell lines such as HepG2. Furthermore, the mutant seemed to follow an intracellular route different from wild type AAV-2 since compounds such as bafilomycin A2 (an inhibitor of endosomal acidification) did not inhibit transduction. Taken together, all studies underline the potential value of the 587 site of the AAV-2 capsid, which is positioned at the tip the GH loop (Xie et al. 2002) for the generation of cell-specific AAV-2

vectors by the direct targeting approach (Fig. 2C) (Girod et al. 1999; Nicklin et al. 2001; Ried et al. 2002).

This strategy was successfully repeated by Grifman et al. (2001). They also used a sequence alignment approach to identify potential targeting sites of the AAV-2 capsid by expanding their comparisons to parvoviruses other than CPV and to the other AAV serotypes (AAV-1, -3, -4 and -5). They identified identical regions to Girod et al. (1999), and finally used sites 448 and 587 for their studies. Grifman et al. (2001) inserted the Myc epitope and a CD13 (NGR receptor expressed on angiogenic vasculature and in many tumor cell lines) specific peptide with the sequence NGRAHA, identified by phage display. The insertion of NGRAHA at 587 allowed a cell-specific targeting to different cell lines (KS1767 (Kaposi sarcoma) and RD (rhabdomyosarcoma)). Interestingly, deletion of the 6 amino acids (GNRQAA) at position 586-591 resulted in the loss of heparin binding, whereas the insertion of the targeting peptide (NGRAHA) restored the heparin binding ability. Taking into account that HSPG has a negative charge, the R at position 588 might have an essential role for HSPG binding.

For a systematic characterization of functional domains of the AAV capsid proteins, Wu et al. (2000) constructed 93 mutants at 59 different positions on the AAV-2 capsid by site directed mutagenesis. They identified several putative regions, which were involved in HSPG binding and/or exposed on the capsid surface, with the potential to tolerate the insertion of a ligand. These positions were 34 (in VP1), the N-terminus of VP2 (138), as well as 266, 328, 447, 522, 553, 591, 664 (in VP3). Although all VP3 insertion mutants were precipitated by an antibody against the inserted HA epitope, only 266, 447, 591 and 664 were still infectious. For insertion mutant 522, this could be explained by the loss of the HSPG binding ability (Rabinowitz et al. 1999; Wu et al. 2000). For the other mutants, a simple explanation is lacking. Wu et al. (2000) tested only the position 34 in the VP1 sequence (FVFLI substitution) and the N-terminus of VP2 (KFNKPFVFLI insertion) for targeting of AAV-2 to IB3 cells via serpin receptor. It was shown that targeting and infection was possible. In this approach the N-terminal VP-2 insertion mutant was 15-fold and the VP1 mutant approximately 62-fold more infectious than the wild type. In both cases, the insertions were placed outside the potential HSPG binding regions. Therefore it was not surprising that the transduction of the target cells by these mutants was blocked by heparin, suggesting that the serpin-tagged mutants continued to use HSPG as primary receptor and used the serpin receptor as alternative (co-)receptor.

Using insertional mutagenesis, Shi et al. (2001) also tried to identify positions in the AAV-2 capsid which might tolerate the insertion of heterologous peptide ligands. In addition to the VP2 N-terminal insertion mutants mentioned above, mutants with insertions into the capsid sequences were generated. These mutants contained either an insertion of two amino acids (TG or AG) or of longer epitopes derived from the bovine papillomavirus (BPV; TPFYLK), from the human luteinizing hormone (LH; HCSTCYHKS) or a cyclic RGD-containing peptide specific for α_v integrins (4C-RGD, CDCRGDCFC). None of these mutants were tested for retargeting, but three important observations were made:

1. Five different capsid regions were identified which allowed the surface display of the BPV peptide ligand. These were 139 (N-terminus of VP2), 161 (in the VP2 region), 459, 584 and 587 (in the VP3 region). The positions 139 and 587 confirmed earlier results (Girod et al. 1999; Wu et al. 2000). The other sites remain to be tested for functional targeting, because the surface display of a ligand alone is a prerequisite but not sufficient for a ligand dependent infection by the virus mutant (Girod et al. 1999).
2. The scaffold sequences flanking the heterologous ligand are important for epitope display, HSPG binding ability and titers. Using for example the amino acids ALS to flank the BPV ligand inserted at 584 resulted in mutants that showed surface display of the epitope, HSPG binding and the production of infectious particles. In contrast, LLA and GLS used as scaffold sequences did not allow the production of infectious particles and reduced the surface display of the BPV ligand. In contrast, the GLS scaffold sequence was better tolerated than LLA or ALS at position 587.
3. Not every ligand, even if comparable in length, is tolerated at a specific insertion site. Shi et al. (2001) inserted either the BPV or the LH ligand both flanked by the GLS scaffold sequences at site 459 and observed that the BPV ligand (a 6 amino acid insertion) generated fully infectious particles, whereas the insertion of the 10 amino acid LH peptide created non-infectious virus particles. Our laboratory made similar observations when trying to insert multimers of the L14 sequence at position 587: larger insertions at position 587 resulted in a decrease of the packaging efficiency although the insertion of a 34 amino acid containing the Z34C protein A domain of *Staphylococcus aureus* (see below) was well tolerated. These results show that the maximal length of the peptide tolerated at this position depends on the sequence itself. The precise determinants of this phenomenon are unknown.

Generation of universal targeting vectors by combining two principles of vector targeting

Inspired by an earlier attempt for Sindbis virus (Ohno et al. 1997), we tried to use a general targeting vector using a truncated 34 amino acid peptide, Z34C, from protein A of *Staphylococcus aureus* (Ried et al. 2002). Protein A recognizes and binds the Fc part of immunoglobulins (Ig), but not the variable Ig domain, which therefore remains free to bind the antigen. Z34C is derived from the protein A subunit B, which encompasses 56 amino acids and binds the Fc portion with a dissociation constant of about 10-50 nM (Sinha et al. 1999). A 38 residue truncation of this domain, selected by phage display, was further truncated and stabilized by insertion of disulfide bonds and showed thereafter a dissociation constant of 20 nM. The insertion of Z34C at position 587 in the AAV-2 capsid (587Z34C) resulted in a 10-fold decrease of packaging efficiency in comparison to wild type AAV-2. In contrast, the combination of the insertion with a 9 amino acid deletion (587 Δ 9Z34C) resulted in a packaging efficiency similar to wild type AAV-2. Electron microscopy and A20-ELISA revealed a wild type capsid morphology for both mutants, although empty capsids were observed 3-fold more frequently. Interestingly, the wild type tropism of the Z34C insertion mutants decreased by 4 orders of magnitude, in agreement with the results of Nicklin et al. (2001). The insertion of Z34C at position 587 allowed a functional expression of the IgG binding domain, as shown by binding studies using various antibodies. Interestingly, the capsid mutant 587Z34C bound antibodies more efficiently than 587 Δ 9Z34C, maybe because the binding domain was less accessible with the 9 amino acid deletion. In agreement, Grifman et al. (2001) showed that a substitution at 587 was less efficient than an insertion. Coupling 587Z34C virus with antibodies against CD29 (β 1-integrin), CD117 (c-kit-receptor) or CXCR4 resulted in a specific, antibody mediated transduction of hematopoietic cell lines. No transduction could be detected without antibody, whereas the targeted infection was blocked with soluble protein A or with IgG molecules. In addition, no inhibition of transduction by the targeting vector was observed with heparin, demonstrating that the interaction of the 587Z34C mutants with the natural AAV-2 receptor HSPG was not essential for infection or transduction. Taken together, this targeting approach shows that a universal AAV targeting vector can be generated and loaded with different targeting molecules to transduce the desired cells via specific receptors. However, this approach leaves room for improvement, since the titers obtained with these vectors were relatively low.

Future prospects: understand the infectious biology of AAV

To efficiently retarget AAV vectors a better understanding of the infectious biology of AAV will be required. This includes the virus-cell surface interactions, mechanisms of uptake, endosomal processing and release, nuclear transport and mechanisms leading to gene expression. The structure determination of the AAV-2 capsid (Xie et al. 2002) will tremendously enhance our knowledge of the location and function of different capsid domains.

The identification of HSPG as primary attachment receptor for AAV-2 was an important achievement. However, no distinct binding motif within the capsid has been identified so far, despite some useful information presented in the work of Rabinowitz et al. (1999) and Wu et al. (2000). Such knowledge will be required to specifically modify the natural viral tropism of AAV-2.

A better understanding of the intracellular processing of AAV targeting vectors is essential, because AAV targeting vectors may be transferred into a cellular compartment from which they will never be released, or in which they will be processed in ways preventing nuclear processing or gene expression. Therefore, the success of creating AAV targeting vectors will ultimately depend on our ability to unveil the detailed mechanisms of AAV transport and processing. Some pieces of the puzzle are already known (Bartlett et al. 2000; Sanlioglu et al. 2000; Seisenberger et al. 2001), but the picture is not complete. With regard to this, single virus tracing (Seisenberger et al. 2001) will be a very important tool to understand which receptors and cellular compartments need to be used to efficiently re-target AAV. On the other hand, the technique of AAV vector targeting will help to uncover some important, basic functions of AAV capsid proteins, as well as mechanisms of the infectious biology of AAV.

The third important issue is the identification of the optimal ligand or targeting receptor. For the genetic modification strategy chosen by our group, the length and sequence of the ligand are critical, as the insertion of a peptide may result in profound alterations of the three-dimensional capsid structure. One possibility of overcoming this problem is the combination of the insertion with one or more deletions. Another possibility is the insertion of a sequence which is able to form its own secondary structure, for example a loop closed by a cysteine bridge.

These difficulties are overcome when using an antibody or another bridging molecule to mediate the interaction between the viral surface and the target cell. However, this

approach will encounter other problems such as the stability of the virus-ligand complex, limitations to scale up the vector production, and steric hindrance of the virus uptake by large virus-ligand complexes. To identify new ligands, phage display has been proven to be a valid approach. However, the ligand sequences are selected in an architectural context that is different from that of the final vector. This means that once inserted in the context of AAV, they could destabilize the capsid structure (resulting in low packaging efficiency) or lose their biological properties (resulting in low infectious titers). To overcome these difficulties the screening for new “retargeting” peptides to be inserted might be done more efficiently in the context of the AAV capsid itself (vector display), where a pool of randomized peptide sequences is inserted into the capsid sequence and the viral pool is then screened directly on the target cells (Perabo et al. 2003). The exciting results obtained by this approach together with the rapid advance of our knowledge of the structure and biology of AAV raise the expectations of dramatic improvement in AAV vector technology in the near future.

The ultimate goal of all these attempts will be the generation of a recombinant AAV vector, which allows gene delivery exclusively to the desired cells or tissue, thereby widening the therapeutic window of this vector for clinical application.

Acknowledgments

This work was supported by the Deutsche Forschungsgemeinschaft (SFB 455), the Wilhelm Sander-Stiftung and the Bayerische Forschungstiftung. The authors thank all members of the laboratory for many inspiring discussions and help during the work presented in this review, and Dr. Susan King for critically reading the manuscript. The authors apologize to investigators whose work was not cited owing to limited space.

CHAPTER VI

References

- Agbandje M, Kajigaya S, McKenna R, Young NS, and Rossmann MG. (1994)** The structure of human parvovirus B19 at 8 Å resolution. *Virology* **203**: 106-115.
- Agbandje M, McKenna R, Rossmann MG, Strassheim ML, and Parrish CR. (1993)** Structure determination of feline panleukopenia virus empty particles. *Proteins* **16**: 155-171.
- Agbandje-McKenna M, Llamas-Saiz AL, Wang F, Tattersall P, and Rossmann MG. (1998)** Functional implications of the structure of the murine parvovirus, minute virus of mice. *Structure* **6**: 1369-1381.
- Anderson R, Macdonald I, Corbett T, Hacking G, Lowdell MW, and Prentice HG. (1997)** Construction and biological characterization of an interleukin-12 fusion protein (Flexi-12): delivery to acute myeloid leukemic blasts using adeno-associated virus. *Hum Gene Ther* **8**: 1125-1135.
- Atchison RW, Casto BC, and Hammon WM. (1965)** Adenovirus-associated defective virus particles. *Science* **149**: 754-756.
- Aumailley M, Gerl M, Sonnenberg A, Deutzmann R, and Timpl R. (1990)** Identification of the Arg-Gly-Asp sequence in laminin A chain as a latent cell-binding site being exposed in fragment P1. *FEBS Lett* **262**: 82-86.
- Balague C, Kalla M, and Zhang WW. (1997)** Adeno-associated virus Rep78 protein and terminal repeats enhance integration of DNA sequences into the cellular genome. *J Virol* **71**: 3299-3306.
- Bantel-Schaal U, Delius H, Schmidt R, and zur Hausen H. (1999)** Human adeno-associated virus type 5 is only distantly related to other known primate helper-dependent parvoviruses. *J Virol* **73**: 939-947.
- Bartlett JS, Kleinschmidt J, Boucher RC, and Samulski RJ. (1999)** Targeted adeno-associated virus vector transduction of nonpermissive cells mediated by a bispecific F(ab \prime)₂ antibody. *Nat Biotechnol* **17**: 181-186.
- Bartlett JS, and Samulski RJ. (1998)** Fluorescent viral vectors: a new technique for the pharmacological analysis of gene therapy. *Nat Med* **4**: 635-637.

-
- Bartlett JS, Wilcher R, and Samulski RJ. (2000)** Infectious entry pathway of adeno-associated virus and adeno-associated virus vectors. *J Virol* **74**: 2777-2785.
- Becerra SP, Koczot F, Fabisch P, and Rose JA. (1988)** Synthesis of adeno-associated virus structural proteins requires both alternative mRNA splicing and alternative initiations from a single transcript. *J Virol* **62**: 2745-2754.
- Becerra SP, Rose JA, Hardy M, Baroudy BM, and Anderson CW. (1985)** Direct mapping of adeno-associated virus capsid proteins B and C: a possible ACG initiation codon. *Proc Natl Acad Sci U S A* **82**: 7919-7923.
- Berns KI, Bergoin M, Bloom ME, Lederman M, Muzyczka N, Siegl N, Tal G, and Tattersall P. (2000)** Parvoviridae. VIIth Report of the International Committee on Taxonomy of Viruses. In: van Regenmortel MHV, Fauquet CM, Bishop DHL, et al., eds. *Virus Taxonomy: Classification and Nomenclature of Viruses*. San Diego: Academic Press. 311-323.
- Berns KI, and Giraud C. (1996)** Biology of adeno-associated virus. *Curr Top Microbiol Immunol* **218**: 1-23.
- Berns KI, and Linden RM. (1995)** The cryptic life style of adeno-associated virus. *Bioessays* **17**: 237-245.
- Blacklow NR. (1988)** Adeno-associated virus of humans. In: Pattison J, ed. *Parvoviruses and human disease*. Boca Raton, FL: CRC Press. 165-174.
- Blacklow NR, Hoggan MD, Kapikian AZ, Austin JB, and Rowe WP. (1968a)** Epidemiology of adenovirus-associated virus infection in a nursery population. *Am J Epidemiol* **88**: 368-378.
- Blacklow NR, Hoggan MD, and Rowe WP. (1968b)** Serologic evidence for human infection with adenovirus-associated viruses. *J Natl Cancer Inst* **40**: 319-327.
- Blacklow NR, Hoggan MD, Sereno MS, Brandt CD, Kim HW, Parrott RH, and Chanock RM. (1971)** A seroepidemiologic study of adenovirus-associated virus infection in infants and children. *Am J Epidemiol* **94**: 359-366.

- Blaese RM, Culver KW, Miller AD, Carter CS, Fleisher T, Clerici M, Shearer G, Chang L, Chiang Y, Tolstoshev P, and et al. (1995)** T lymphocyte-directed gene therapy for ADA- SCID: initial trial results after 4 years. *Science* **270**: 475-480.
- Brister JR, and Muzyczka N. (2000)** Mechanism of Rep-mediated adeno-associated virus origin nicking. *J Virol* **74**: 7762-7771.
- Brockstedt DG, Podsakoff GM, Fong L, Kurtzman G, Mueller-Ruchholtz W, and Engleman EG. (1999)** Induction of immunity to antigens expressed by recombinant adeno-associated virus depends on the route of administration. *Clin Immunol* **92**: 67-75.
- Burguete T, Rabreau M, Fontanges-Darriet M, Roset E, Hager HD, Koppel A, Bischof P, and Schlehofer JR. (1999)** Evidence for infection of the human embryo with adeno-associated virus in pregnancy. *Hum Reprod* **14**: 2396-2401.
- Carter BJ, and Rose JA. (1974)** Transcription in vivo of a defective parvovirus: sedimentation and electrophoretic analysis of RNA synthesized by adenovirus-associated virus and its helper adenovirus. *Virology* **61**: 182-199.
- Carter PJ, and Samulski RJ. (2000)** Adeno-associated viral vectors as gene delivery vehicles. *Int J Mol Med* **6**: 17-27.
- Chang SF, Sgro JY, and Parrish CR. (1992)** Multiple amino acids in the capsid structure of canine parvovirus coordinately determine the canine host range and specific antigenic and hemagglutination properties. *J Virol* **66**: 6858-6867.
- Chapman MS, and Rossmann MG. (1993)** Structure, sequence, and function correlations among parvoviruses. *Virology* **194**: 491-508.
- Chejanovsky N, and Carter BJ. (1989)** Replication of a human parvovirus nonsense mutant in mammalian cells containing an inducible amber suppressor. *Virology* **171**: 239-247.
- Cheung AK, Hoggan MD, Hauswirth WW, and Berns KI. (1980)** Integration of the adeno-associated virus genome into cellular DNA in latently infected human Detroit 6 cells. *J Virol* **33**: 739-748.

-
- Chiorini JA, Kim F, Yang L, and Kotin RM. (1999)** Cloning and characterization of adeno-associated virus type 5. *J Virol* **73**: 1309-1319.
- Chiorini JA, Wendtner CM, Urcelay E, Safer B, Hallek M, and Kotin RM. (1995)** High-efficiency transfer of the T cell co-stimulatory molecule B7-2 to lymphoid cells using high-titer recombinant adeno-associated virus vectors. *Hum Gene Ther* **6**: 1531-1541.
- Chiorini JA, Wiener SM, Yang L, Smith RH, Safer B, Kilcoin NP, Liu Y, Urcelay E, and Kotin RM. (1996)** The roles of AAV Rep proteins in gene expression and targeted integration. *Curr Top Microbiol Immunol* **218**: 25-33.
- Chiorini JA, Yang L, Liu Y, Safer B, and Kotin RM. (1997)** Cloning of adeno-associated virus type 4 (AAV4) and generation of recombinant AAV4 particles. *J Virol* **71**: 6823-6833.
- Chipman PR, Agbandje-McKenna M, Kajigaya S, Brown KE, Young NS, Baker TS, and Rossmann MG. (1996)** Cryo-electron microscopy studies of empty capsids of human parvovirus B19 complexed with its cellular receptor. *Proc Natl Acad Sci U S A* **93**: 7502-7506.
- Chirmule N, Propert K, Magosin S, Qian Y, Qian R, and Wilson J. (1999)** Immune responses to adenovirus and adeno-associated virus in humans. *Gene Ther* **6**: 1574-1583.
- Chirmule N, Xiao W, Truneh A, Schnell MA, Hughes JV, Zoltick P, and Wilson JM. (2000)** Humoral immunity to adeno-associated virus type 2 vectors following administration to murine and nonhuman primate muscle. *J Virol* **74**: 2420-2425.
- Cosset FL, and Russell SJ. (1996)** Targeting retrovirus entry. *Gene Ther* **3**: 946-956.
- Costello E, Saudan P, Winocour E, Pizer L, and Beard P. (1997)** High mobility group chromosomal protein 1 binds to the adeno-associated virus replication protein (Rep) and promotes Rep-mediated site-specific cleavage of DNA, ATPase activity and transcriptional repression. *Embo J* **16**: 5943-5954.

- Curiel DT, Agarwal S, Wagner E, and Cotten M. (1991)** Adenovirus enhancement of transferrin-polylysine-mediated gene delivery. *Proc Natl Acad Sci U S A* **88**: 8850-8854.
- Curiel DT, Wagner E, Cotten M, Birnstiel ML, Agarwal S, Li CM, Loechel S, and Hu PC. (1992)** High-efficiency gene transfer mediated by adenovirus coupled to DNA-polylysine complexes. *Hum Gene Ther* **3**: 147-154.
- Davidson BL, Stein CS, Heth JA, Martins I, Kotin RM, Derksen TA, Zabner J, Ghodsi A, and Chiorini JA. (2000)** Recombinant adeno-associated virus type 2, 4, and 5 vectors: transduction of variant cell types and regions in the mammalian central nervous system. *Proc Natl Acad Sci U S A* **97**: 3428-3432.
- de la Maza LM, and Carter BJ. (1981)** Inhibition of adenovirus oncogenicity in hamsters by adeno-associated virus DNA. *J Natl Cancer Inst* **67**: 1323-1326.
- Dong JY, Fan PD, and Frizzell RA. (1996)** Quantitative analysis of the packaging capacity of recombinant adeno-associated virus. *Hum Gene Ther* **7**: 2101-2112.
- Douar AM, Poulard K, Stockholm D, and Danos O. (2001)** Intracellular trafficking of adeno-associated virus vectors: routing to the late endosomal compartment and proteasome degradation. *J Virol* **75**: 1824-1833.
- Duan D, Li Q, Kao AW, Yue Y, Pessin JE, and Engelhardt JF. (1999)** Dynamin is required for recombinant adeno-associated virus type 2 infection. *J Virol* **73**: 10371-10376.
- Duan D, Yue Y, Yan Z, and Engelhardt JF. (2000)** A new dual-vector approach to enhance recombinant adeno-associated virus-mediated gene expression through intermolecular cis activation. *Nat Med* **6**: 595-598.
- Dubielzig R, King JA, Weger S, Kern A, and Kleinschmidt JA. (1999)** Adeno-associated virus type 2 protein interactions: formation of pre-encapsulation complexes. *J Virol* **73**: 8989-8998.

-
- Dutheil N, Shi F, Dupressoir T, and Linden RM. (2000)** Adeno-associated virus site-specifically integrates into a muscle-specific DNA region. *Proc Natl Acad Sci U S A* **97**: 4862-4866.
- Dyall J, Szabo P, and Berns KI. (1999)** Adeno-associated virus (AAV) site-specific integration: formation of AAV-AAVS1 junctions in an in vitro system. *Proc Natl Acad Sci U S A* **96**: 12849-12854.
- Erles K, Rohde V, Thaele M, Roth S, Edler L, and Schlehofer JR. (2001)** DNA of adeno-associated virus (AAV) in testicular tissue and in abnormal semen samples. *Hum Reprod* **16**: 2333-2337.
- Erles K, Sebkova P, and Schlehofer JR. (1999)** Update on the prevalence of serum antibodies (IgG and IgM) to adeno-associated virus (AAV). *J Med Virol* **59**: 406-411.
- Ferrari FK, Samulski T, Shenk T, and Samulski RJ. (1996)** Second-strand synthesis is a rate-limiting step for efficient transduction by recombinant adeno-associated virus vectors. *J Virol* **70**: 3227-3234.
- Ferrari FK, Xiao X, McCarty D, and Samulski RJ. (1997)** New developments in the generation of Ad-free, high-titer rAAV gene therapy vectors. *Nat Med* **3**: 1295-1297.
- Fisher KJ, Gao GP, Weitzman MD, DeMatteo R, Burda JF, and Wilson JM. (1996)** Transduction with recombinant adeno-associated virus for gene therapy is limited by leading-strand synthesis. *J Virol* **70**: 520-532.
- Fisher KJ, Jooss K, Alston J, Yang Y, Haecker SE, High K, Pathak R, Raper SE, and Wilson JM. (1997)** Recombinant adeno-associated virus for muscle directed gene therapy. *Nat Med* **3**: 306-312.
- Fisher-Adams G, Wong KK, Jr., Podsakoff G, Forman SJ, and Chatterjee S. (1996)** Integration of adeno-associated virus vectors in CD34+ human hematopoietic progenitor cells after transduction. *Blood* **88**: 492-504.
- Flannery JG, Zolotukhin S, Vaquero MI, LaVail MM, Muzyczka N, and Hauswirth WW. (1997)** Efficient photoreceptor-targeted gene expression in vivo by recombinant adeno-associated virus. *Proc Natl Acad Sci U S A* **94**: 6916-6921.

- Flotte TR, Afione SA, Conrad C, McGrath SA, Solow R, Oka H, Zeitlin PL, Guggino WB, and Carter BJ. (1993)** Stable in vivo expression of the cystic fibrosis transmembrane conductance regulator with an adeno-associated virus vector. *Proc Natl Acad Sci U S A* **90**: 10613-10617.
- Flotte TR, and Carter BJ. (1995)** Adeno-associated virus vectors for gene therapy. *Gene Ther* **2**: 357-362.
- Gao X, and Huang L. (1996)** Potentiation of cationic liposome-mediated gene delivery by polycations. *Biochemistry* **35**: 1027-1036.
- Giraud C, Winocour E, and Berns KI. (1994)** Site-specific integration by adeno-associated virus is directed by a cellular DNA sequence. *Proc Natl Acad Sci U S A* **91**: 10039-10043.
- Giraud C, Winocour E, and Berns KI. (1995)** Recombinant junctions formed by site-specific integration of adeno-associated virus into an episome. *J Virol* **69**: 6917-6924.
- Girod A, Ried M, Wobus C, Lahm H, Leike K, Kleinschmidt J, Deleage G, and Hallek M. (1999)** Genetic capsid modifications allow efficient re-targeting of adeno-associated virus type 2. *Nat Med* **5**: 1052-1056.
- Girod A, Wobus CE, Zadori Z, Ried M, Leike K, Tijssen P, Kleinschmidt JA, and Hallek M. (2002)** The VP1 capsid protein of adeno-associated virus type 2 is carrying a phospholipase A2 domain required for virus infectivity. *J Gen Virol* **83**: 973-978.
- Griesenbach U, Ferrari S, Geddes DM, and Alton EW. (2002)** Gene therapy progress and prospects: cystic fibrosis. *Gene Ther* **9**: 1344-1350.
- Grifman M, Trepel M, Speece P, Gilbert LB, Arap W, Pasqualini R, and Weitzman MD. (2001)** Incorporation of tumor-targeting peptides into recombinant adeno-associated virus capsids. *Mol Ther* **3**: 964-975.
- Grimm D, Kern A, Pawlita M, Ferrari F, Samulski R, and Kleinschmidt J. (1999)** Titration of AAV-2 particles via a novel capsid ELISA: packaging of genomes can limit production of recombinant AAV-2. *Gene Ther* **6**: 1322-1330.

-
- Grimm D, and Kleinschmidt JA. (1999)** Progress in adeno-associated virus type 2 vector production: promises and prospects for clinical use. *Hum Gene Ther* **10**: 2445-2450.
- Hacein-Bey-Abina S, von Kalle C, Schmidt M, Le Deist F, Wulffraat N, McIntyre E, Radford I, Villeval JL, Fraser CC, Cavazzana-Calvo M, and Fischer A. (2003)** A serious adverse event after successful gene therapy for X-linked severe combined immunodeficiency. *N Engl J Med* **348**: 255-256.
- Halbert CL, Allen JM, and Miller AD. (2001)** Adeno-associated virus type 6 (AAV6) vectors mediate efficient transduction of airway epithelial cells in mouse lungs compared to that of AAV2 vectors. *J Virol* **75**: 6615-6624.
- Halbert CL, Rutledge EA, Allen JM, Russell DW, and Miller AD. (2000)** Repeat transduction in the mouse lung by using adeno-associated virus vectors with different serotypes. *J Virol* **74**: 1524-1532.
- Halbert CL, Standaert TA, Wilson CB, and Miller AD. (1998)** Successful readministration of adeno-associated virus vectors to the mouse lung requires transient immunosuppression during the initial exposure. *J Virol* **72**: 9795-9805.
- Handa A, Muramatsu S, Qiu J, Mizukami H, and Brown KE. (2000)** Adeno-associated virus (AAV)-3-based vectors transduce haematopoietic cells not susceptible to transduction with AAV-2-based vectors. *J Gen Virol* **81**: 2077-2084.
- Hansen J, Qing K, and Srivastava A. (2001)** Infection of purified nuclei by adeno-associated virus 2. *Mol Ther* **4**: 289-296.
- Harlow E, and Lane D. (1988)** *Antibodies. A laboratory manual*. Cold Spring Harbor Laboratory, Cold Spring Harbor, NY.
- Harper SQ, Hauser MA, DelloRusso C, Duan D, Crawford RW, Phelps SF, Harper HA, Robinson AS, Engelhardt JF, Brooks SV, and Chamberlain JS. (2002)** Modular flexibility of dystrophin: implications for gene therapy of Duchenne muscular dystrophy. *Nat Med* **8**: 253-261.

- Heilbronn R, Schlehofer JR, Yalkinoglu AO, and Zur Hausen H. (1985)** Selective DNA-amplification induced by carcinogens (initiators): evidence for a role of proteases and DNA polymerase alpha. *Int J Cancer* **36**: 85-91.
- Hermens WT, ter Brake O, Dijkhuizen PA, Sonnemans MA, Grimm D, Kleinschmidt JA, and Verhaagen J. (1999)** Purification of recombinant adeno-associated virus by iodixanol gradient ultracentrifugation allows rapid and reproducible preparation of vector stocks for gene transfer in the nervous system. *Hum Gene Ther* **10**: 1885-1891.
- Hermonat PL. (1989)** The adeno-associated virus Rep78 gene inhibits cellular transformation induced by bovine papillomavirus. *Virology* **172**: 253-261.
- Hermonat PL. (1994)** Down-regulation of the human c-fos and c-myc proto-oncogene promoters by adeno-associated virus Rep78. *Cancer Lett* **81**: 129-136.
- Hermonat PL, Labow MA, Wright R, Berns KI, and Muzyczka N. (1984)** Genetics of adeno-associated virus: isolation and preliminary characterization of adeno-associated virus type 2 mutants. *J Virol* **51**: 329-339.
- Hernandez YJ, Wang J, Kearns WG, Loiler S, Poirier A, and Flotte TR. (1999)** Latent adeno-associated virus infection elicits humoral but not cell-mediated immune responses in a nonhuman primate model. *J Virol* **73**: 8549-8558.
- Hildinger M, Auricchio A, Gao G, Wang L, Chirmule N, and Wilson JM. (2001)** Hybrid vectors based on adeno-associated virus serotypes 2 and 5 for muscle-directed gene transfer. *J Virol* **75**: 6199-6203.
- Hinshaw JE, and Schmid SL. (1995)** Dynamin self-assembles into rings suggesting a mechanism for coated vesicle budding. *Nature* **374**: 190-192.
- Hoggan MD, Blacklow NR, and Rowe WP. (1966)** Studies of small DNA viruses found in various adenovirus preparations: physical, biological, and immunological characteristics. *Proc Natl Acad Sci U S A* **55**: 1467-1474.

-
- Hoque M, Ishizu K, Matsumoto A, Han SI, Arisaka F, Takayama M, Suzuki K, Kato K, Kanda T, Watanabe H, and Handa H. (1999)** Nuclear transport of the major capsid protein is essential for adeno-associated virus capsid formation. *J Virol* **73**: 7912-7915.
- Huttner NA, Girod A, Schnittger S, Schoch C, Hallek M, and Buning H. (2003)** Analysis of site-specific transgene integration following co-transduction with recombinant adeno-associated virus and a rep encoding plasmid. *J Gene Med* **5**: 120-129.
- Im DS, and Muzyczka N. (1990)** The AAV origin binding protein Rep68 is an ATP-dependent site-specific endonuclease with DNA helicase activity. *Cell* **61**: 447-457.
- Im DS, and Muzyczka N. (1992)** Partial purification of adeno-associated virus Rep78, Rep52, and Rep40 and their biochemical characterization. *J Virol* **66**: 1119-1128.
- Jomary C, Vincent KA, Grist J, Neal MJ, and Jones SE. (1997)** Rescue of photoreceptor function by AAV-mediated gene transfer in a mouse model of inherited retinal degeneration. *Gene Ther* **4**: 683-690.
- Jooss K, Yang Y, Fisher KJ, and Wilson JM. (1998)** Transduction of dendritic cells by DNA viral vectors directs the immune response to transgene products in muscle fibers. *J Virol* **72**: 4212-4223.
- Kaludov N, Brown KE, Walters RW, Zabner J, and Chiorini JA. (2001)** Adeno-associated virus serotype 4 (AAV4) and AAV5 both require sialic acid binding for hemagglutination and efficient transduction but differ in sialic acid linkage specificity. *J Virol* **75**: 6884-6893.
- Kaplitt MG, Leone P, Samulski RJ, Xiao X, Pfaff DW, O'Malley KL, and During MJ. (1994)** Long-term gene expression and phenotypic correction using adeno-associated virus vectors in the mammalian brain. *Nat Genet* **8**: 148-154.
- Kay MA, Manno CS, Ragni MV, Larson PJ, Couto LB, McClelland A, Glader B, Chew AJ, Tai SJ, Herzog RW, Arruda V, Johnson F, Scallan C, Skarsgard E, Flake AW, and High KA. (2000)** Evidence for gene transfer and expression of factor IX in haemophilia B patients treated with an AAV vector. *Nat Genet* **24**: 257-261.

- Kearns WG, Afione SA, Fulmer SB, Pang MC, Erikson D, Egan M, Landrum MJ, Flotte TR, and Cutting GR. (1996)** Recombinant adeno-associated virus (AAV-CFTR) vectors do not integrate in a site-specific fashion in an immortalized epithelial cell line. *Gene Ther* **3**: 748-755.
- Kessler PD, Podsakoff GM, Chen X, McQuiston SA, Colosi PC, Matelis LA, Kurtzman GJ, and Byrne BJ. (1996)** Gene delivery to skeletal muscle results in sustained expression and systemic delivery of a therapeutic protein. *Proc Natl Acad Sci U S A* **93**: 14082-14087.
- Khleif SN, Myers T, Carter BJ, and Trempe JP. (1991)** Inhibition of cellular transformation by the adeno-associated virus rep gene. *Virology* **181**: 738-741.
- King JA, Dubielzig R, Grimm D, and Kleinschmidt JA. (2001)** DNA helicase-mediated packaging of adeno-associated virus type 2 genomes into preformed capsids. *Embo J* **20**: 3282-3291.
- Klein RL, Meyer EM, Peel AL, Zolotukhin S, Meyers C, Muzyczka N, and King MA. (1998)** Neuron-specific transduction in the rat septohippocampal or nigrostriatal pathway by recombinant adeno-associated virus vectors. *Exp Neurol* **150**: 183-194.
- Kotin RM. (1994)** Prospects for the use of adeno-associated virus as a vector for human gene therapy. *Hum Gene Ther* **5**: 793-801.
- Kotin RM, and Berns KI. (1989)** Organization of adeno-associated virus DNA in latently infected Detroit 6 cells. *Virology* **170**: 460-467.
- Kotin RM, Linden RM, and Berns KI. (1992)** Characterization of a preferred site on human chromosome 19q for integration of adeno-associated virus DNA by non-homologous recombination. *Embo J* **11**: 5071-5078.
- Kotin RM, Siniscalco M, Samulski RJ, Zhu XD, Hunter L, Laughlin CA, McLaughlin S, Muzyczka N, Rocchi M, and Berns KI. (1990)** Site-specific integration by adeno-associated virus. *Proc Natl Acad Sci U S A* **87**: 2211-2215.

-
- Kronenberg S, Kleinschmidt JA, and Bottcher B. (2001)** Electron cryo-microscopy and image reconstruction of adeno-associated virus type 2 empty capsids. *EMBO Rep* **2**: 997-1002.
- Kwoh DY, Coffin CC, Lollo CP, Jovenal J, Banaszczyk MG, Mullen P, Phillips A, Amini A, Fabrycki J, Bartholomew RM, Brostoff SW, and Carlo DJ. (1999)** Stabilization of poly-L-lysine/DNA polyplexes for in vivo gene delivery to the liver. *Biochim Biophys Acta* **1444**: 171-190.
- Kyostio SR, Owens RA, Weitzman MD, Antoni BA, Chejanovsky N, and Carter BJ. (1994)** Analysis of adeno-associated virus (AAV) wild-type and mutant Rep proteins for their abilities to negatively regulate AAV p5 and p19 mRNA levels. *J Virol* **68**: 2947-2957.
- Labow MA, and Berns KI. (1988)** The adeno-associated virus rep gene inhibits replication of an adeno-associated virus/simian virus 40 hybrid genome in cos-7 cells. *J Virol* **62**: 1705-1712.
- Lamartina S, Sporeno E, Fattori E, and Toniatti C. (2000)** Characteristics of the adeno-associated virus preintegration site in human chromosome 19: open chromatin conformation and transcription-competent environment. *J Virol* **74**: 7671-7677.
- Laughlin CA, Cardellicchio CB, and Coon HC. (1986)** Latent infection of KB cells with adeno-associated virus type 2. *J Virol* **60**: 515-524.
- Lee RJ, and Huang L. (1996)** Folate-targeted, anionic liposome-entrapped polylysine-condensed DNA for tumor cell-specific gene transfer. *J Biol Chem* **271**: 8481-8487.
- Lewin AS, Drenser KA, Hauswirth WW, Nishikawa S, Yasumura D, Flannery JG, and LaVail MM. (1998)** Ribozyme rescue of photoreceptor cells in a transgenic rat model of autosomal dominant retinitis pigmentosa. *Nat Med* **4**: 967-971.
- Lichter P, Cremer T, Borden J, Manuelidis L, and Ward DC. (1988)** Delineation of individual human chromosomes in metaphase and interphase cells by in situ suppression hybridization using recombinant DNA libraries. *Hum Genet* **80**: 224-234.

- Linden RM, Ward P, Giraud C, Winocour E, and Berns KI. (1996a)** Site-specific integration by adeno-associated virus. *Proc Natl Acad Sci U S A* **93**: 11288-11294.
- Linden RM, Winocour E, and Berns KI. (1996b)** The recombination signals for adeno-associated virus site-specific integration. *Proc Natl Acad Sci U S A* **93**: 7966-7972.
- Macville M, Schrock E, Padilla-Nash H, Keck C, Ghadimi BM, Zimonjic D, Popescu N, and Ried T. (1999)** Comprehensive and definitive molecular cytogenetic characterization of HeLa cells by spectral karyotyping. *Cancer Res* **59**: 141-150.
- Mandel RJ, Spratt SK, Snyder RO, and Leff SE. (1997)** Midbrain injection of recombinant adeno-associated virus encoding rat glial cell line-derived neurotrophic factor protects nigral neurons in a progressive 6-hydroxydopamine-induced degeneration model of Parkinson's disease in rats. *Proc Natl Acad Sci U S A* **94**: 14083-14088.
- Manning WC, Paliard X, Zhou S, Pat Bland M, Lee AY, Hong K, Walker CM, Escobedo JA, and Dwarki V. (1997)** Genetic immunization with adeno-associated virus vectors expressing herpes simplex virus type 2 glycoproteins B and D. *J Virol* **71**: 7960-7962.
- Manning WC, Zhou S, Bland MP, Escobedo JA, and Dwarki V. (1998)** Transient immunosuppression allows transgene expression following readministration of adeno-associated viral vectors. *Hum Gene Ther* **9**: 477-485.
- Marks B, Stowell MH, Vallis Y, Mills IG, Gibson A, Hopkins CR, and McMahon HT. (2001)** GTPase activity of dynamin and resulting conformation change are essential for endocytosis. *Nature* **410**: 231-235.
- Marsh M, and Helenius A. (1989)** Virus entry into animal cells. *Adv Virus Res* **36**: 107-151.
- Mayor HD, Houlditch GS, and Mumford DM. (1973)** Influence of adeno-associated satellite virus on adenovirus-induced tumours in hamsters. *Nat New Biol* **241**: 44-46.
- Mayor HD, Torikai K, Melnick JL, and Mandel M. (1969)** Plus and minus single-stranded DNA separately encapsidated in adeno-associated satellite virions. *Science* **166**: 1280-1282.

-
- McCarty DM, Monahan PE, and Samulski RJ. (2001)** Self-complementary recombinant adeno-associated virus (scAAV) vectors promote efficient transduction independently of DNA synthesis. *Gene Ther* **8**: 1248-1254.
- McCarty DM, Pereira DJ, Zolotukhin I, Zhou X, Ryan JH, and Muzyczka N. (1994)** Identification of linear DNA sequences that specifically bind the adeno-associated virus Rep protein. *J Virol* **68**: 4988-4997.
- McCown TJ, Xiao X, Li J, Breese GR, and Samulski RJ. (1996)** Differential and persistent expression patterns of CNS gene transfer by an adeno-associated virus (AAV) vector. *Brain Res* **713**: 99-107.
- McKenna R, Olson NH, Chipman PR, Baker TS, Booth TF, Christensen J, Aasted B, Fox JM, Bloom ME, Wolfinbarger JB, and Agbandje-McKenna M. (1999)** Three-dimensional structure of Aleutian mink disease parvovirus: implications for disease pathogenicity. *J Virol* **73**: 6882-6891.
- McLaughlin SK, Collis P, Hermonat PL, and Muzyczka N. (1988)** Adeno-associated virus general transduction vectors: analysis of proviral structures. *J Virol* **62**: 1963-1973.
- Meneses P, Berns KI, and Winocour E. (2000)** DNA sequence motifs which direct adeno-associated virus site-specific integration in a model system. *J Virol* **74**: 6213-6216.
- Miller AD. (1996)** Cell-surface receptors for retroviruses and implications for gene transfer. *Proc Natl Acad Sci U S A* **93**: 11407-11413.
- Monahan PE, and Samulski RJ. (2000)** Adeno-associated virus vectors for gene therapy: more pros than cons? *Mol Med Today* **6**: 433-440.
- Moskalenko M, Chen L, van Roey M, Donahue BA, Snyder RO, McArthur JG, and Patel SD. (2000)** Epitope mapping of human anti-adeno-associated virus type 2 neutralizing antibodies: implications for gene therapy and virus structure. *J Virol* **74**: 1761-1766.
- Muramatsu S, Mizukami H, Young NS, and Brown KE. (1996)** Nucleotide sequencing and generation of an infectious clone of adeno-associated virus 3. *Virology* **221**: 208-217.

- Murphy JE, Zhou S, Giese K, Williams LT, Escobedo JA, and Dwarki VJ. (1997)** Long-term correction of obesity and diabetes in genetically obese mice by a single intramuscular injection of recombinant adeno-associated virus encoding mouse leptin. *Proc Natl Acad Sci U S A* **94**: 13921-13926.
- Muzyczka N, and Berns KI. (2001)** Parvoviridae: The viruses and their replication. In: Knipe DM, Howley PM, Griffin DE, et al., eds. *Fields Virology*. 4th ed. Philadelphia: Lippincott Williams & Wilkins. 2327-2359.
- Nakai H, Storm TA, and Kay MA. (2000)** Increasing the size of rAAV-mediated expression cassettes in vivo by intermolecular joining of two complementary vectors. *Nat Biotechnol* **18**: 527-532.
- Nguyen JT, Wu P, Clouse ME, Hlatky L, and Terwilliger EF. (1998)** Adeno-associated virus-mediated delivery of antiangiogenic factors as an antitumor strategy. *Cancer Res* **58**: 5673-5677.
- Nicklin SA, Buening H, Dishart KL, de Alwis M, Girod A, Hacker U, Thrasher AJ, Ali RR, Hallek M, and Baker AH. (2001)** Efficient and selective AAV2-mediated gene transfer directed to human vascular endothelial cells. *Mol Ther* **4**: 174-181.
- Ohno K, Sawai K, Iijima Y, Levin B, and Meruelo D. (1997)** Cell-specific targeting of Sindbis virus vectors displaying IgG-binding domains of protein A. *Nat Biotechnol* **15**: 763-767.
- Perabo L, Büning H, Kofler D, Ried MU, Girod A, Enssle J, and Hallek M. (2003)** In vitro selection of viral vectors with modified tropism: the adeno-associated virus display. *Mol Ther* **8**: 151-157.
- Qing K, Mah C, Hansen J, Zhou S, Dwarki V, and Srivastava A. (1999)** Human fibroblast growth factor receptor 1 is a co-receptor for infection by adeno-associated virus 2. *Nat Med* **5**: 71-77.
- Qiu J, and Brown KE. (1999)** Integrin alphaVbeta5 is not involved in adeno-associated virus type 2 (AAV2) infection. *Virology* **264**: 436-440.

-
- Qiu J, Mizukami H, and Brown KE. (1999)** Adeno-associated virus 2 co-receptors? *Nat Med* **5**: 467-468.
- Rabinowitz JE, Rolling F, Li C, Conrath H, Xiao W, Xiao X, and Samulski RJ. (2002)** Cross-packaging of a single adeno-associated virus (AAV) type 2 vector genome into multiple AAV serotypes enables transduction with broad specificity. *J Virol* **76**: 791-801.
- Rabinowitz JE, and Samulski RJ. (2000)** Building a better vector: the manipulation of AAV virions. *Virology* **278**: 301-308.
- Rabinowitz JE, Xiao W, and Samulski RJ. (1999)** Insertional mutagenesis of AAV2 capsid and the production of recombinant virus. *Virology* **265**: 274-285.
- Raj K, Ogston P, and Beard P. (2001)** Virus-mediated killing of cells that lack p53 activity. *Nature* **412**: 914-917.
- Redemann BE, Mendelson E, and Carter BJ. (1989)** Adeno-associated virus rep protein synthesis during productive infection. *J Virol* **63**: 873-882.
- Ried MU, Girod A, Leike K, Buning H, and Hallek M. (2002)** Adeno-associated virus capsids displaying immunoglobulin-binding domains permit antibody-mediated vector retargeting to specific cell surface receptors. *J Virol* **76**: 4559-4566.
- Rivadeneira ED, Popescu NC, Zimonjic DB, Cheng GS, Nelson PJ, Ross MD, DiPaolo JA, and Klotman ME. (1998)** Sites of recombinant adeno-associated virus integration. *Int J Oncol* **12**: 805-810.
- Ruffing M, Zentgraf H, and Kleinschmidt JA. (1992)** Assembly of viruslike particles by recombinant structural proteins of adeno-associated virus type 2 in insect cells. *J Virol* **66**: 6922-6930.
- Russell DW, Alexander IE, and Miller AD. (1995)** DNA synthesis and topoisomerase inhibitors increase transduction by adeno-associated virus vectors. *Proc Natl Acad Sci USA* **92**: 5719-5723.
- Russell DW, and Kay MA. (1999)** Adeno-associated virus vectors and hematology. *Blood* **94**: 864-874.

- Rutledge EA, Halbert CL, and Russell DW. (1998)** Infectious clones and vectors derived from adeno-associated virus (AAV) serotypes other than AAV type 2. *J Virol* **72**: 309-319.
- Rutledge EA, and Russell DW. (1997)** Adeno-associated virus vector integration junctions. *J Virol* **71**: 8429-8436.
- Samulski RJ, Berns KI, Tan M, and Muzyczka N. (1982)** Cloning of adeno-associated virus into pBR322: rescue of intact virus from the recombinant plasmid in human cells. *Proc Natl Acad Sci U S A* **79**: 2077-2081.
- Samulski RJ, Chang LS, and Shenk T. (1987)** A recombinant plasmid from which an infectious adeno-associated virus genome can be excised in vitro and its use to study viral replication. *J Virol* **61**: 3096-3101.
- Samulski RJ, Chang LS, and Shenk T. (1989)** Helper-free stocks of recombinant adeno-associated viruses: normal integration does not require viral gene expression. *J Virol* **63**: 3822-3828.
- Samulski RJ, Zhu X, Xiao X, Brook JD, Housman DE, Epstein N, and Hunter LA. (1991)** Targeted integration of adeno-associated virus (AAV) into human chromosome 19. *Embo J* **10**: 3941-3950.
- Sanlioglu S, Benson PK, Yang J, Atkinson EM, Reynolds T, and Engelhardt JF. (2000)** Endocytosis and nuclear trafficking of adeno-associated virus type 2 are controlled by rac1 and phosphatidylinositol-3 kinase activation. *J Virol* **74**: 9184-9196.
- Sarukhan A, Camugli S, Gjata B, von Boehmer H, Danos O, and Jooss K. (2001)** Successful interference with cellular immune responses to immunogenic proteins encoded by recombinant viral vectors. *J Virol* **75**: 269-277.
- Saudan P, Vlach J, and Beard P. (2000)** Inhibition of S-phase progression by adeno-associated virus Rep78 protein is mediated by hypophosphorylated pRb. *Embo J* **19**: 4351-4361.

-
- Seiler M, Halbert CL, Chiorini JA, Miller AD, and Zabner J. (2002)** AAV5 and AAV6 mediate gene transfer to human airway epithelia via different receptors. *Mol. Ther.* **5**: abstract No. 117.
- Seisenberger G, Ried MU, Endress T, Buning H, Hallek M, and Brauchle C. (2001)** Real-time single-molecule imaging of the infection pathway of an adeno-associated virus. *Science* **294**: 1929-1932.
- Sever S, Damke H, and Schmid SL. (2000)** Dynamin:GTP controls the formation of constricted coated pits, the rate limiting step in clathrin-mediated endocytosis. *J Cell Biol* **150**: 1137-1148.
- Shelling AN, and Smith MG. (1994)** Targeted integration of transfected and infected adeno-associated virus vectors containing the neomycin resistance gene. *Gene Ther* **1**: 165-169.
- Shi W, Arnold GS, and Bartlett JS. (2001)** Insertional mutagenesis of the adeno-associated virus type 2 (AAV2) capsid gene and generation of AAV2 vectors targeted to alternative cell-surface receptors. *Hum Gene Ther* **12**: 1697-1711.
- Sinha P, Sengupta J, and Ray PK. (1999)** Functional mimicry of protein A of *Staphylococcus aureus* by a proteolytically cleaved fragment. *Biochem Biophys Res Commun* **260**: 111-116.
- Smith RH, and Kotin RM. (1998)** The Rep52 gene product of adeno-associated virus is a DNA helicase with 3'-to-5' polarity. *J Virol* **72**: 4874-4881.
- Smith RH, and Kotin RM. (2000)** An adeno-associated virus (AAV) initiator protein, Rep78, catalyzes the cleavage and ligation of single-stranded AAV ori DNA. *J Virol* **74**: 3122-3129.
- Smith TJ. (2001)** Antibody interactions with rhinovirus: lessons for mechanisms of neutralization and the role of immunity in viral evolution. *Curr Top Microbiol Immunol* **260**: 1-28.

- Smuda JW, and Carter BJ. (1991)** Adeno-associated viruses having nonsense mutations in the capsid genes: growth in mammalian cells containing an inducible amber suppressor. *Virology* **184**: 310-318.
- Snyder RO, Im DS, Ni T, Xiao X, Samulski RJ, and Muzyczka N. (1993)** Features of the adeno-associated virus origin involved in substrate recognition by the viral Rep protein. *J Virol* **67**: 6096-6104.
- Snyder RO, Miao C, Meuse L, Tubb J, Donahue BA, Lin HF, Stafford DW, Patel S, Thompson AR, Nichols T, Read MS, Bellinger DA, Brinkhous KM, and Kay MA. (1999)** Correction of hemophilia B in canine and murine models using recombinant adeno-associated viral vectors. *Nat Med* **5**: 64-70.
- Snyder RO, Miao CH, Patijn GA, Spratt SK, Danos O, Nagy D, Gown AM, Winther B, Meuse L, Cohen LK, Thompson AR, and Kay MA. (1997)** Persistent and therapeutic concentrations of human factor IX in mice after hepatic gene transfer of recombinant AAV vectors. *Nat Genet* **16**: 270-276.
- Snyder RO, Samulski RJ, and Muzyczka N. (1990)** In vitro resolution of covalently joined AAV chromosome ends. *Cell* **60**: 105-113.
- Strassheim ML, Gruenberg A, Veijalainen P, Sgro JY, and Parrish CR. (1994)** Two dominant neutralizing antigenic determinants of canine parvovirus are found on the threefold spike of the virus capsid. *Virology* **198**: 175-184.
- Summerford C, Bartlett JS, and Samulski RJ. (1999)** AlphaVbeta5 integrin: a co-receptor for adeno-associated virus type 2 infection. *Nat Med* **5**: 78-82.
- Summerford C, and Samulski RJ. (1998)** Membrane-associated heparan sulfate proteoglycan is a receptor for adeno-associated virus type 2 virions. *J Virol* **72**: 1438-1445.
- Summerford C, and Samulski RJ. (1999)** Viral receptors and vector purification: new approaches for generating clinical-grade reagents. *Nat Med* **5**: 587-588.
- Sun L, Li J, and Xiao X. (2000)** Overcoming adeno-associated virus vector size limitation through viral DNA heterodimerization. *Nat Med* **6**: 599-602.

-
- Surosky RT, Urabe M, Godwin SG, McQuiston SA, Kurtzman GJ, Ozawa K, and Natsoulis G. (1997)** Adeno-associated virus Rep proteins target DNA sequences to a unique locus in the human genome. *J Virol* **71**: 7951-7959.
- Tal J. (2000)** Adeno-associated virus-based vectors in gene therapy. *J Biomed Sci* **7**: 279-291.
- Teichler Zallen D. (2000)** US gene therapy in crisis. *Trends Genet* **16**: 272-275.
- Tratschin JD, Miller IL, and Carter BJ. (1984)** Genetic analysis of adeno-associated virus: properties of deletion mutants constructed in vitro and evidence for an adeno-associated virus replication function. *J Virol* **51**: 611-619.
- Tsao J, Chapman MS, Agbandje M, Keller W, Smith K, Wu H, Luo M, Smith TJ, Rossmann MG, Compans RW, and et al. (1991)** The three-dimensional structure of canine parvovirus and its functional implications. *Science* **251**: 1456-1464.
- Tsunoda H, Hayakawa T, Sakuragawa N, and Koyama H. (2000)** Site-specific integration of adeno-associated virus-based plasmid vectors in lipofected HeLa cells. *Virology* **268**: 391-401.
- Urabe M, Hasumi Y, Kume A, Surosky RT, Kurtzman GJ, Tobita K, and Ozawa K. (1999)** Charged-to-alanine scanning mutagenesis of the N-terminal half of adeno-associated virus type 2 Rep78 protein. *J Virol* **73**: 2682-2693.
- Wagner E, Cotten M, Foisner R, and Birnstiel ML. (1991)** Transferrin-polycation-DNA complexes: the effect of polycations on the structure of the complex and DNA delivery to cells. *Proc Natl Acad Sci U S A* **88**: 4255-4259.
- Wagner E, Zatloukal K, Cotten M, Kirlappos H, Mechtler K, Curiel DT, and Birnstiel ML. (1992)** Coupling of adenovirus to transferrin-polylysine/DNA complexes greatly enhances receptor-mediated gene delivery and expression of transfected genes. *Proc Natl Acad Sci U S A* **89**: 6099-6103.
- Wagner E, Zenke M, Cotten M, Beug H, and Birnstiel ML. (1990)** Transferrin-polycation conjugates as carriers for DNA uptake into cells. *Proc Natl Acad Sci U S A* **87**: 3410-3414.

- Walsh CE, Liu JM, Xiao X, Young NS, Nienhuis AW, and Samulski RJ. (1992)** Regulated high level expression of a human gamma-globin gene introduced into erythroid cells by an adeno-associated virus vector. *Proc Natl Acad Sci U S A* **89**: 7257-7261.
- Walter W, and Stein U. (1996)** Cell type specific and inducible promoters for vectors in gene therapy as an approach for cell targeting. *J Mol Med* **74**: 379-392.
- Wang K, Huang S, Kapoor-Munshi A, and Nemerow G. (1998)** Adenovirus internalization and infection require dynamin. *J Virol* **72**: 3455-3458.
- Wang L, Takabe K, Bidlingmaier SM, III CR, and Verma IM. (1999)** Sustained correction of bleeding disorder in hemophilia B mice by gene therapy. *Proc Natl Acad Sci U S A* **96**: 3906-3910.
- Weichert WS, Parker JS, Wahid AT, Chang SF, Meier E, and Parrish CR. (1998)** Assaying for structural variation in the parvovirus capsid and its role in infection. *Virology* **250**: 106-117.
- Weitzman MD, Kyostio SR, Kotin RM, and Owens RA. (1994)** Adeno-associated virus (AAV) Rep proteins mediate complex formation between AAV DNA and its integration site in human DNA. *Proc Natl Acad Sci U S A* **91**: 5808-5812.
- Wendtner CM, Kofler DM, Theiss HD, Kurzeder C, Buhmann R, Schweighofer C, Perabo L, Danhauser-Riedl S, Baumert J, Hiddemann W, Hallek M, and Buning H. (2002)** Efficient gene transfer of CD40 ligand into primary B-CLL cells using recombinant adeno-associated virus (rAAV) vectors. *Blood* **100**: 1655-1661.
- White JM. (1993)** Integrins as virus receptors. *Curr Biol* **3**: 596-599.
- Wistuba A, Kern A, Weger S, Grimm D, and Kleinschmidt JA. (1997)** Subcellular compartmentalization of adeno-associated virus type 2 assembly. *J Virol* **71**: 1341-1352.
- Wistuba A, Weger S, Kern A, and Kleinschmidt JA. (1995)** Intermediates of adeno-associated virus type 2 assembly: identification of soluble complexes containing Rep and Cap proteins. *J Virol* **69**: 5311-5319.

-
- Wobus CE, Hugle-Dorr B, Girod A, Petersen G, Hallek M, and Kleinschmidt JA. (2000)** Monoclonal antibodies against the adeno-associated virus type 2 (AAV-2) capsid: epitope mapping and identification of capsid domains involved in AAV-2-cell interaction and neutralization of AAV-2 infection. *J Virol* **74**: 9281-9293.
- Wolfert MA, and Seymour LW. (1996)** Atomic force microscopic analysis of the influence of the molecular weight of poly(L)lysine on the size of polyelectrolyte complexes formed with DNA. *Gene Ther* **3**: 269-273.
- Wu P, Xiao W, Conlon T, Hughes J, Agbandje-McKenna M, Ferkol T, Flotte T, and Muzyczka N. (2000)** Mutational analysis of the adeno-associated virus type 2 (AAV2) capsid gene and construction of AAV2 vectors with altered tropism. *J Virol* **74**: 8635-8647.
- Xiao W, Chirmule N, Berta SC, McCullough B, Gao G, and Wilson JM. (1999)** Gene therapy vectors based on adeno-associated virus type 1. *J Virol* **73**: 3994-4003.
- Xiao W, Chirmule N, Schnell MA, Tazelaar J, Hughes JV, and Wilson JM. (2000)** Route of administration determines induction of T-cell-independent humoral responses to adeno-associated virus vectors. *Mol Ther* **1**: 323-329.
- Xiao X, Li J, and Samulski RJ. (1996)** Efficient long-term gene transfer into muscle tissue of immunocompetent mice by adeno-associated virus vector. *J Virol* **70**: 8098-8108.
- Xiao X, Li J, and Samulski RJ. (1998)** Production of high-titer recombinant adeno-associated virus vectors in the absence of helper adenovirus. *J Virol* **72**: 2224-2232.
- Xiao X, McCown TJ, Li J, Breese GR, Morrow AL, and Samulski RJ. (1997a)** Adeno-associated virus (AAV) vector antisense gene transfer in vivo decreases GABA(A) alpha1 containing receptors and increases inferior collicular seizure sensitivity. *Brain Res* **756**: 76-83.
- Xiao X, Xiao W, Li J, and Samulski RJ. (1997b)** A novel 165-base-pair terminal repeat sequence is the sole cis requirement for the adeno-associated virus life cycle. *J Virol* **71**: 941-948.

- Xie Q, Bu W, Bhatia S, Hare J, Somasundaram T, Azzi A, and Chapman MS. (2002)** The atomic structure of adeno-associated virus (AAV-2), a vector for human gene therapy. *Proc Natl Acad Sci U S A* **99**: 10405-10410.
- Yakobson B, Hrynko TA, Peak MJ, and Winocour E. (1989)** Replication of adeno-associated virus in cells irradiated with UV light at 254 nm. *J Virol* **63**: 1023-1030.
- Yakobson B, Koch T, and Winocour E. (1987)** Replication of adeno-associated virus in synchronized cells without the addition of a helper virus. *J Virol* **61**: 972-981.
- Yalkinoglu AO, Zentgraf H, and Hubscher U. (1991)** Origin of adeno-associated virus DNA replication is a target of carcinogen-inducible DNA amplification. *J Virol* **65**: 3175-3184.
- Yalkinoglu AO, Heilbronn R, Burkle A, Schlehofer JR, and zur Hausen H. (1988)** DNA amplification of adeno-associated virus as a response to cellular genotoxic stress. *Cancer Res* **48**: 3123-3129.
- Yan Z, Zhang Y, Duan D, and Engelhardt JF. (2000)** Trans-splicing vectors expand the utility of adeno-associated virus for gene therapy. *Proc Natl Acad Sci U S A* **97**: 6716-6721.
- Yang CC, Xiao X, Zhu X, Ansardi DC, Epstein ND, Frey MR, Matera AG, and Samulski RJ. (1997)** Cellular recombination pathways and viral terminal repeat hairpin structures are sufficient for adeno-associated virus integration in vivo and in vitro. *J Virol* **71**: 9231-9247.
- Yang Q, Mamounas M, Yu G, Kennedy S, Leaker B, Merson J, Wong-Staal F, Yu M, and Barber JR. (1998)** Development of novel cell surface CD34-targeted recombinant adenoassociated virus vectors for gene therapy. *Hum Gene Ther* **9**: 1929-1937.
- Young SM, Jr., McCarty DM, Degtyareva N, and Samulski RJ. (2000)** Roles of adeno-associated virus Rep protein and human chromosome 19 in site-specific recombination. *J Virol* **74**: 3953-3966.

-
- Yuasa K, Sakamoto M, Miyagoe-Suzuki Y, Tanouchi A, Yamamoto H, Li J, Chamberlain JS, Xiao X, and Takeda S. (2002)** Adeno-associated virus vector-mediated gene transfer into dystrophin-deficient skeletal muscles evokes enhanced immune response against the transgene product. *Gene Ther* **9**: 1576-1588.
- Zabner J, Seiler M, Walters R, Kotin RM, Fulgeras W, Davidson BL, and Chiorini JA. (2000)** Adeno-associated virus type 5 (AAV5) but not AAV2 binds to the apical surfaces of airway epithelia and facilitates gene transfer. *J Virol* **74**: 3852-3858.
- Zadori Z, Szelei J, Lacoste MC, Li Y, Gariepy S, Raymond P, Allaire M, Nabi IR, and Tijssen P. (2001)** A viral phospholipase A2 is required for parvovirus infectivity. *Dev Cell* **1**: 291-302.
- Zaiss AK, Liu Q, Bowen GP, Wong NC, Bartlett JS, and Muruve DA. (2002)** Differential activation of innate immune responses by adenovirus and adeno-associated virus vectors. *J Virol* **76**: 4580-4590.
- Zenke M, Steinlein P, Wagner E, Cotten M, Beug H, and Birnstiel ML. (1990)** Receptor-mediated endocytosis of transferrin-polycation conjugates: an efficient way to introduce DNA into hematopoietic cells. *Proc Natl Acad Sci U S A* **87**: 3655-3659.
- Zhang Y, Chirmule N, Gao G, and Wilson J. (2000)** CD40 ligand-dependent activation of cytotoxic T lymphocytes by adeno-associated virus vectors in vivo: role of immature dendritic cells. *J Virol* **74**: 8003-8010.
- Zhou S, Murphy JE, Escobedo JA, and Dwarki VJ. (1998)** Adeno-associated virus-mediated delivery of erythropoietin leads to sustained elevation of hematocrit in nonhuman primates. *Gene Ther* **5**: 665-670.
- Zhou X, Zolotukhin I, Im DS, and Muzyczka N. (1999)** Biochemical characterization of adeno-associated virus rep68 DNA helicase and ATPase activities. *J Virol* **73**: 1580-1590.
- Ziady AG, Perales JC, Ferkol T, Gerken T, Beegen H, Perlmutter DH, and Davis PB. (1997)** Gene transfer into hepatoma cell lines via the serpin enzyme complex receptor. *Am J Physiol* **273**: G545-552.

- Zolotukhin S, Byrne BJ, Mason E, Zolotukhin I, Potter M, Chesnut K, Summerford C, Samulski RJ, and Muzyczka N. (1999)** Recombinant adeno-associated virus purification using novel methods improves infectious titer and yield. *Gene Ther* **6**: 973-985.

ABBREVIATIONS

aa	amino acid	B19	B19 human parvovirus
AAV	adeno-associated virus, specifically adeno-associated virus type 2	bp	base pair
AAVS1	AAV integration site 1 (located in human chromosome 19)	BSA	bovine serum albumin
Ab	antibody	Cap	capsid protein
Ad	adenovirus	cDNA	complementary DNA
AFM	atomic force microscopy	ch	chromosome
		CLL	chronic lymphocytic leukemia
		CMV	cytomegalovirus
		CPV	canine parvovirus
		CTL	cytotoxic T-lymphocyte
		Cy3, Cy5	indocarbocyanine dyes
		Da	Dalton
		DMEM	Dulbecco's Modified Eagle Medium
		e.g.	for example (Lat.: <i>exempli gratia</i>)
		ELISA	enzyme-linked immunosorbent assay
		FACS	fluorescence-activated cell sorting
		FCS	fetal calf serum
		FGFR	fibroblast growth factor receptor 1
		Fig.	figure
		FISH	fluorescence <i>in situ</i> hybridization
		FITC	fluorescein isothiocyanate
		FPV	feline panleukopenia virus
		GFP	green fluorescence protein
		Gy	Gray
		h	hour
		HA	hemagglutinin
		HSPG	heparan sulfate proteoglycan
		i.e.	that is (Lat.: <i>id est</i>)
		i.m.	intra muscular
		ITR	inverted terminal repeat
		kb	kilobases
		K _d	dissociation constant
		mAb	monoclonal antibody
		MHC	major histocompatibility complex
		min	minute
		MOI	multiplicity of infection
		NPC	nuclear pore complex

<u>Amino acids:</u>	
A (Ala)	alanine
C (Cys)	cysteine
D (Asp)	aspartate
E (Glu)	glutamate
F (Phe)	phenylalanine
G (Gly)	glycine
H (His)	histidine
I (Ile)	isoleucine
K (Lys)	lysine
L (Leu)	leucine
M (Met)	methionine
N (Asn)	asparagine
P (Pro)	proline
Q (Gln)	glutamine
R (Arg)	arginine
S (Ser)	serine
T (Thr)	threonine
V (Val)	valine
W (Trp)	tryptophan
Y (Tyr)	tyrosine

<u>Bases:</u>	
A	adenin
C	cytosin
G	guanin
T	thymin

nt	nucleotide	RT	room temperature
ori	origin of replication	SDS	sodium dodecyl sulfate
ORF	open reading frame	Stav	streptavidin
PLL	poly-L-lysine	Stpl	Streptavidin linked to polylysine
rAAV	recombinant AAV	T	triangulation number
RBS	Rep binding site	TRS	terminal resolution site
Rep	viral regulatory protein	VP	viral protein (AAV capsid protein)
rpm	rounds per minute	wtAAV	wild-type AAV

CURRICULUM VITAE

Persönliche Daten

Nadja Angelika Huttner
Bäckerstr. 16
81241 München
geboren am 2. September 1971 in München
ledig

Schulbildung und Studium

1982 – 1991	Bertolt-Brecht-Gymnasium in München Abschluss: Allgemeine Hochschulreife
1991 – 1996	Studium der Pharmazie an der LMU München
Juli 1997	Abschluss des Studiums - Erteilung der Approbation als Apothekerin

Promotion

seit Sept. 1997 Promotion am Institut für Biochemie der LMU München in der
Arbeitsgruppe von Prof. Dr. Michael Hallek
*„Adeno-associated virus type 2 as vector for human gene therapy:
Characterization of virus-host interactions.“*

Publikationen

Huttner NA, Girod A, Schnittger S, Schoch C, Hallek M, and Büning H. (2003) Analysis of site-specific transgene integration following co-transduction with recombinant adeno-associated virus and a rep encoding plasmid. *J Gene Med* 5: 120-129

Huttner NA, Girod A, Perabo L, Edbauer D, Kleinschmidt JA, Büning H, and Hallek M. (2003) Genetic modifications of the adeno-associated virus type 2 capsid reduce the affinity and the neutralizing effects of human serum antibodies. *Gene Ther* (in press)

Büning H, Ried MU, Perabo L, Gerner FM, **Huttner NA**, Enssle J, and Hallek M. (2003) Receptor targeting of adeno-associated virus vectors. *Gene Ther* 10, 1142-1151

Teilnahme an internationalen Kongressen

XI. International Parvovirus Workshop in Bologna, Italy (2002):

Vortrag: Genetic modifications of the adeno-associated virus type 2 capsid reduce the affinity to human serum antibodies and overcome the limitations of high prevalence of neutralizing antibodies

Cold Spring Harbor Laboratories - Vector Targeting Strategies for Human Gene Therapy, USA (2003):

Posterpräsentation: Genetic modification of the AAV capsid reduce antibody binding and neutralization

Patente

Internationale Patentanmeldung WO 03/054197: A library of modified structural genes or capsid modified particles useful for the identification of viral clones with desired cell tropism.

